ORNL-5285

Use of Ultimate Tensile Strength to Correlate and Estimate Creep and Creep-Rupture Behavior of Types 304 and 316 Stainless Steel

V. K. Sikka
M. K. Booker
C. R. Brinkman

OAK RIDGE NATIONAL LABORATORY
OPERATED BY UNION CARBIDE CORPORATION FOR THE ENERGY RESEARCH AND DEVELOPMENT ADMINISTRATION

Printed in the United States of America. Available from
the Energy Research and Development Administration,
Technical Information Center
P. O. Box 62, Oak Ridge, Tennessee 37830
Price: Printed Copy $~~5.00~~ 6.00; Microfiche $3.00

ORNL-5285
Dist. Category UC-79b, -k
(Liquid Metal Fast Breeder Reactors)

Contract No. W-7405-eng-26

METALS AND CERAMICS DIVISION

USE OF ULTIMATE TENSILE STRENGTH TO CORRELATE AND ESTIMATE CREEP AND CREEP-RUPTURE BEHAVIOR OF TYPES 304 AND 316 STAINLESS STEEL*

V. K. Sikka M. K. Booker C. R. Brinkman

Date Published: October 1977

OAK RIDGE NATIONAL LABORATORY
Oak Ridge, Tennessee 37830
operated by
UNION CARBIDE CORPORATION
for the
ENERGY RESEARCH AND DEVELOPMENT ADMINISTRATION

CONTENTS

USE OF ULTIMATE TENSILE STRENGTH TO CORRELATE AND ESTIMATE CREEP AND CREEP-RUPTURE BEHAVIOR OF TYPES 304 AND 316 STAINLESS STEEL*

V. K. Sikka, M. K. Booker, and C. R. Brinkman

ABSTRACT

Elevated-temperature tensile and creep properties of several heats of types 304 and 316 stainless steels were used to show that the short-term ultimate tensile strength of a given heat at the creep-test temperature and at a fixed strain rate can be used as an index for correlating and predicting creep and creep-rupture behavior. The short-term elevated-temperature ultimate tensile strength helps to account for changes in creep properties due to test temperature as well as due to heat-to-heat variations. Generalized models of time to rupture and minimum creep rate were defined in terms of stress, temperature and ultimate tensile strength.

Ultimate tensile strength was used in a creep equation to predict the strain-time behavior of individual heats. Several possible reasons are presented for the observed relationships between the short-term ultimate tensile strength and the long-term creep properties.

Design and materials engineering implications of the observed relationships between short-term elevated-temperature ultimate tensile strength and creep properties are also discussed.

1. INTRODUCTION

Types 304 and 316 stainless steel are prime structural steels for construction of many components of liquid-metal fast breeder nuclear reactors. These materials, even when purchased in accordance with ASTM material specifications, show wide variations in creep and creep-rupture properties (Figs. 1–3). Presented here are data from an ongoing program at Oak Ridge National Laboratory (ORNL) studying heat-to-heat variations in tensile and creep properties of types 304 and 316 stainless steels. For example, at a given stress and temperature, time to rupture (t_r) can vary by factors of 40–50. Orders of magnitude of variations are approximately the same for all test temperatures (Fig. 1). Moreover, for a given stress and temperature, $\dot{e}_m$ can vary by factors of 140–200. Large magnitudes of variations can be displayed by actual creep curves (Fig. 3).

In general, large variations in short-term creep data (rupture time of $<10^4$ hr) appear reduced in the long-term data (rupture times $>10^4$ hr). However, this is probably due to the relatively few data available for such long test times (Fig. 4).

Heat-to-heat variations for creep and creep-rupture properties of type 304 (Figs. 1–3) are also observed[1,2] in type 316 stainless steel. An analysis of such variations has been done by Sikka and Booker[2] for data collected from sources in the United States, Japan and Great Britain. That analysis showed that the variations in creep-rupture properties were smaller for type 316 than for type 304 stainless steel. It was also

*Work performed under ERDA/RDD 189a No. OHO50, Mechanical Properties for Structural Materials.

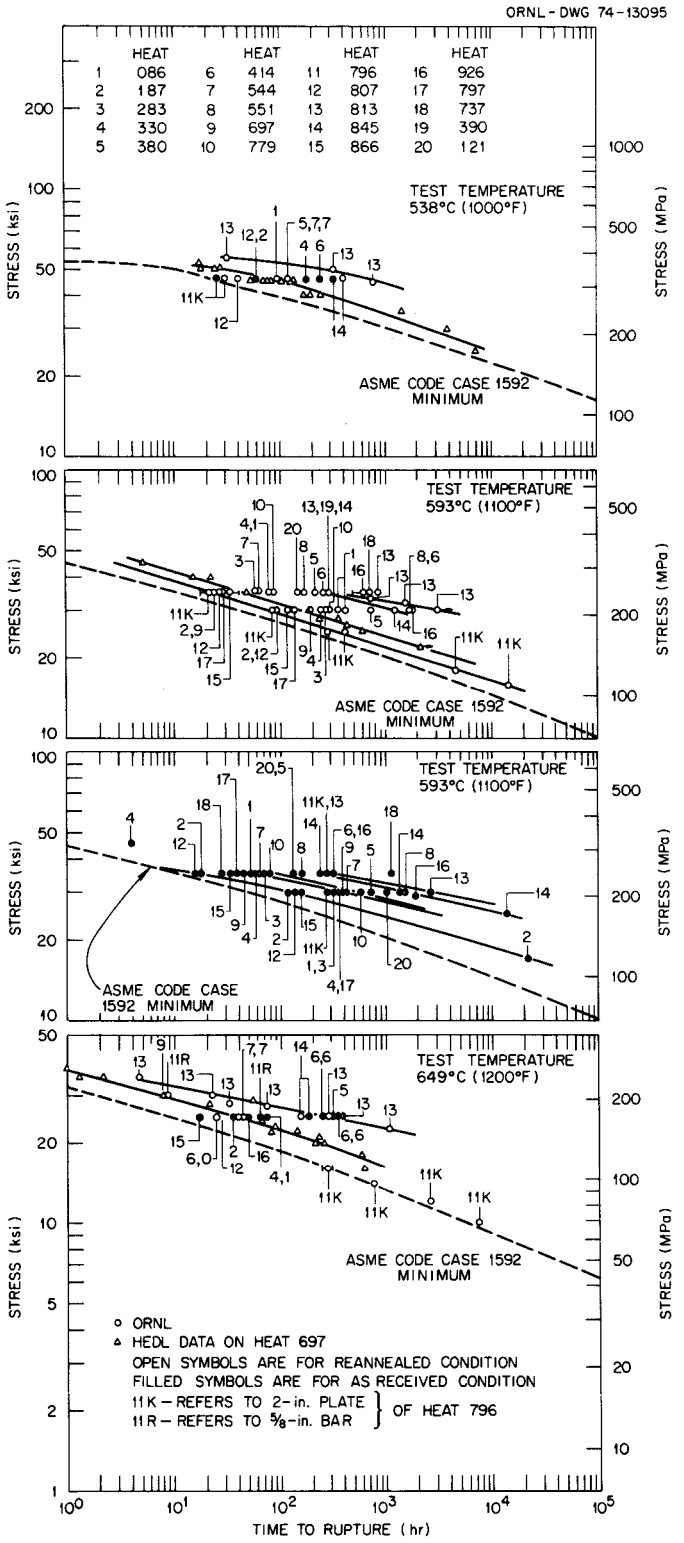

Fig. 1. Heat-to-Heat Variations in Stress-Rupture Data at 538, 593, and 649°C (1000, 1100, and 1200°F) for 20 Heats of Type 304 Stainless Steel in Both As-Received and Reannealed Conditions. ASME Code Case 1592 minimum value curves are included for comparison.

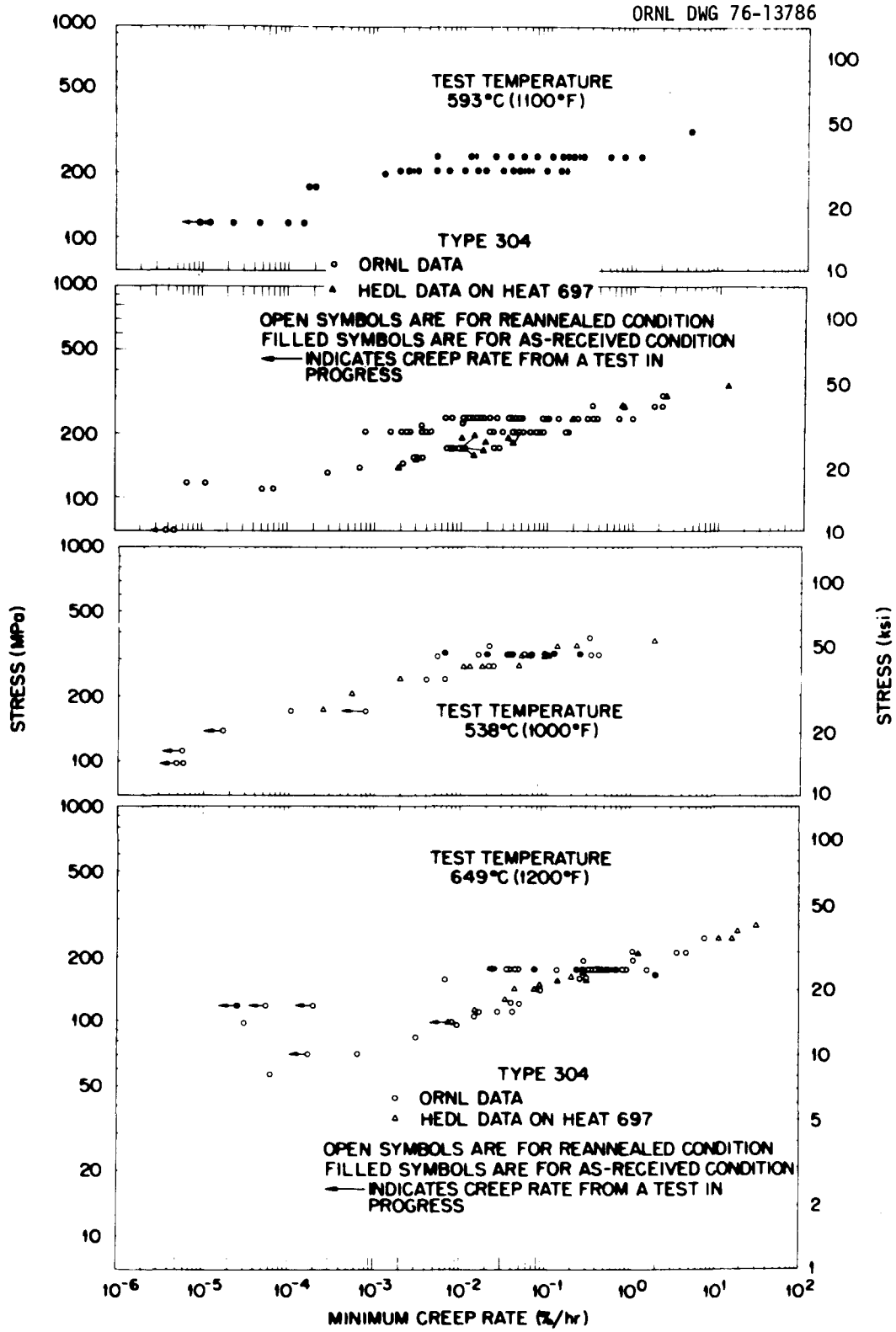

Fig. 2. Heat-to-Heat Variations in Minimum Creep-Rate Data at 538, 593, and 649°C (1000, 1100, and 1200°F) for 20 Heats of Type 304 Stainless Steel in Both the As-Received and Reannealed Conditions.

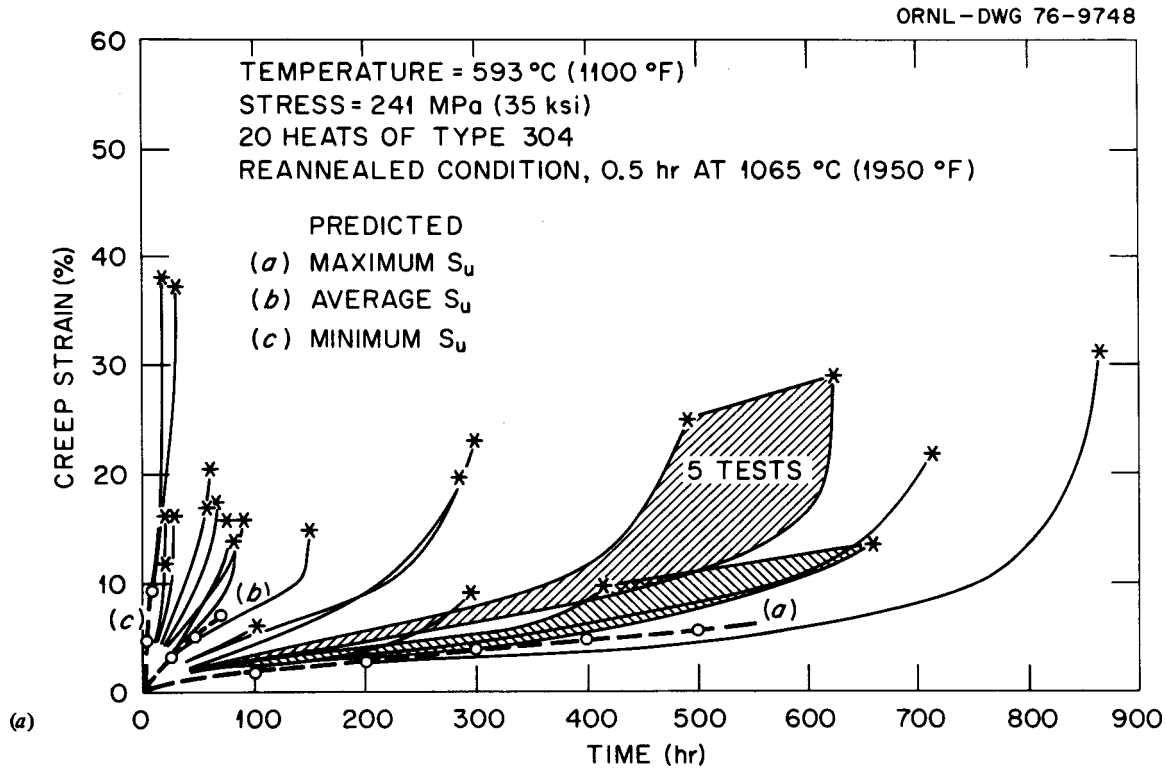

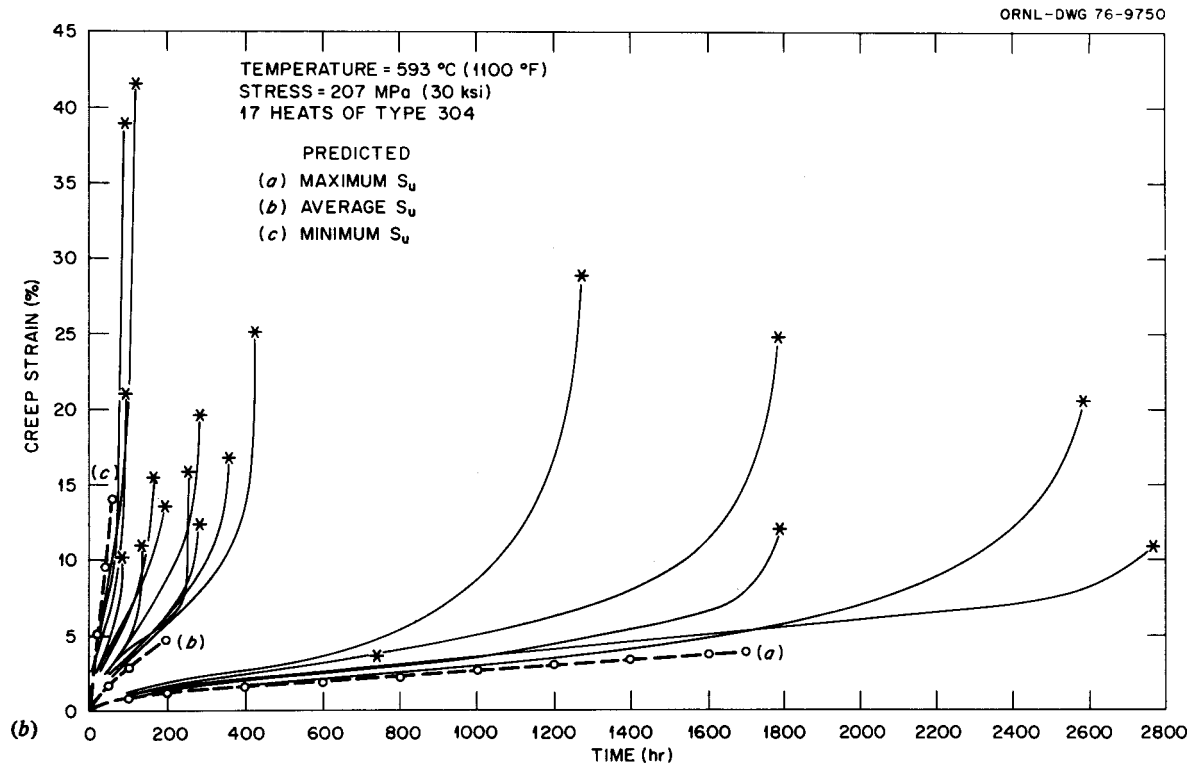

Fig. 3. Heat-to-Heat Variations in Creep Curves of Several Reannealed Heats of Type 304 Stainless Steel. (*a*) Creep tests at 241 MPa (35 ksi) and 593°C (1100°F). (*b*) Creep tests at 207 MPa (30 ksi) and 593°C (1100°F).

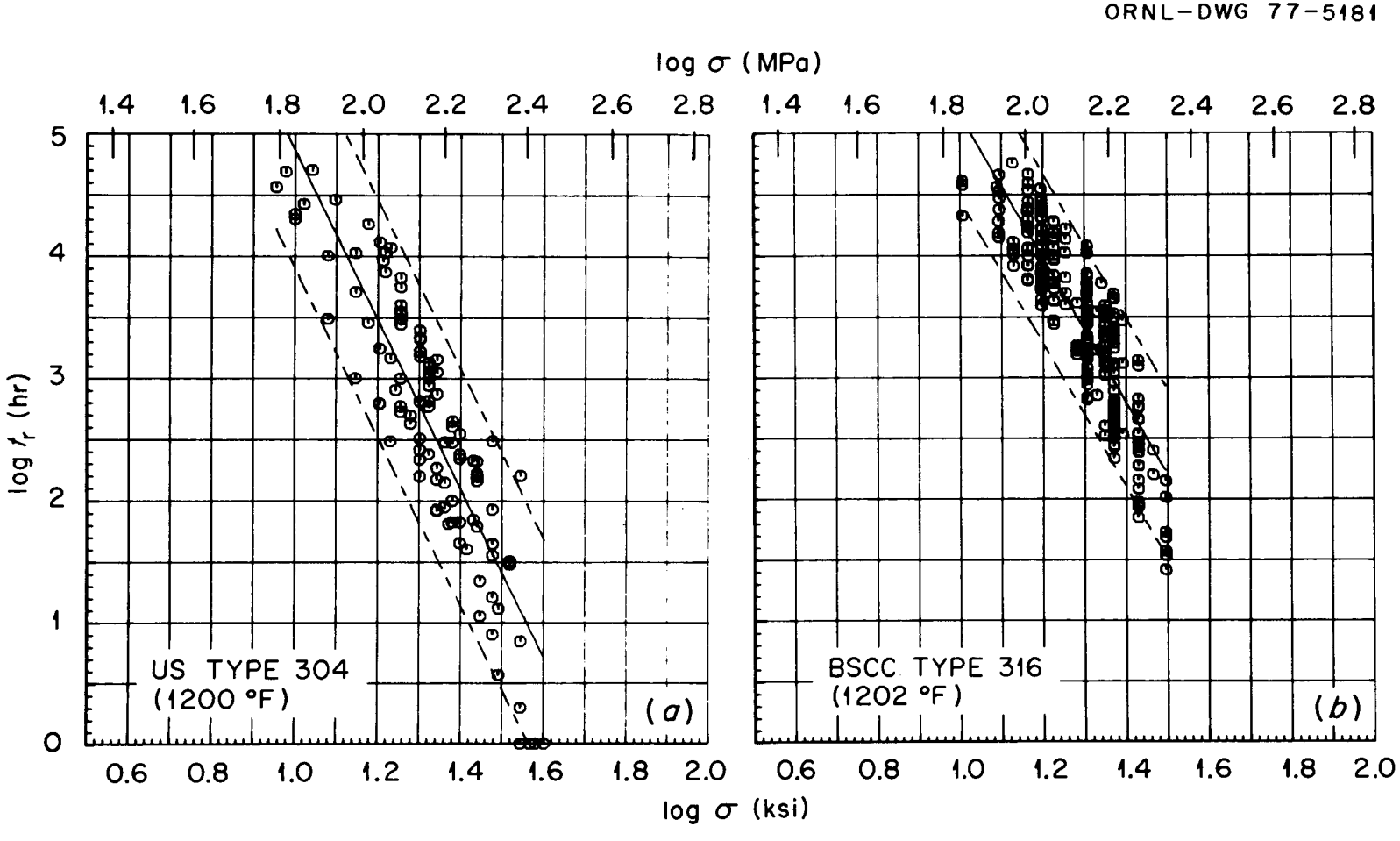

Fig. 4. Plots of Time to Rupture as a Function of Stress Illustrating the Uniformity of Heat-to-Heat Variations for Short- and Long-Term Data. (*a*) Type 304 and (*b*) type 316.

concluded from this study[2] that the 10^4-hr creep-rupture strengths of type 316 stainless steels, meeting ASTM material specifications, were essentially indistinguishable for tests done in the three different countries. However, the same could not be said for variations in properties of type 304 stainless steel.

It is important to understand the reasons for observed variations in elevated-temperature creep properties in order to effectively use these materials. Our investigation at ORNL seeks to understand and explain heat-to-heat variations in properties. One method for doing this is the micro- or chemical analysis and grain size method.

In this method a chemical analysis of various heats of types 304 and 316 stainless steel narrows down any systematic variations in strengthening elements, such as C, N, Nb, Ta, Ti, and B. Once the influence of a chemical element or elements responsible for heat-to-heat variations has been characterized, it may be possible to modify the material specifications. Progress has been made in this area and results will be presented in a forthcoming report.[3]

The micro- or chemical analysis method, although the most fundamental approach, may have some economic and technical disadvantages. The economic disadvantage is the expected increase in cost due to tighter control of specifications. The technical disadvantage is the difficulty of using correlations containing chemical analyses in design calculations. Therefore, more practical indices were needed to explain and relate heat-to-heat variations. Short-term elevated-temperature ultimate tensile strength is such an index.[4] This report will present the following:

1. review of the literature on the use of ultimate tensile strength to correlate and predict creep and creep-rupture properties,
2. stress-based correlations of creep and creep-rupture strength as a function of ultimate tensile strength,
3. time to rupture and minimum creep-rate modeling,
4. extension of models to time and strain to onset of tertiary creep via empirical relations,
5. a creep equation and associated isochronous stress-strain curves,
6. metallurgical considerations for observed relations between short- and long-term properties, and
7. implication of results in design and materials engineering applications.

2. LITERATURE REVIEW ON THE USE OF ULTIMATE TENSILE STRENGTH TO CORRELATE AND PREDICT CREEP AND CREEP-RUPTURE PROPERTIES

One of the first attempts to relate elevated-temperature short- and long-term properties was made by Bens,[5] who measured the hot-hardness at 871°C (1500°F) of a wide variety of chromium-base alloys for which the rupture times at that temperature were known. Although the scatter was considerable, the trend was evident: an increase in hot-hardness resulted in an increase in the short-term rupture life (data for rupture times of $\leqslant$2000 hr). Trends observed by Bens could be expressed as:

$$H = A \log t_r + B \ , \tag{1}$$

where

H = hot-hardness at the creep-test temperature,

t_r = time to rupture for a fixed stress, and

A and B are constants.

Bens concluded that the hardness of stable alloys at elevated temperatures appears to be a useful index of elevated-temperature strength.

A similar attempt to correlate hot-hardness with creep-rupture strength was made by Garofalo et al.[6] for carbon and 18 Cr-8Ni stainless steels. In this study hot-hardness at the creep temperature was plotted against the stress for rupture in 1, 100 and 1000 hr for carbon steels tested at 455°C (850°F) and stainless steels tested at 593, 704 and 815°C (1100, 1300 and 1500°F). They also plotted hot-hardness against the creep strength (stress to cause a creep rate of 1% in 10,000 hrs) of the same steels. This study showed a relationship between hot-hardness and the creep and creep-rupture strengths at elevated temperatures. Also Garofalo et al. suggested that the relation between hot-hardness and strength was *independent* of structure or temperature within the limits of their investigation. This same study showed a linear relationship between hot-hardness and ultimate tensile strength and suggested therefore that ultimate tensile strength and creep and creep-rupture strengths were related.

In a written discussion[6] of the work by Garofalo et al.,[6] Miller pointed out that they used the depth of penetration of the indentor at 649°C (1200°F) as a measure of hot-hardness. Their results showed that the ranking of the stress-rupture (10^4 hr) and the creep strength (1% in 10,000 hr) for several alloys [e.g., 7 Cu-14 Mo, 16 Cr-13 Ni-3 Mo, 18 Cr-8 Ni, 25 Cr-20 Ni, Croloy 2¼ (2¼ Cr-1 Mo), Croloy 5 (5 Cr-1 Mo) and Croloy 5 Si (5 Cr-1 Mo-Si) was consistent with the depth of the indention. Miller also referred to similar results by Soviet investigators.[7]

Underwood[8] suggested that if the hot-hardness of a particular alloy is known, one can determine not only the ultimate tensile strength but also the creep-rupture strength and the time to rupture at a given temperature.

The literature shows that Soviet investigators have spent considerable effort in developing relations between the short-term and long-term strength properties. For example, Novik and Klypin[9] investigated the relations between properties of various groups of heat-resistant alloys at room and elevated temperature and on the basis of these results suggested a relation between the ultimate tensile strength and creep strength. They correlated the data according to a linear relationship of the form:

$$y = a + bx \,, \tag{2}$$

where y is the predicted property (creep strength), and x is an easily determined characteristic of the alloy (e.g., ultimate tensile strength). It was concluded[9] that a linear relationship did exist between ultimate tensile strength and creep strength for test times up to 10,000 hr; but there was no linear relationship between short-term and 100,000-hr creep strength.

Krivenyuk[10] suggested that since variations in strength characteristics are often associated with variations in ductility characteristics, it is useful to consider the relationship between S_u and S_r^t in a more general form:

$$f(S_u)\, f(\delta, \psi, \zeta) = p \sim S_r^t \,, \tag{3}$$

where

δ = relative elongation after fracture,
ψ = reduction of area,
ζ = impact strength, and
$p \sim S_r^t$ = long-time creep-rupture strengths.

Sherby and Dorn[11] showed a correlation between creep and tensile data for binary alpha solid solutions of magnesium, copper, germanium, zinc and silver in aluminum based on the Zener-Holloman relationship:

$$\sigma \equiv \sigma(\dot{e}_m e^{\Delta H/RT}), \tag{4}$$

where

σ = creep stress or ultimate tensile strength,
ΔH = activation energy, and
$\dot{e}_m$ = minimum creep rate or tensile strain rate.

It was shown[11] that a similar substracture developed at the same value of the Zener-Holloman parameter ($\dot{e}_m e^{\Delta H/RT}$), at least for creep and tensile data for pure aluminum and its dilute alloys at high temperatures. The correlation between creep and tensile data was observed only for temperatures in excess of about 127°C (261°F) or 0.43 T_m, where recovery phenomena became important. The authors suggested that at lower temperatures the more complex phenomenon associated with strain hardening invalidates the use of the Zener-Holloman equation.

The results of the above studies tend to show a relationship between hot-hardness or hot-tensile strength and creep and creep-rupture properties. In all studies, short-term tensile and creep and creep-rupture properties were measured at the same test temperature. For 2¼ Cr-1 Mo steel, room-temperature ultimate tensile strength has been correlated[12–14] with corresponding increases in creep-rupture strength. Minimum creep rate has been expressed as a function of stress, temperature, and room-temperature ultimate tensile strength for this material.[15]

To summarize, several attempts have been made in the past to correlate short-term tensile properties with long-term creep properties. The Soviet work[9,10] was more elaborate since they looked at correlations for many different materials. However, that work differed from the American work in that a linear relationship between the two types of properties was used by the former as opposed to an exponential reationship used by the latter.[4]

3. DATA

The creep and tensile data used here were obtained primarily from the heat-to-heat variations program[1,16,17] at ORNL. Additional data were obtained from the literature[18,19] (Tables A1–A6). The ORNL tensile and creep data were on 20 heats of type 304 and 7 heats of type 316 stainless steel. The ultimate tensile strength values for each heat were measured at the creep-test temperature and a nominal strain rate of 6.7×10^{-4} per sec.

4. RESULTS

4.1 STRESS-BASED CORRELATIONS

Log $\dot{e}_m$ and log t_r are plotted against S_u for ORNL data on up to 20 heats of type 304 stainless steel (Figs. 5–7). Figure 8 shows a similar plot for ORNL data on 7 heats of type 316 stainless steel. The S_u values in these plots were obtained at the creep-test temperature. Although scatter is considerable, the trend shows that for a fixed stress and temperature, $\dot{e}_m$ decreases and t_r increases with increasing S_u. The lines shown in these figures are from the ultimate tensile strength model described in Sect. 4.2.

Creep-rupture strength, $S_r{}^t$ (10^3, 10^4 and 10^5 hr) was a function of S_u for ORNL data and data from the literature[18,19] for several heats of types 304 and 316 stainless steels (Figs. 9 and 10). These data were for several test temperatures in the range of 538–816°C (1000–1500°F) as opposed to data shown for a single test temperature (Figs. 5–8). Similar plots for creep strength ($S_{1\%}{}^t$) of types 304 and 316 stainless steels (Figs. 11 and 12) show that $S_r{}^t$ and $S_{1\%}{}^t$ can be represented by the following equations:

$$S_r{}^t = \alpha \exp(\beta S_u) , \tag{5}$$

and

$$S_{1\%}{}^t = \alpha_1 \exp(\beta_1 S_u) . \tag{6}$$

The constants α, α_1, and β and β_1 were determined by the method of least squares (Tables 1 and 2). Equations (5) and (6) are independent of test temperatures, although α and α_1 depend on test time and relate to β and β_1. Equations (5) and (6) are similar to Eq. (1) from Bens.[5] Furthermore, these equations are consistent with suggestions made by Garofalo et al.[6] that the relationships between ultimate tensile strength, creep, and creep-rupture strength were independent of structure or temperature.

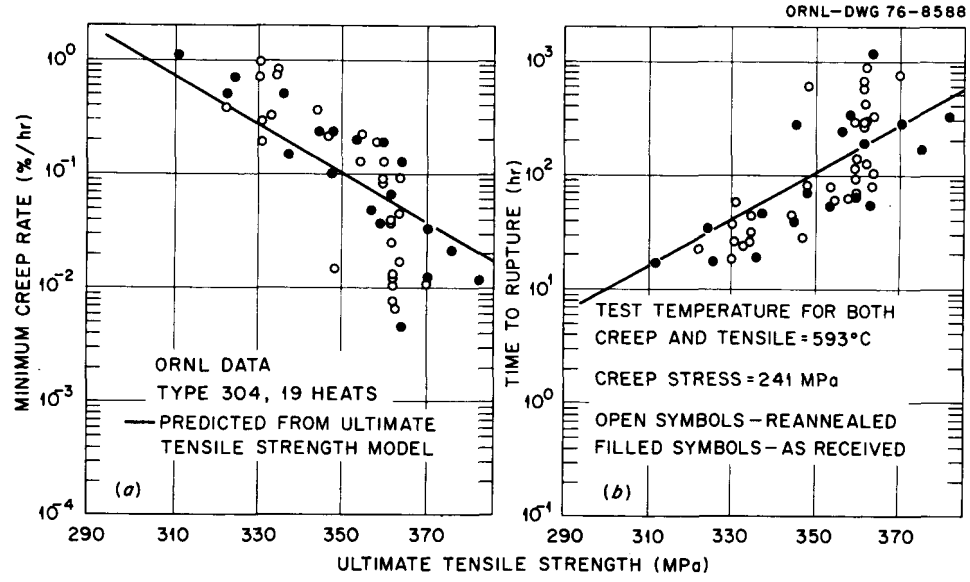

Fig. 5. Comparison of Experimental Minimum Creep Rate and Time to Rupture as a Function of Elevated-Temperature Ultimate Tensile Strength (S_u) with Values Predicted from Rupture Model with S_u for Different Heats of Type 304 Stainless. Tests were at 593°C (1100°F) and 241 MPa (ksi).

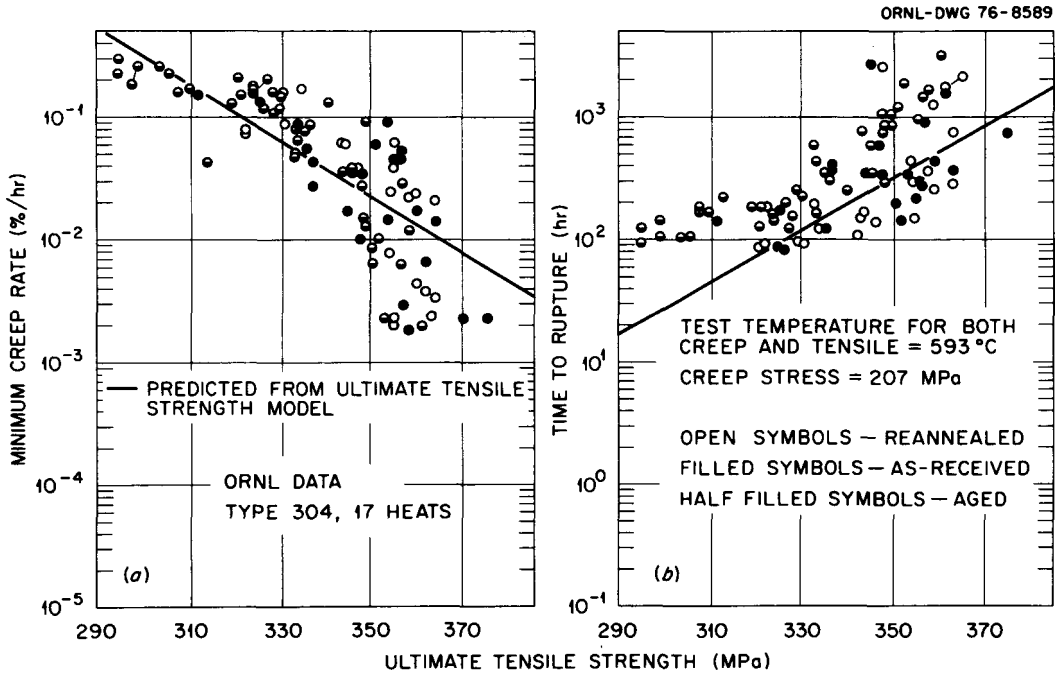

Fig. 6. Comparison of Experimental Minimum Creep Rate and Time to Rupture as a Function of Elevated-Temperature Ultimate Tensile Strength (S_u) with Values Predicted from Rupture Model with S_u for Different Heats of Type 304 Stainless. Tests were made at 593°C (1100°F) and 207 MPa (30 ksi).

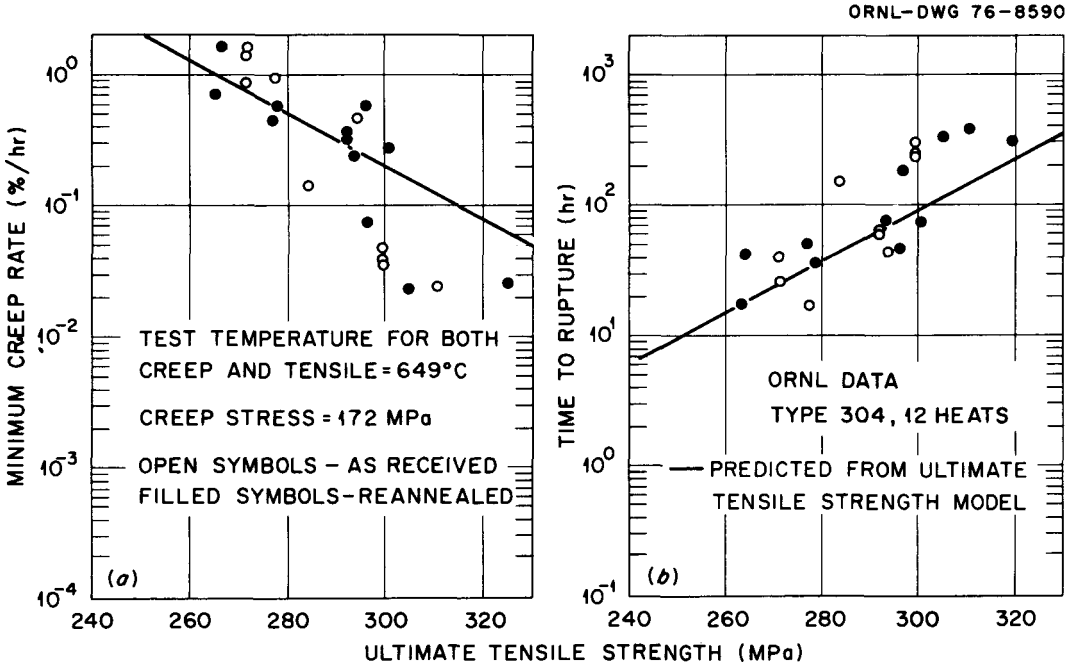

Fig. 7. Comparison of Experimental Minimum Creep Rate and Time to Rupture as a Function of Elevated-Temperature Ultimate Tensile Strength (S_u) with Values Predicted from Rupture Model with S_u for Different Heats of Type 304 Stainless. Tests were made at 649°C (1200°F) and 172 MPa (25 ksi)

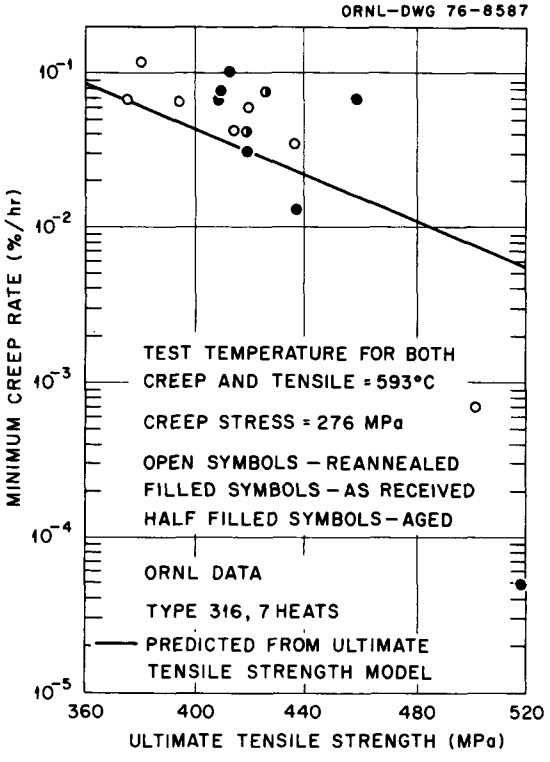

Fig. 8. Comparison of Experimental Minimum Creep Rate as a Function of Elevated-Temperature Ultimate Tensile Strength (S_u) with Values Predicted from Rupture Model with S_u for Different Heats of Type 316 Stainless. Tests were at 593°C (1100°F) and 276 MPa (40 ksi).

Results (Figs. 5–12) have shown clearly that the changes in the short-term elevated-temperature ultimate tensile strength indicate trends in creep properties that result from both the temperature and heat-to-heat variations. Therefore, S_u should be useful for predicting the differences among the weak and strong heats (Fig. 13). Plots in this figure were made according to both the conventional and S_u modified power law for both the ORNL data and data from the literature.[18,19] The conventional power law expression is:

$$t_r = A_r S^{-n_r} , \tag{7}$$

where

n_r = stress exponent, and

A_r = structure constant.

The S_u modified power law expression is:

$$t_r = A_r^* S^{*-n_r^*} = A_r^* \left[S \exp(-\beta S_u)\right]^{-n_r^*} , \tag{8}$$

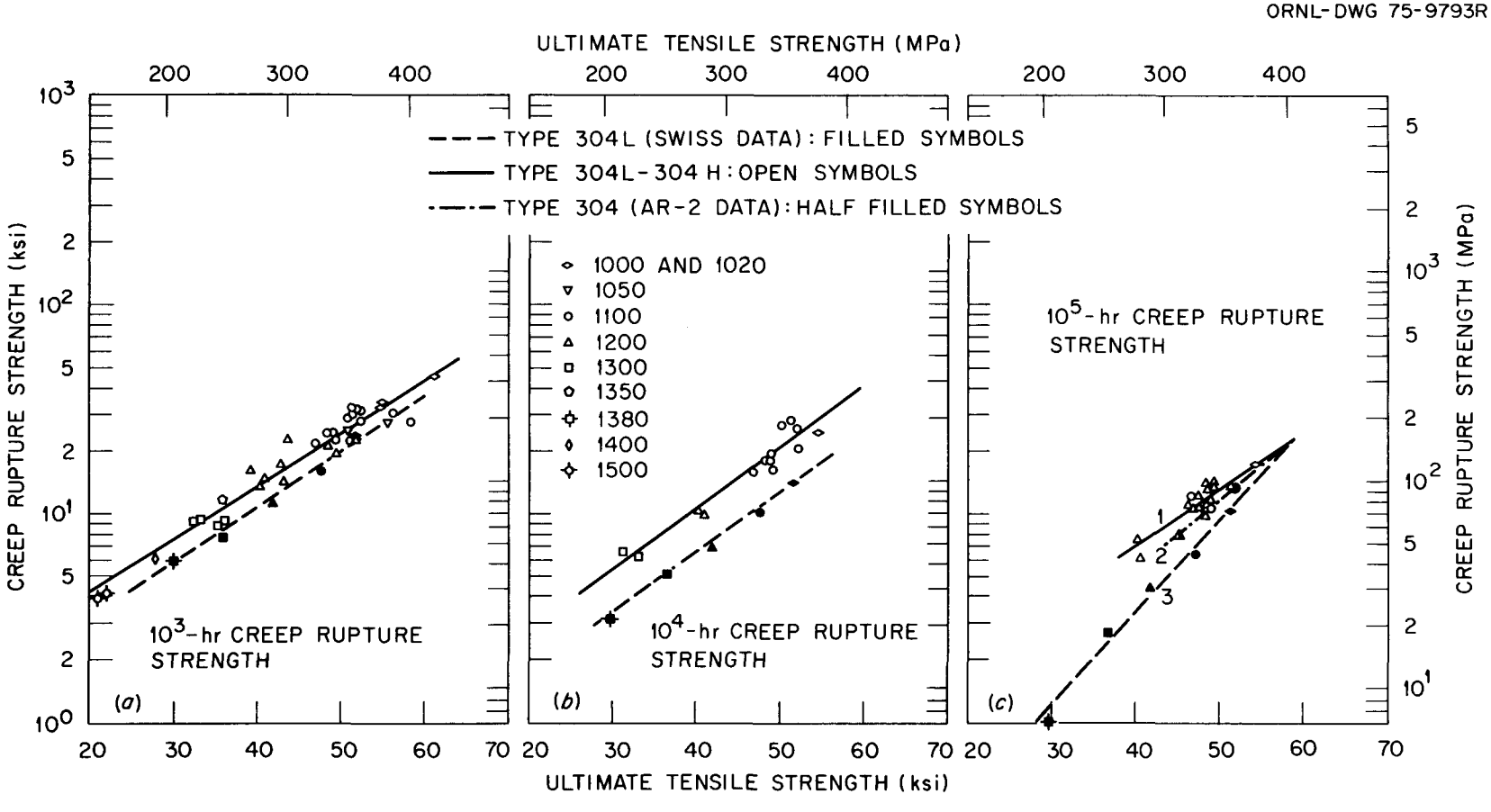

Fig. 9. Creep-Rupture Strength as a Function of Ultimate Tensile Strength at the Creep-Test Temperature for Various Heats and Variations of Type 304 Stainless Steel. (*a*) 10^3 hr. (*b*) 10^4 hr. (*c*) 10^5 hr. Lines 1, 2, and 3 in (*c*) represent extrapolated values from 10,000 to 20,000 hr, from 50,000 to 60,000 hr, and nonextrapolated data respectively. In °C the temperatures listed are 538, 549, 566, 593, 649, 704, 732, 749, 760, and 816.

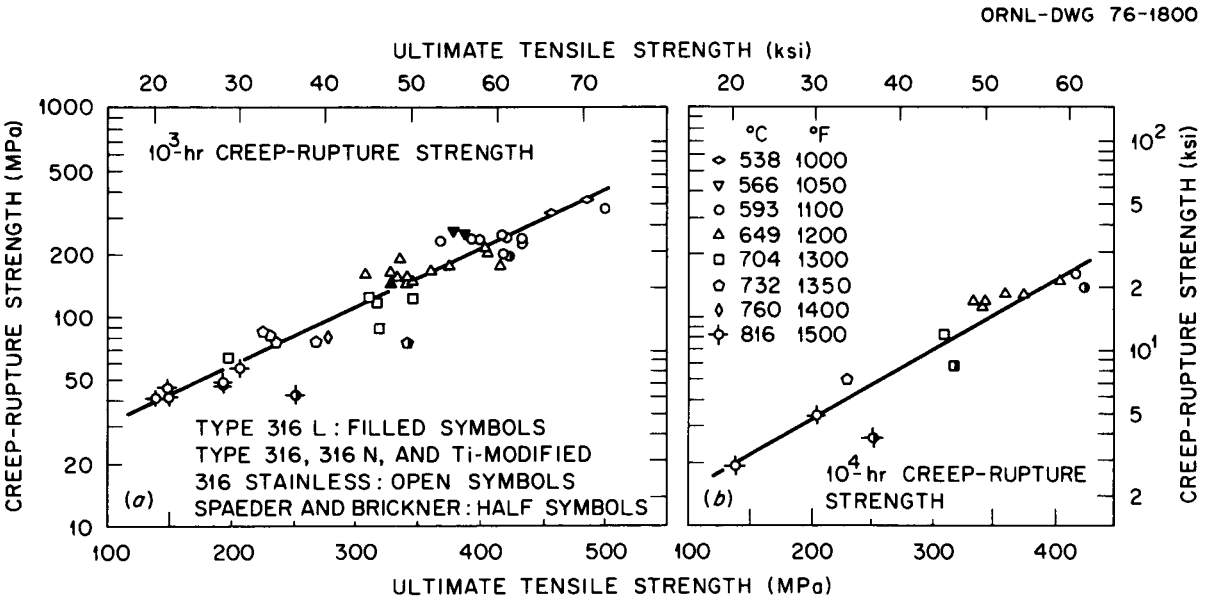

Fig. 10. Creep-Rupture Strength as a Function of Ultimate Tensile Strength at the Creep-Test Temperature for Various Heats of Type 316 Stainless Steel. (*a*) 10^3 hr. (*b*) 10^4 hr.

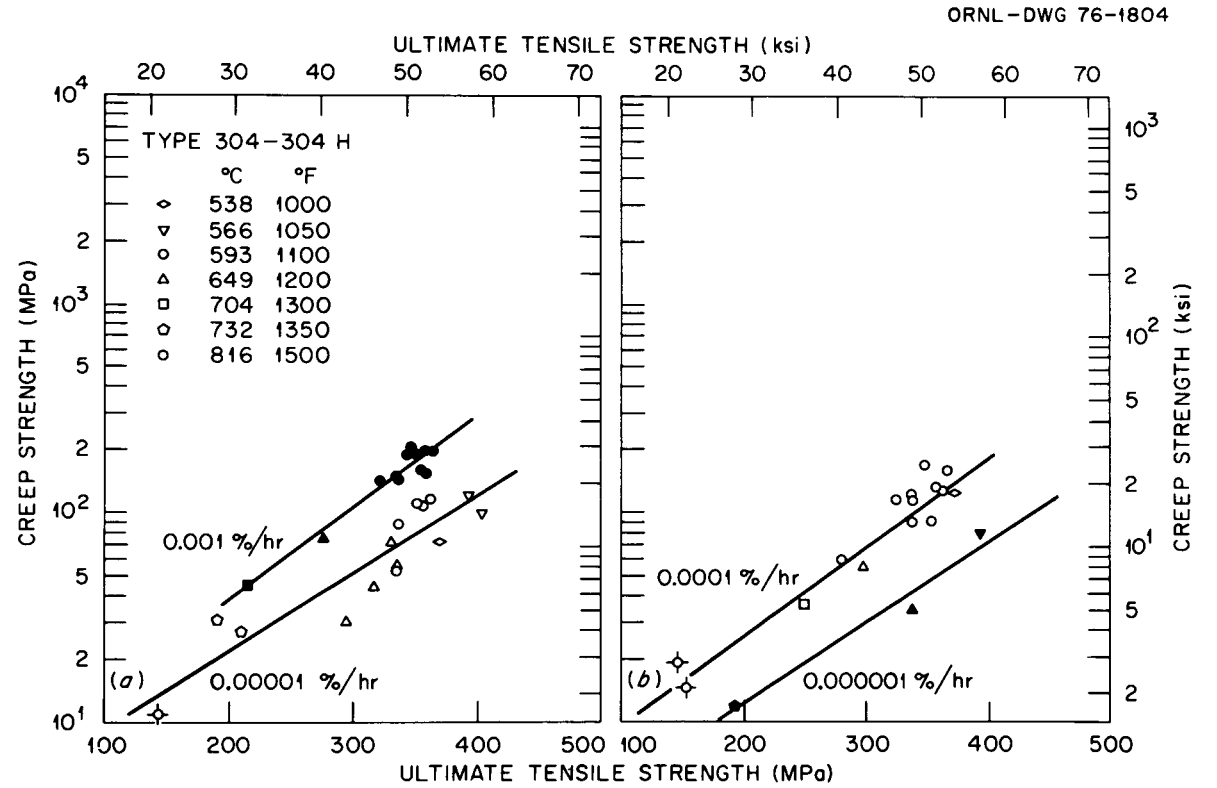

Fig. 11. Creep Strength as a Function of Ultimate Tensile Strength at the Creep-Test Temperature for Various Heats and Variations of Type 304 Stainless Steel. (*a*) 0.001%/hr and 0.00001%/hr. (*b*) 0.0001%/hr and 0.000001%/hr.

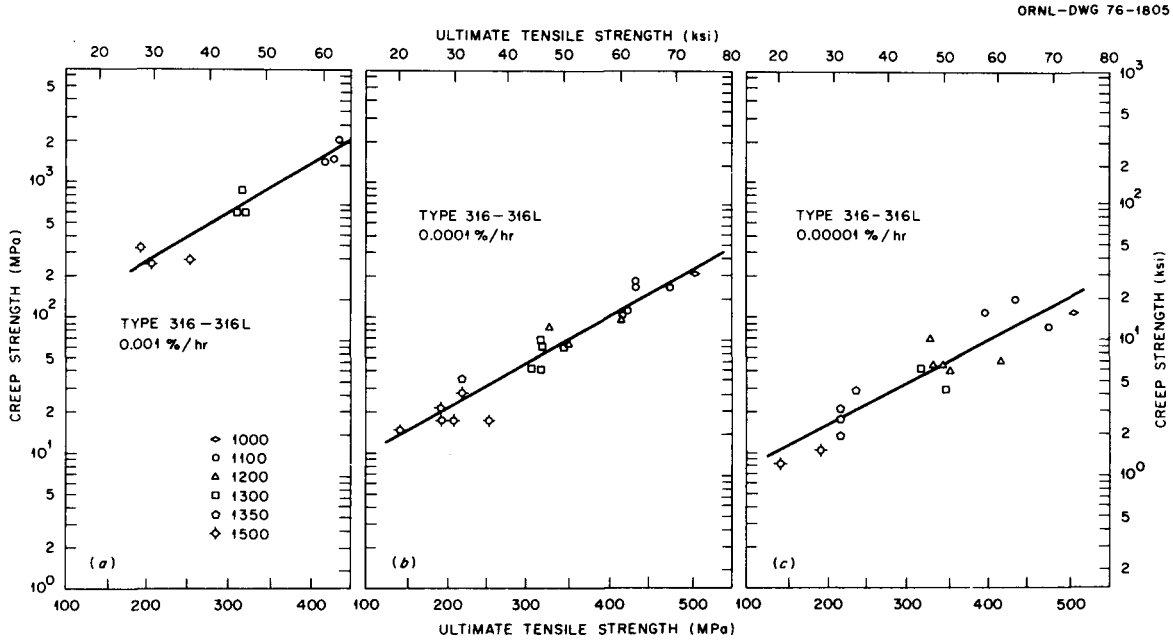

Fig. 12. Creep Strength as a Function of Ultimate Tensile Strength at the Creep-Test Temperature for Various Heats and Variations of Type 316 Stainless Steel. (*a*) 0.001%/hr. (*b*) 0.0001%/hr. (*c*) 0.00001%/hr.

Table 1. Creep-rupture-strength constants in equation $S_R^t = \alpha \exp(\beta S_u)$ for several austenitic stainless steels

Stainless steel type	Number of data points	Temperature range (°C)	Temperature range (°F)	Constants[a] α (ksi)	Constants[a] β(1/ksi)
		10^3-hr rupture strength			
304, 304L, 304H, 304N	38	538–816	1000–1500	1.3198	0.05807
304L[b]	5	550–750	1020–1380	0.9088	0.06111
316L, 316N, 316 (Ti modified)	45	538–816	1000–1500	2.3761	0.04352
347, 347L	23	538–816	1000–1500	1.9154	0.05151
347[b]	5	550–750	1020–1380	0.2439	0.08335
321	21	566–816	1050–1500	1.4670	0.05720
201, 202, 303	7	538–816	1000–1500	1.6753	0.04980
		10^4-hr rupture strength			
304, 304L, 304H, 304N	14	538–704	1000–1300	0.6919	0.06774
304L[b]	5	550–750	1020–1380	0.4449	0.06680
316L, 316N	14	593–816	1100–1500	0.9753	0.05330
347, 347L	13	566–732	1050–1350	0.8981	0.06001
347[b]	5	550–750	1020–1380	0.0536	0.09961
321	9	566–732	1050–1350	1.4942	0.05413
201, 202, 303	5	566–816	1050–1500	0.3999	0.07004
		10^5-hr rupture strength			
304, 304H[c]	19	538–704	1000–1300	0.5745	0.06224
304[d]	2	593–649	1100–1200	0.2558	0.07634
304L[b]	5	550–750	1020–1320	0.0596	0.10055
347[c]	2	593–649	1100–1200	1.8965	0.03958
347[b]	5	550–750	1020–1380	0.0131	0.11110
201[c]	3	566–732	1050–1350	0.0392	0.10705

[a] To convert to MPa, multiply α and divide β by 6.895.

[b] Creep-rupture strength was from 11 years of creep testing, but tensile-strength values were obtained by multiplying average room-temperature value listed by Smith with his tensile-strength ratio.

[c] Creep-rupture strength obtained by extrapolation.

[d] AR-2 data extrapolated from test times of 50,000 to 65,000 hr.

Table 2. Creep-strength constants in equation $S_R^t = \alpha \exp(\beta S_u)$ for several austenitic stainless steels

Stainless steel type	Number of data points	Temperature range (°C)	Temperature range (°F)	Constants α_1 (ksi)	Constants α_1 (MPa)	Constants β_1 (1/ksi)	Constants β_1 (1/MPa)
0.001%/hr creep strength							
304[a]	12	593–704	1100–1300	0.7498	5.1697	0.06917	0.010032
316[a]	9	593–816	1100–1500	0.7149	4.9291	0.05689	0.008251
347	3	593–816	1100–1500	0.4235	2.9199	0.07344	0.010652
321	4	593–816	1100–1500	0.4066	2.8034	0.08020	0.011632
0.0001%/hr creep strength							
304	15	593–816	1100–1500	0.5272	3.6349	0.06698	0.009715
316	21	538–816	1000–1500	0.6686	4.5823	0.05304	0.007693
347	12	593–816	1100–1500	0.6949	4.7912	0.06232	0.009039
321	11	565–816	1050–1500	0.1323	0.9122	0.09963	0.014450
0.00001%/hr creep strength							
304	15	538–816	1000–1500	0.6032	4.1589	0.05753	0.008344
316	17	538–816	1000–1500	0.5408	3.7287	0.04913	0.007126
347	14	538–816	1000–1500	0.3579	2.4676	0.06966	0.010103
321	4	565–649	1050–1500	0.4295	2.9613	0.06813	0.009881
0.000001%/hr creep strength							
304	3	565–732	1050–1350	0.2971	2.0484	0.06120	0.008876

[a]Including modification with controlled carbon or titanium.

where:

$n_r^* = S_u$ modified stress exponent,

$S^* = S_u$ modified stress $= S \exp(-\beta S_u)$, and

$A_r^* = S_u$ modified constant.

Based on Fig. 4 and Table 1, a value of 0.05 was selected for β for plots in Fig. 13 and modified constants summarized in Table 3. The improvement in fit to the data by S_u modification of stress is reflected in the values of the standard error of estimate (SEE) and the coefficient of determination (R^2). The S_u modification of stress significantly improves the correlation at test temperatures of 593 and 649°C (1100 and 1200°F) (Fig. 13 and Table 3). These are the two temperatures at which most data was taken. At other temperatures, little effect can be observed by modifying the stress. The lack of improvement by S_u for a small number of data points from several sources is thought to occur as a result of ultimate tensile strength values reported at different strain rates.

Equations (5) and (6), along with their constants (Table 1 and 2; Figs. 9–12) can be used to estimate the creep or creep-rupture strength of a given heat from known values of its elevated-temperature ultimate tensile strength at a strain rate of 6.67×10^{-4} per sec. Equation (8) along with its constants (Table 3, or Fig. 13) can be used to estimate the time to rupture of a given heat from known value of its elevated-temperature ultimate tensile strength.

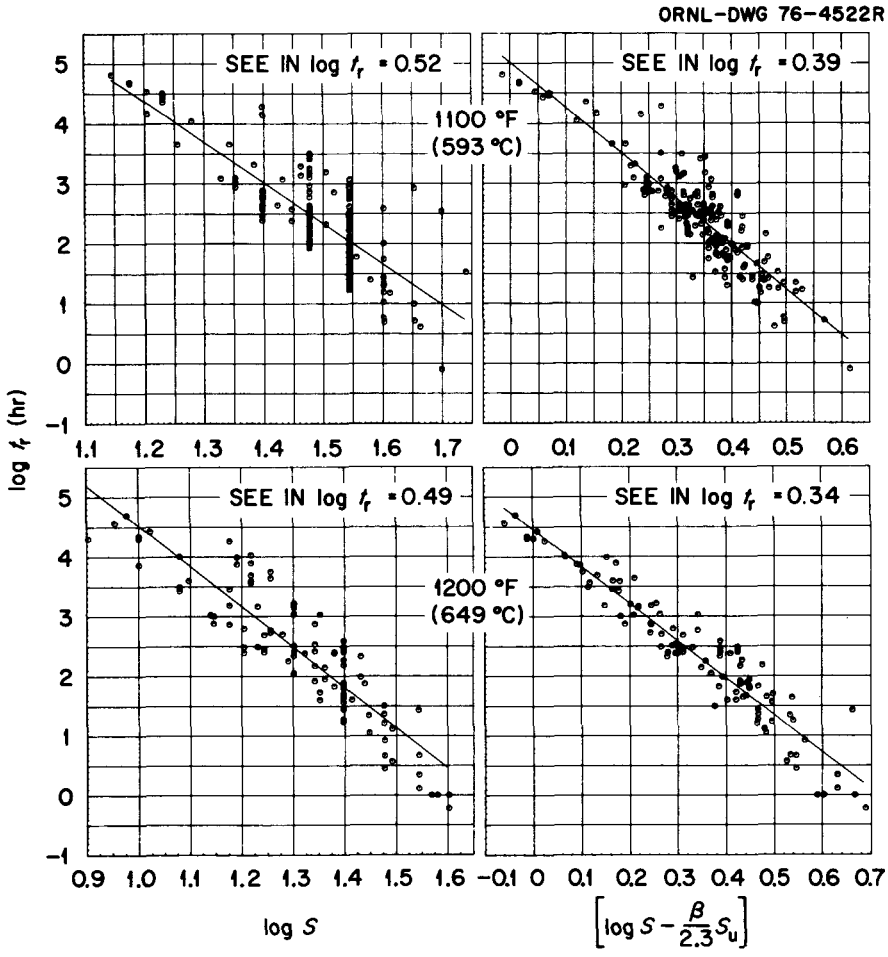

Fig. 13. Plots of log t_r as a Function of log S and log $S - \beta S_u$ for ORNL Data on 20 Heats of Type 304 Stainless Steel. The top two plots are for 593°C and the bottom are for 649°C. There is an improvement in the standard error of estimate (SEE) from 0.52 to 0.39 in log t_r at 593°C and from 0.49 to 0.34 for 649°C.

Table 3. Constants[a] showing decreases in scatter obtained by ultimate tensile-strength modified power law

Test temperature (°C)	Test temperature (°F)	Number of data points	n_r	n_r*	R^2 (%) Conventional	R^2 (%) Modified	Standard error of estimate, log t_r Conventional[b]	Standard error of estimate, log t_r Modified[c]	A_r	A_r*
538	1000	25	8.54	8.50	93.90	94.96	0.178	0.161	100×10^{16}	2.74×10^5
565	1050	8	7.20	6.16	78.96	66.67	0.388	0.489	1.80×10^{14}	4.85×10^4
593	1100	181	6.76	7.56	62.40	79.00	0.517	0.387	3.05×10^{12}	1.03×10^5
649	1200	107	6.76	6.22	80.60	91.00	0.495	0.338	1.90×10^{11}	2.85×10^4
704	1300	21	6.36	6.90	97.54	95.0	0.168	0.239	1.61×10^9	4.26×10^4
732	1350	15	6.28	5.71	90.11	88.1	0.277	0.304	3.20×10^9	7.29×10^4
760	1400	16	5.91	5.78	97.54	96.21	0.194	0.241	5.52×10^7	1.44×10^4
816	1500	8	6.54	6.56	93.91	93.05	0.357	0.381	2.01×10^7	1.70×10^4

[a] Based on ORNL and literature data for type 304 stainless steel.

[b] $t_r = A_r S^{-n_r}$, S in ksi.

[c] $t_r = A_r^* S^{*-n_r^*} = A_r^* [S \exp(-\beta S_u)]^{-n_r^*}$, $\beta = 0.05$, and S_u = ultimate tensile strength at the creep-test temperature. S and S_u in ksi.

4.2 TIME TO RUPTURE (t_r) AND MINIMUM CREEP-RATE ($\dot{e}_m$) MODELING

Although Eqs. (5), (6), and (8) have shown the usefulness of the ultimate tensile strength in correlating and predicting creep properties, a generalized model was needed for t_r and $\dot{e}_m$ in terms of S, T, and S_u. The generalized model development was restricted to ORNL and Blackburn[19] data because these were the only data for which S_u values were known at the creep-test temperature and at a single strain rate of 6.67×10^{-4} per sec. The available t_r and $\dot{e}_m$ data (205 and 226 points) from these two sources were subjected to an analysis using a generalized set of algebraic models for $\log t_r$ and $\log \dot{e}_m$ as a function of S, T, and S_u (ref. 20). The final choice of models was based on:

1. least squares fit to the entire set of data,
2. prediction of long time ($t_r > 2000$ hr) or low rate ($\dot{e}_m < 0.001\%$ per hr) data from fits to short-time or high-rate data, and
3. simplicity and physical reasonableness of the models.

The final models chosen for type 304 stainless steel were:

$$\log t_r = 5.716 - 3915\frac{\log S}{T} + 32.60\frac{S_u}{T} - 0.007303\, S_u \log S\,, \tag{9}$$

and

$$\log \dot{e}_m = -2.765 + 3346\frac{\log S}{T} - 51.84\frac{S_u}{T} + 0.01616\, S_u \log S\,, \tag{10}$$

with S and S_u in MPa and T in K. Equations (9) and (10) are of the same form, both being linear in $\log S - \log t_r$ and $\log S - \log \dot{e}_m$. The analysis of the same t_r and $\dot{e}_m$ data showed[20] that for models not containing an S_u term, the properties could be represented by:

$$\log t_r = -7.889 - 2.395 \log S - 0.00866\, S + 15324/T\,, \tag{11}$$

and

$$\log \dot{e}_m = 15.42 + 3.542 \log S + 0.011199\, S - 23882/T\,, \tag{12}$$

with S in MPa and T in K.

Figure 14 illustrates two plots of predicted versus experimental values of t_r and $\dot{e}_m$ from the models both with and without S_u terms (Eqs. 9–12). The improvement in prediction by models with S_u is clearly reflected by the observed increases in the values of R^2 and SEE for ORNL data on 20 heats of type 304 stainless steel (Table 4).

For type 316 stainless steel there were 132 t_r and 102 $\dot{e}_m$ data points available in the literature[18,19] for which elevated-temperature S_u values were specified. If those tests were run in accordance with ASTM specifications, the strain rate should be 6.67×10^{-4} per sec. These data, when

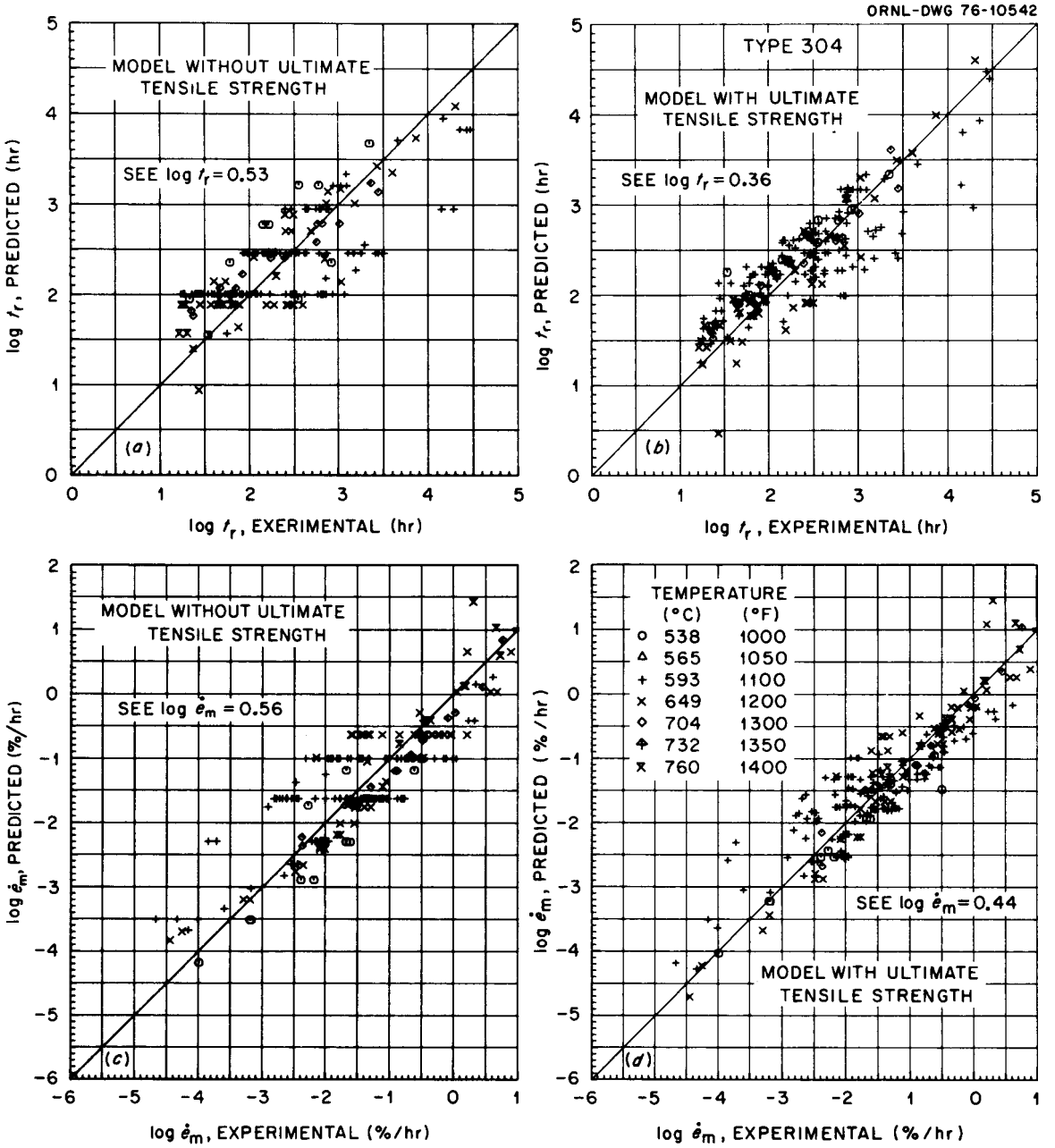

Fig. 14. Comparison of Experimental Time to Rupture and Minimum Creep Rate with Predicted Results from Models With and Without Ultimate Tensile Strength for 20 Heats of Type 304 Stainless Steel.

Table 4. Coefficients of determination (R^2) and standard errors of estimate (SEE) for ORNL data on type 304 and literature data on type 316 stainless steel

Model	Data points	Property	R^2 (%)	SEE ($\log t_r$) and ($\log \dot{e}_m$)
		Type 304		
Without S_u, Eq. (11)	205	t_r	56.19	0.53
With S_u, Eq. (9)	205	t_r	73.37	0.36
Without S_u, Eq. (12)	226	$\dot{e}_m$	73.84	0.56
With S_u, Eq. (10)	226	$\dot{e}_m$	83.67	0.44
		Type 316		
Without S_u, Eq. (13)	132	t_r	88.16	0.29
With S_u, Eq. (14)	132	t_r	91.4	0.25
Without S_u, Eq. (15)	102	$\dot{e}_m$	91.4	0.47
With S_u, Eq. (16)	102	$\dot{e}_m$	94.6	0.37

analyzed similarly to those used for type 304[20] showed that for t_r the optimum models (with and without S_u) were not different in a statistical sense. These models were:

$$\log t_r = -7.801 - 3.047 \log S - 0.009098\, S + \frac{17565}{T} \quad , \tag{13}$$

and

$$\log t_r = -5.138 - 2.181 \log S + \frac{13768}{T} - \frac{3771\, S}{T S_u} \quad , \tag{14}$$

where S and S_u were in MPa and T was in K. The values of R^2 and SEE for the models in Eqs. (13) and (14) are included in Table 4.

However, for $\dot{e}_m$ data, where heat-to-heat variations were almost twice as large as those observed for t_r, the following relations were found in terms of S, T, and S, T, and S_u:

$$\log \dot{e}_m = 9.6223 + 4.592 \log S + 0.00725\, S - \frac{21120}{T} \quad , \tag{15}$$

and

$$\log \dot{e}_m = -3.534 + 2.0734 \log S - 45.064 \frac{S_u}{T} + 0.01836\, S_u \log S \quad , \tag{16}$$

with S and S_u in MPa and T in K. These equations were derived from 102 data points; corresponding values of R^2 and SEE are included in Table 4. The values for R^2 increased (improved) from 91.4 to 94% and SEE in log $\dot{e}_m$ from 0.47 to 0.37 for the model with S_u, Eq. (16) (Table 4). Therefore, including S_u in the calculations will decrease the scatter resulting from heat-to-heat variations of type 316 stainless steel. Fig. 15 shows the plots of predicted versus experimental values of t_r and $\dot{e}_m$ for type 316 from the models both with and without S_u (Eqs. 13, 14, 15, and 16).

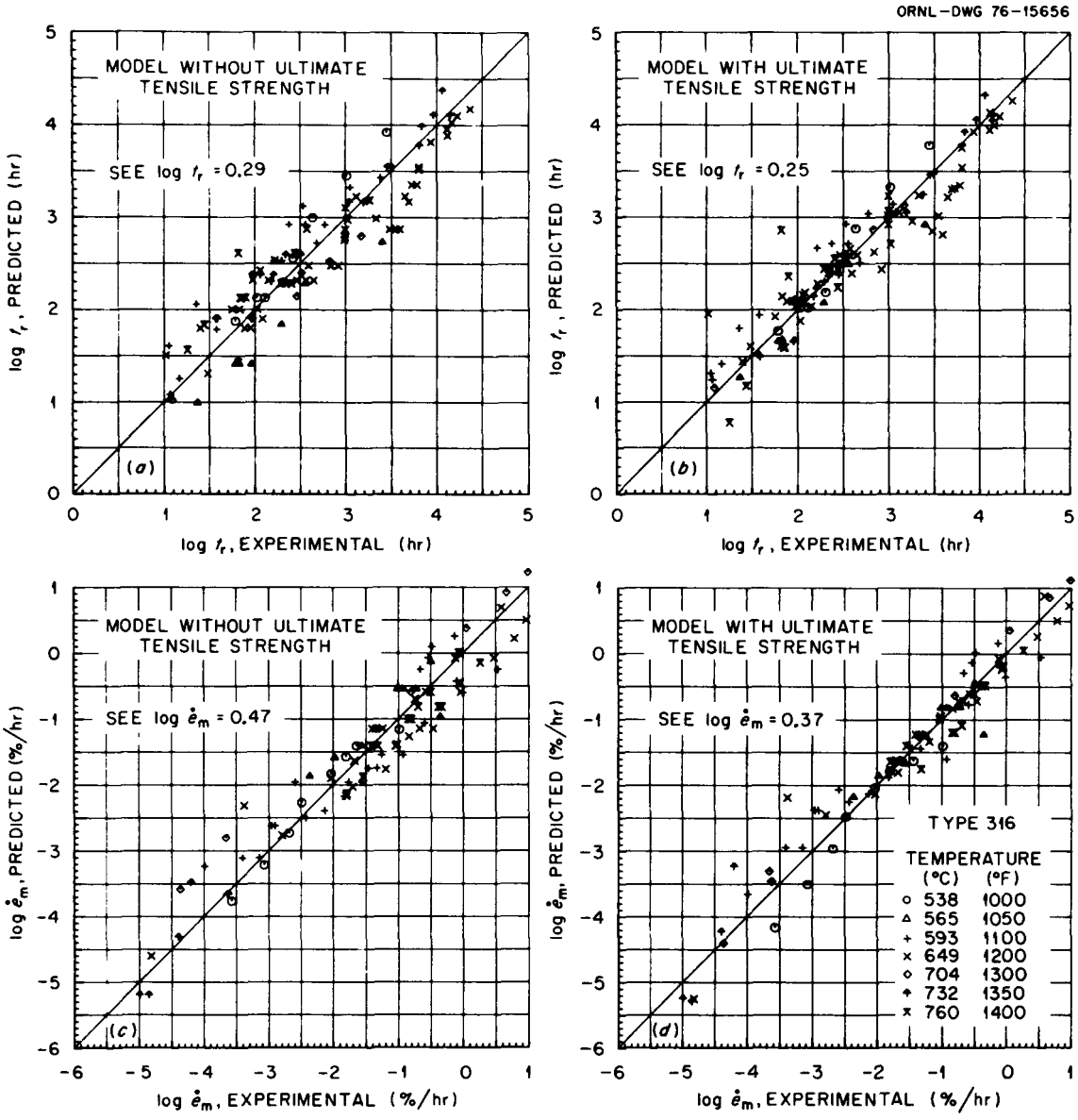

Fig. 15. Comparison of Experimental Time to Rupture and Minimum Creep Rate with Predicted Results from Models With and Without Ultimate Tensile Strength for Several Heats of Type 316 Stainless Steel.

Equations (9), (10), and (16) can be used to predict the average, minimum, and maximum properties, based on corresponding values of S_u. The mean values of S_u, as a function of temperature for type 304 stainless steel, were predicted from:

$$S_u = 639.8 - 1.848\,T_c + 0.00532\,T_c^2 - 5.088 \times 10^{-6} T_c^3 \ , \tag{17}$$

and

$$S_u = 613.0 - 1.510\,T_c + 0.00410\,T_c^2 - 3.896 \times 10^{-6} T_c^3 \ , \tag{18}$$

with S_u in MPa and T in °C. Equation (17) is for as-received material and was developed from 171 ORNL data points in the range from room temperature to 649°C (1200°F). Equation (18) is for reannealed material and was developed[21] from 135 ORNL data points in the range from room temperature to 704°C (1300°F). The standard errors of estimate for Eqs. (17) and (18) were 26.49 and 23.43 MPa respectively.

The mean values of S_u, as a function of temperature for type 316 stainless steel, were predicted from:

$$S_u = 85.15 - 5.89 \times 10^{-2} T_c + 8.84 \times 10^{-5} T_c^2 - 5.13 \times 10^{-8} T_c^3 \ , \tag{19}$$

with S_u in ksi and T in °F. Equation (19) is for the as-received material and was derived[2] from 77 literature[18,19] data points ranging from room temperature to 816°C (1500°F). The SEE for Eq. (19) was 32 MPa.

The maximum and minimum values of S_u were arbitrarily defined as mean value plus or minus two SEE. Although arbitrary, such a definition of maximum and minimum gives values close to those obtained by central tolerance limits ($P = 0.90$, $\lambda = 0.95$).

A comparison of the predicted maximum, average, and minimum values of t_r and $\dot{e}_m$ from Eqs. (9) and (10) and the ORNL experimental values on 20 heats of type 304 stainless steel (Figs. 16 and 17) shows that the total heat-to-heat variations in t_r and $\dot{e}_m$ can be bounded by the predicted maximum-minimum band from corresponding values of S_u. Comparisons were made of predicted and experimental values of $\dot{e}_m$ and t_r as a function of S_u for a fixed stress and temperature for type 304 stainless steel (Figs. 5, 6, and 7) and for type 316 stainless steel (Fig. 8). Predicted variations from generalized models in Eqs. (9), (10), and (16) are in excellent agreement with experimentally observed heat-to-heat variations in types 304 and 316 stainless steel (Figs. 5, 6, and 7).

The Japanese (NRIM)[22] heat-to-heat variations data for 9 heats of type 304 stainless steel were compared with the predicted maximum-minimum band from Eq. (9) (Fig. 18). The average and plus or minus two SEE values were obtained[2] at a strain rate of 1.25×10^{-3} per sec and therefore were corrected to a strain rate of 6.67×10^{-4} per sec, which was used in the derivation of Eqs. (9) and (10). The strain-rate correction[21] was based on the method presented in Appendix B. The predicted maximum-minimum band encloses the observed variations in the data for test temperatures of 600–700°C (1112–1293°F). Thus, Eqs. (9) and (10) are not only accurate for ORNL data but can also be extended to the Japanese data.[22]

Figs. 19 through 27 compare t_r and $\dot{e}_m$ for individual heats of types 304 and 316 stainless steel between experimental data and values predicted from models with and without S_u [Eqs. (9) through (16)]. Fig. 28 shows the plots of minimum creep rate for long-term creep tests on a single heat each of types 304 and 316 stainless steel. These are the first data where the creep rates go to values in the 10^{-7}% per hr range. These data were obtained from NRIM.[23] The predicted values from the model without S_u can differ from the

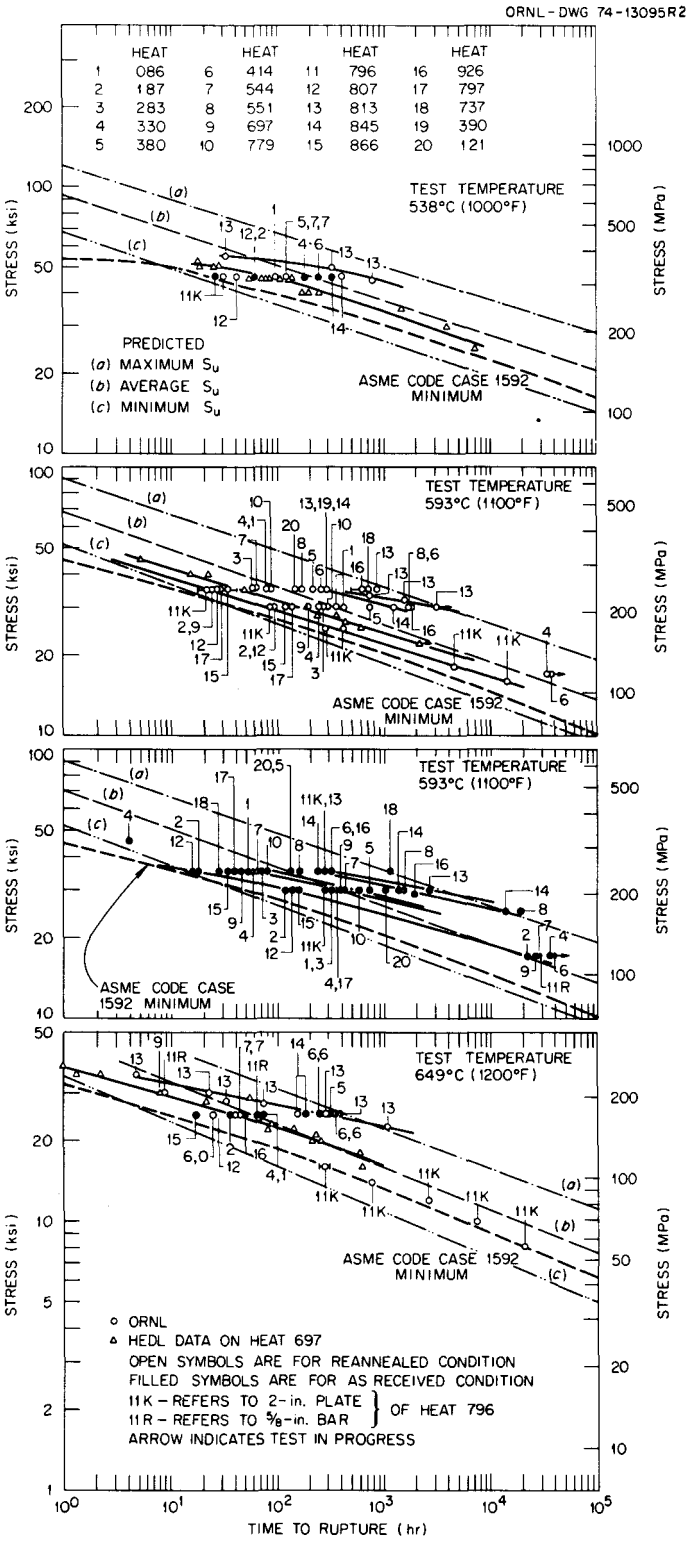

Fig. 16. Comparison of Stress-Rupture Data at 538, 593, and 649°C (1000, 1100, and 1200°F) for 20 Heats of Type 304 Stainless Steel in Both As-Received and Reannealed Conditions with ASME Code Case 1592 Minimum and the Predicted Maximum, Average, and Minimum Curves from the Rupture Model with Elevated-Temperature Ultimate Tensile Strength (S_u).

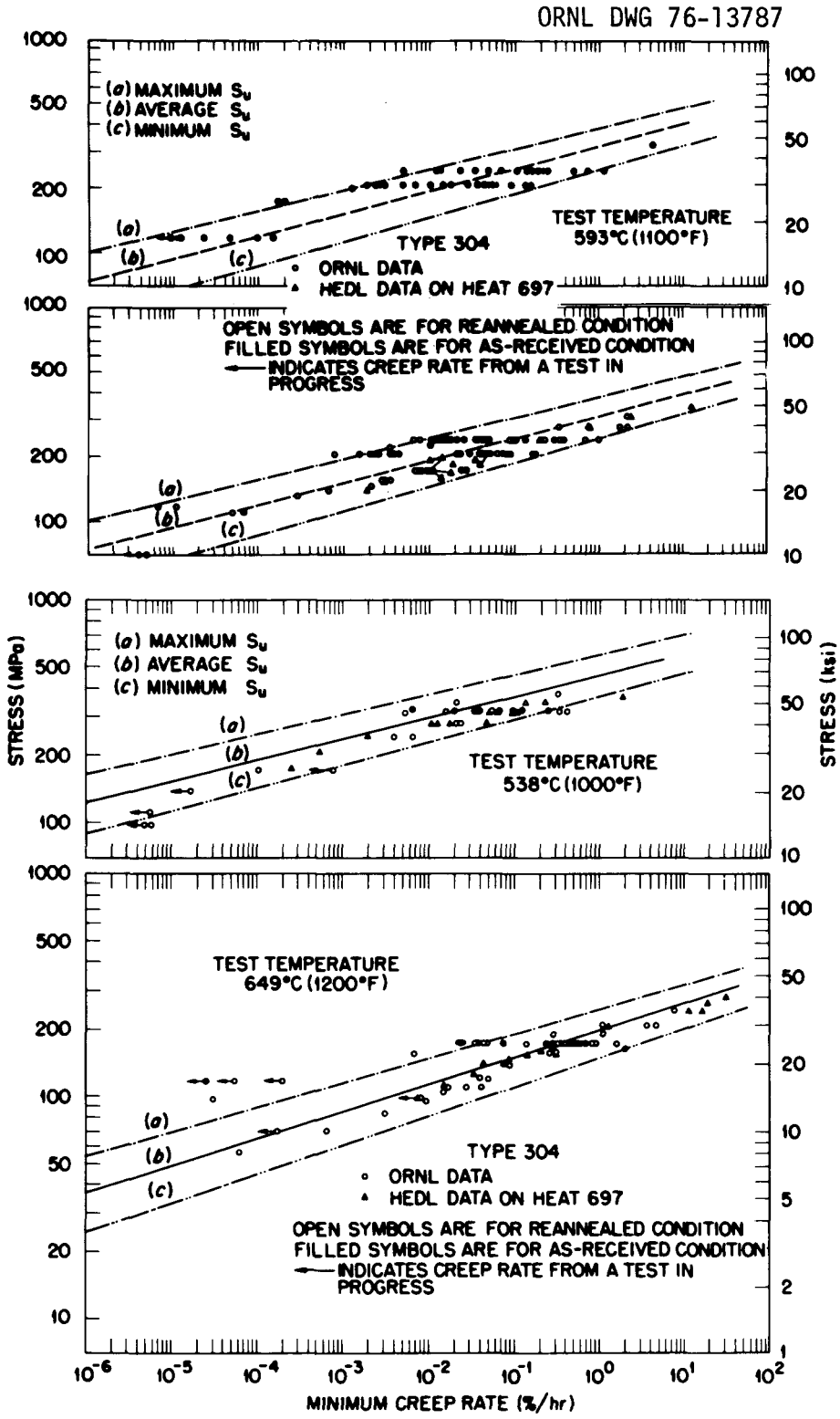

Fig. 17. Comparison of Minimum Creep-Rate Data at 538, 593, and 649°C (1000, 1100, and 1200°F) for 20 Heats of Type 304 Stainless Steel in Both As-Received and Reannealed Conditions with the Predicted Maximum, Average, and Minimum Curves from Minimum Creep Model with Elevated-Temperature Ultimate Tensile Strength (S_u).

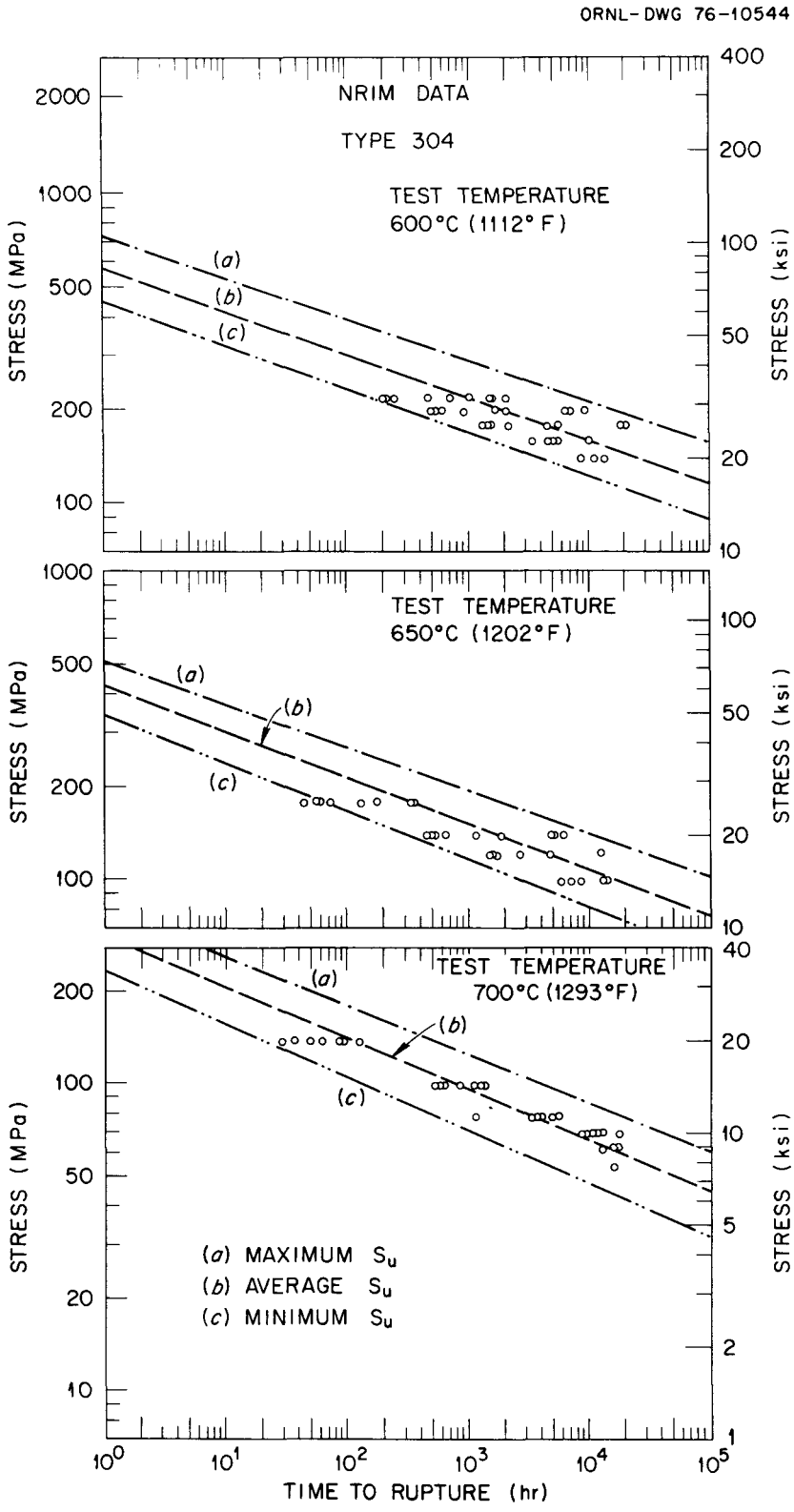

Fig. 18. Comparison of NRIM Stress-Rupture Data at 600, 650, and 700°C (1112, 1202, and 1293°F) for 9 Heats of Type 304 Stainless Steel in As-Received Condition with Predicted Maximum, Average, and Minimum Curves from Rupture Model with Elevated-Temperature Ultimate Tensile Strength (S_u).

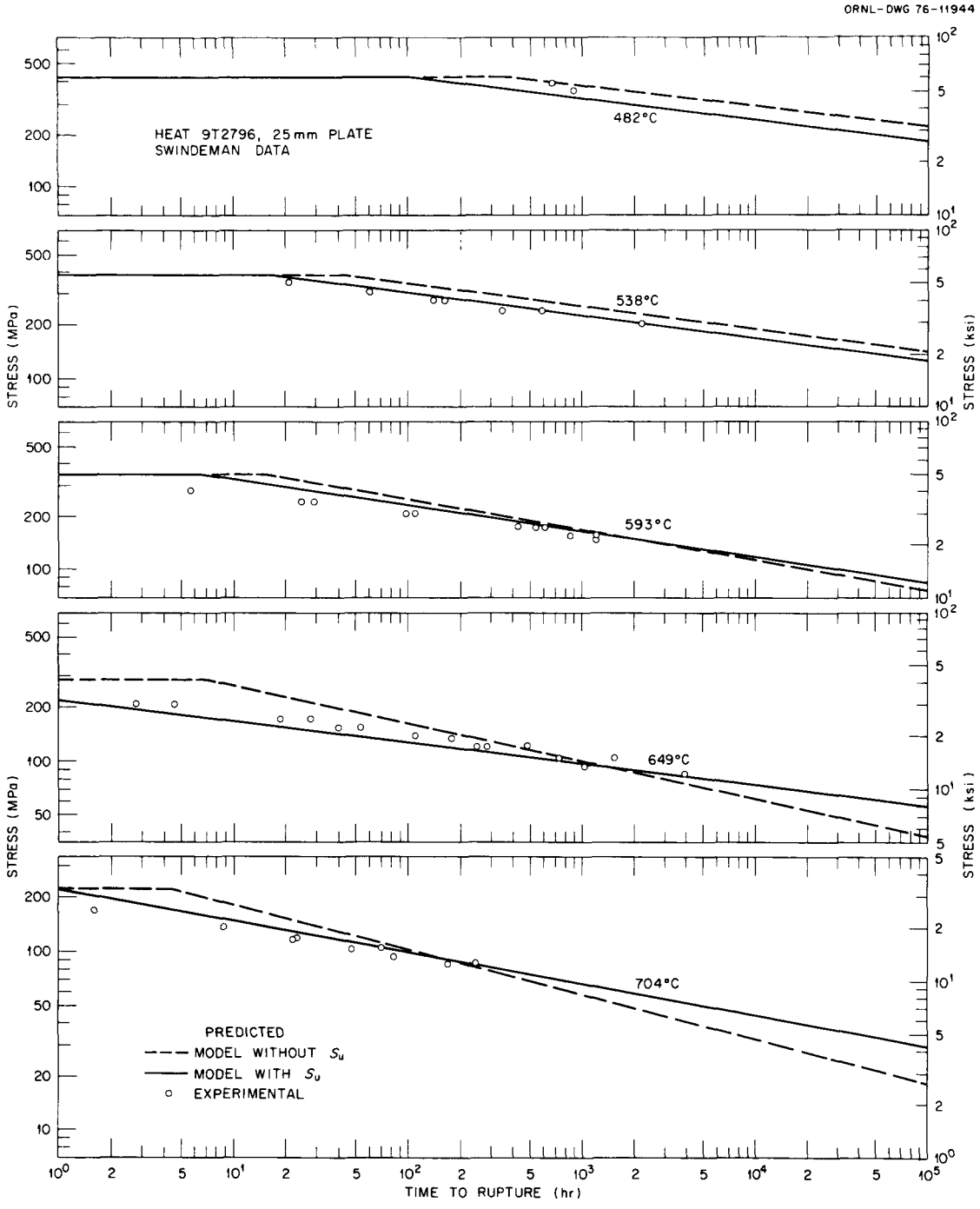

Fig. 19. Comparison of Experimental Time to Rupture with Values Computed from Models With and Without Elevated-Temperature Ultimate Temperature Strength (S_u) for 25-mm (1-in.) Plate of Reannealed Reference Heat of Type 304 Stainless Steel.

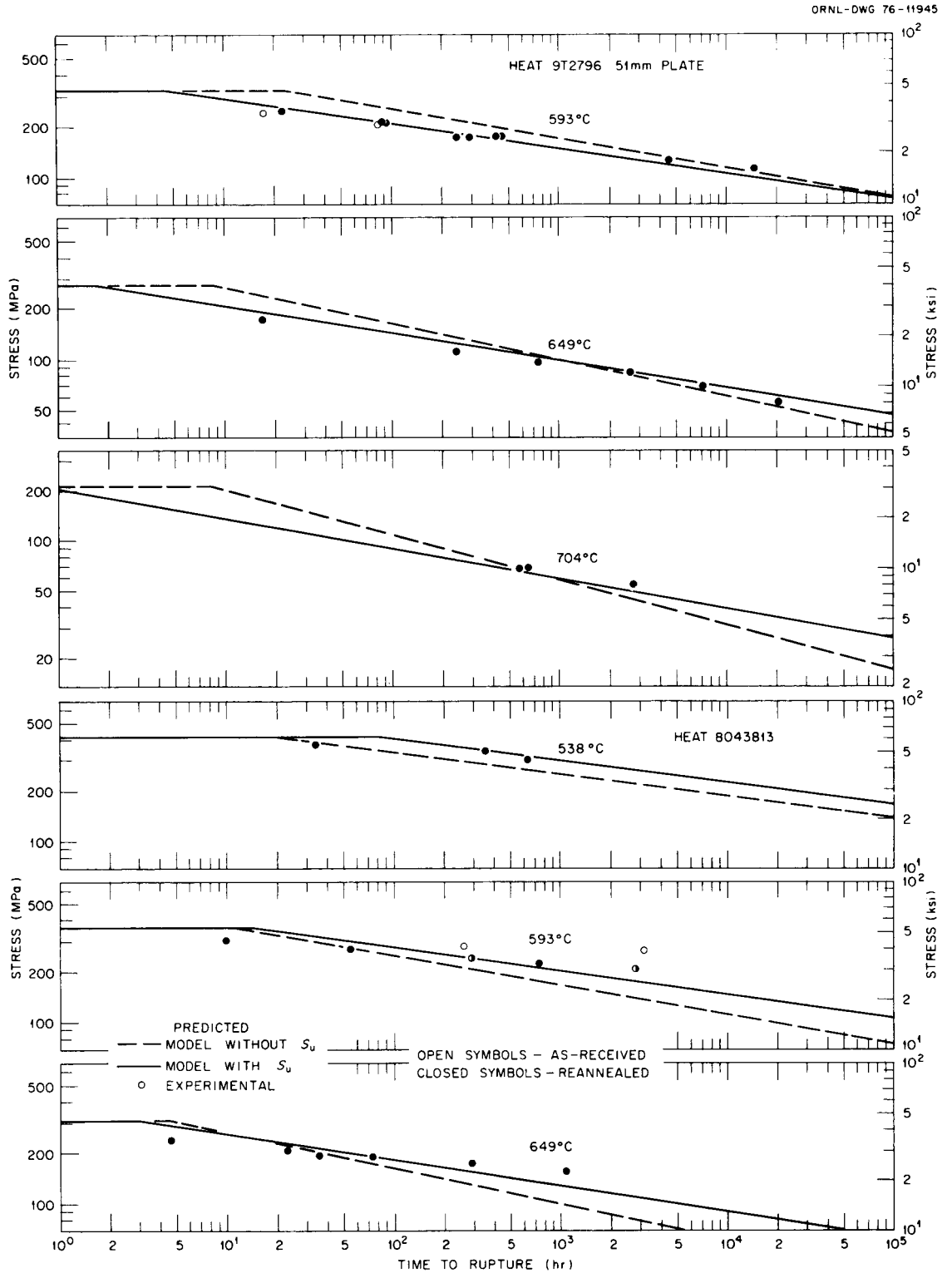

Fig. 20. Comparison of Experimental Time to Rupture with Values Computed from Models With and Without Elevated-Temperature Ultimate Tensile Strength (S_u) for a Weak (9T2796) and a Strong Heat (8043813).

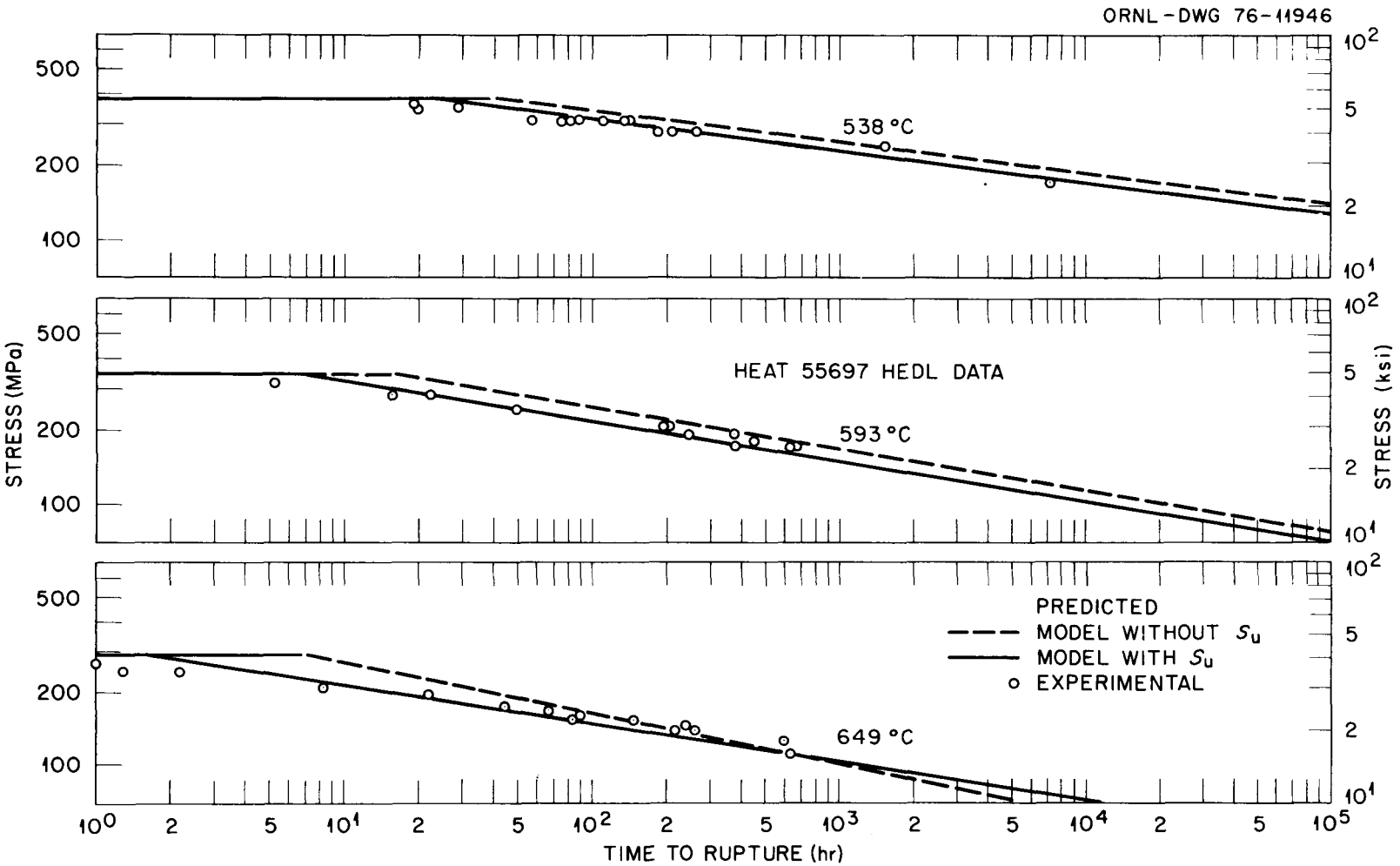

Fig. 21. Comparison of Experimental Time to Rupture with Values Computed from Models With and Without Elevated-Temperature Ultimate Tensile Strength (S_u) for HEDL Data on Reannealed Heat 55697.

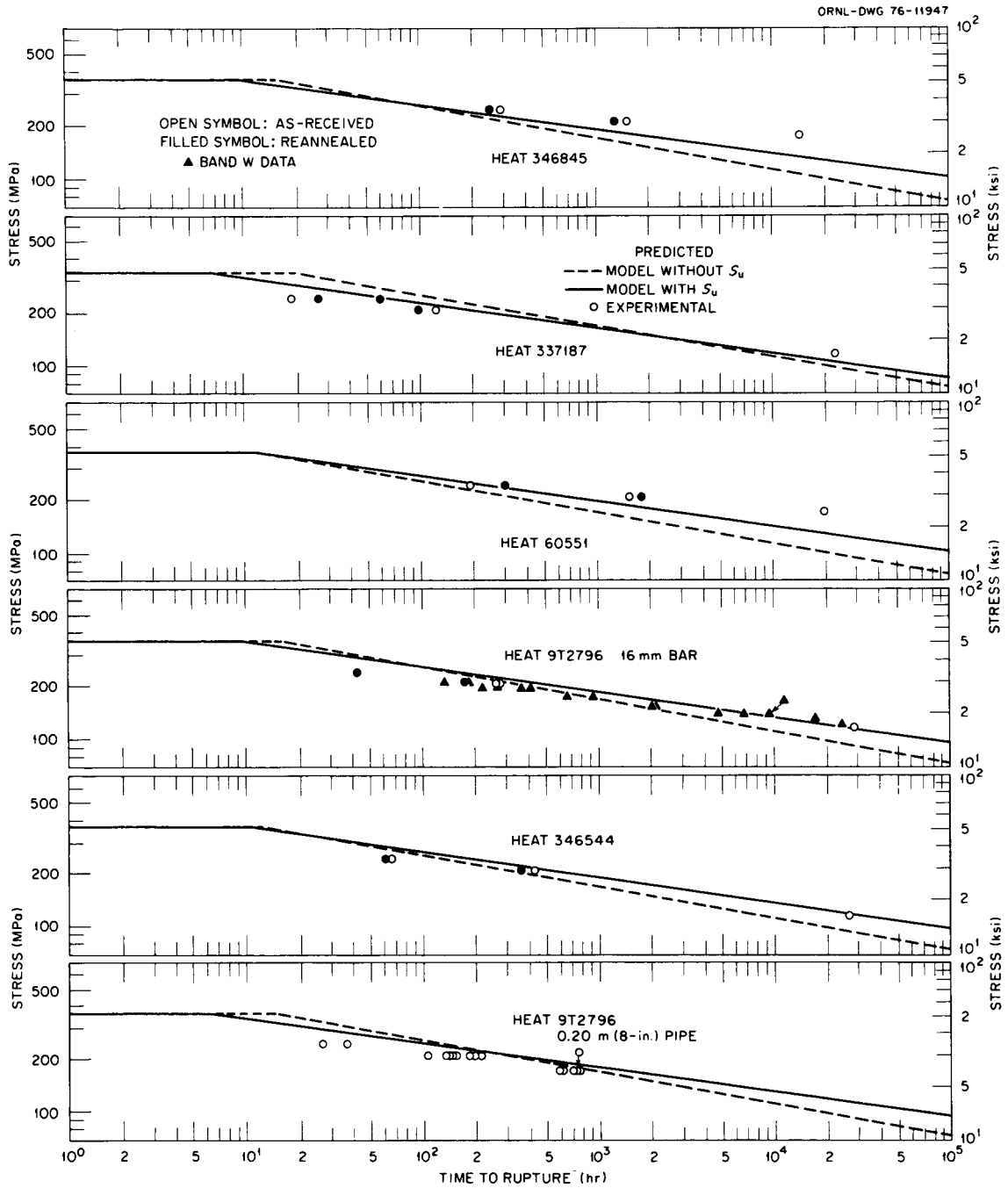

Fig. 22. Comparison of Experimental Time to Rupture with Values Computed from Models With and Without Elevated-Temperature Ultimate Tensile Strength (S_u) for Several Heats of Type 304 Stainless Steel at 593°C.

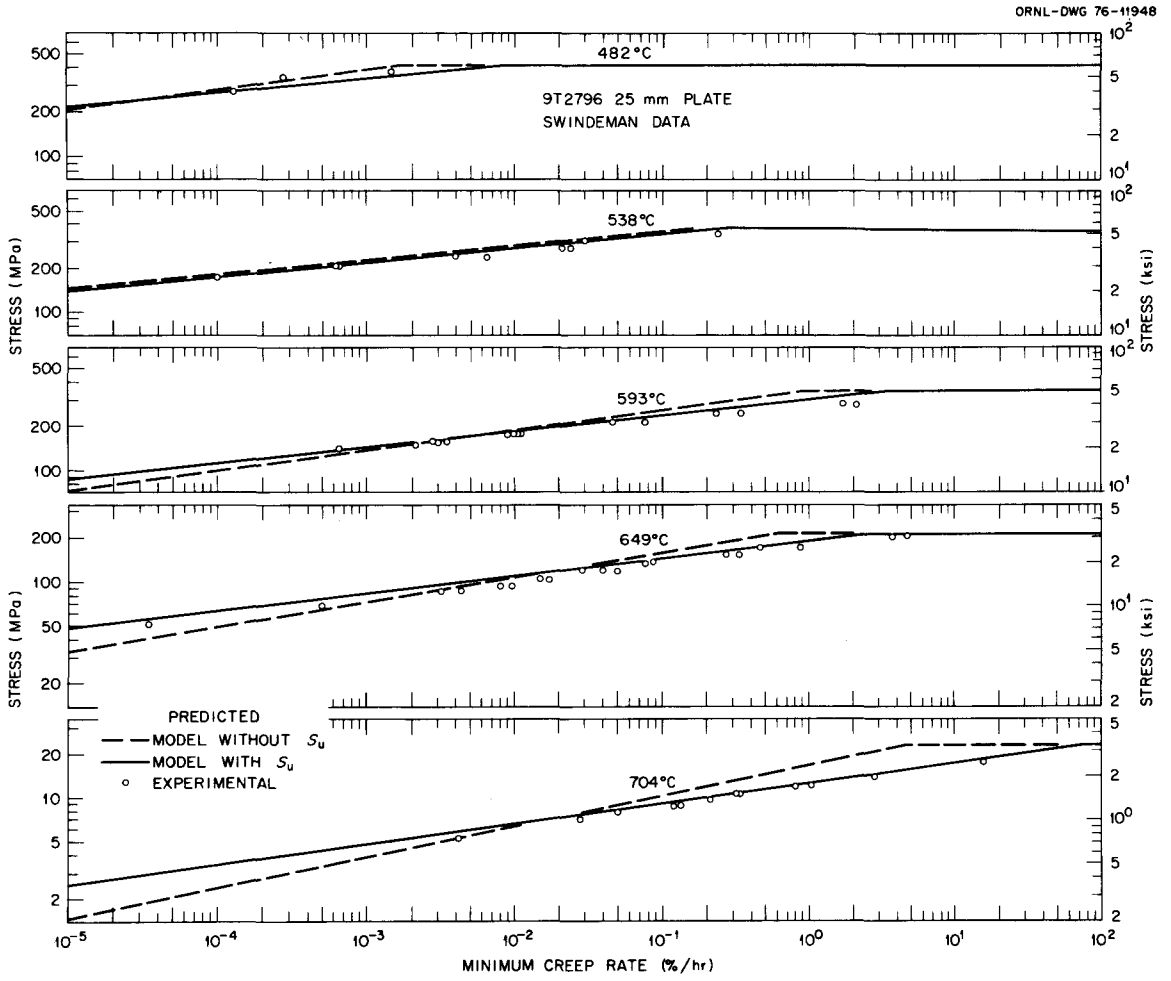

Fig. 23. Comparison of Experimental Minimum Creep Rate with Values Computed from Models With and Without Elevated-Temperature Ultimate Tensile Strength (S_u) for 25-mm (1-in.) Plate of Reannealed Reference Heat of Type 304 Stainless Steel.

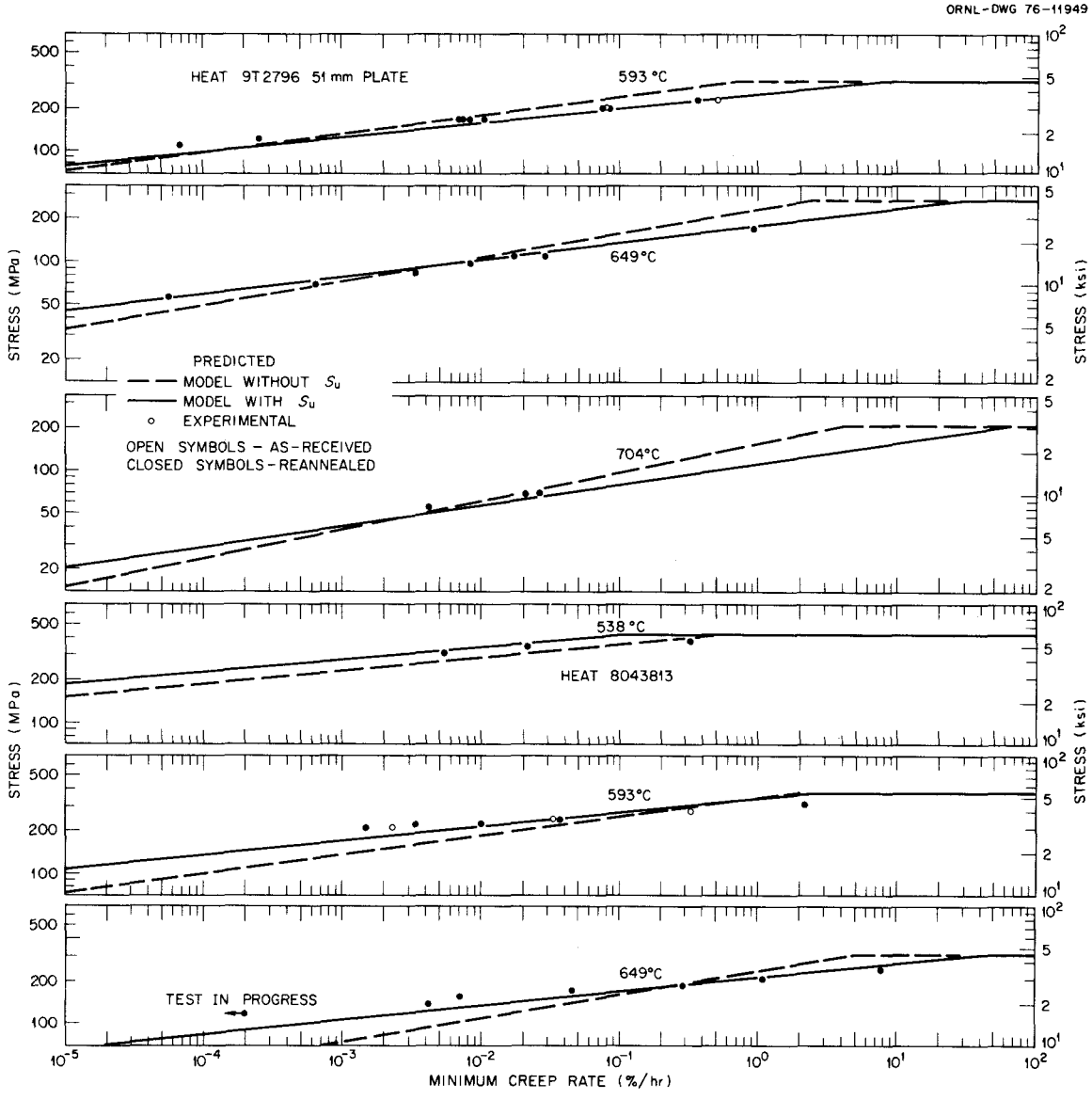

Fig. 24. Comparison of Experimental Minimum Creep Rate with Values Computed from Models With and Without Elevated-Temperature Ultimate Tensile Strength (S_u) for a Weak (9T2796) and a Strong Heat (8043813).

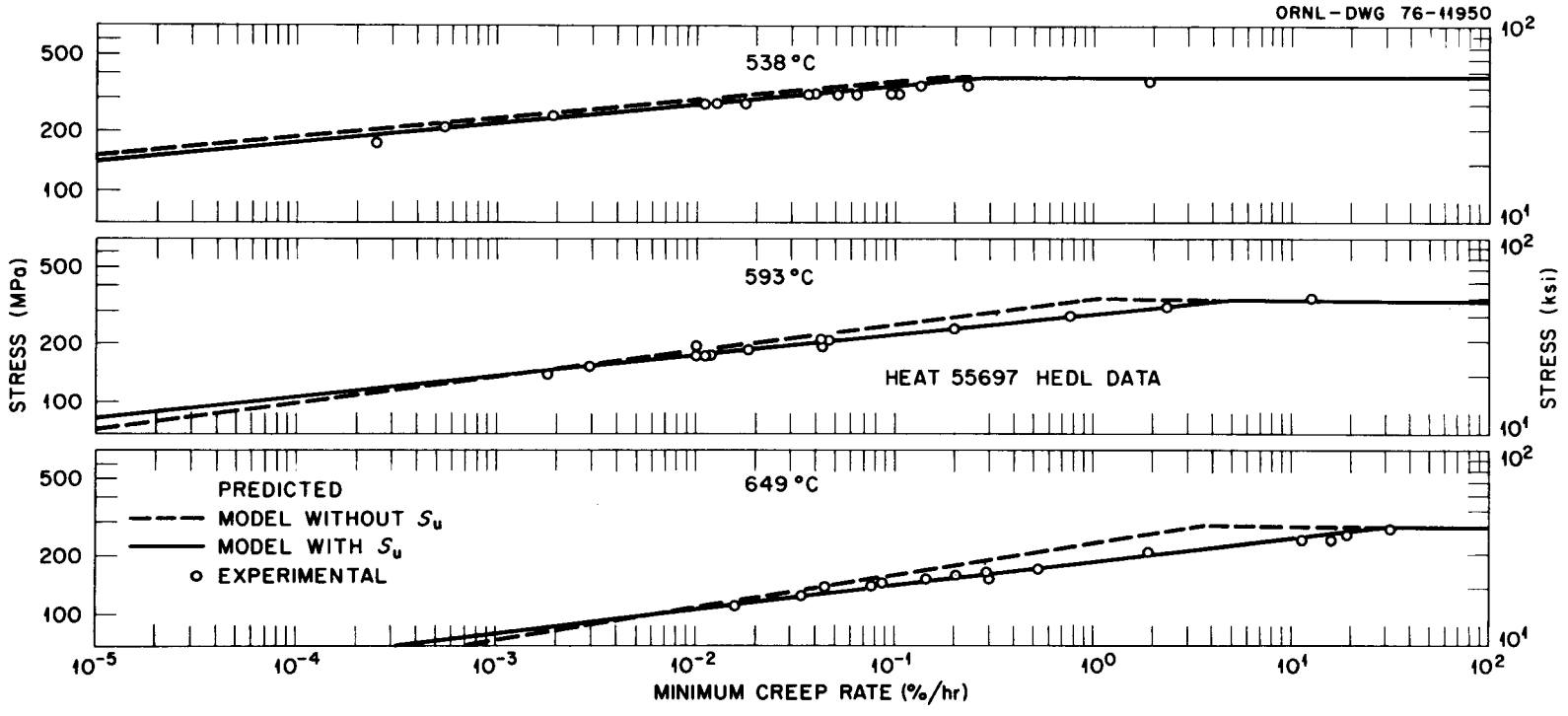

Fig. 25. Comparison of Experimental Minimum Creep Rate with Values Computed from Models With and Without Elevated-Temperature Ultimate Tensile Strength (S_u) for HEDL Data on Reannealed Heat 55697.

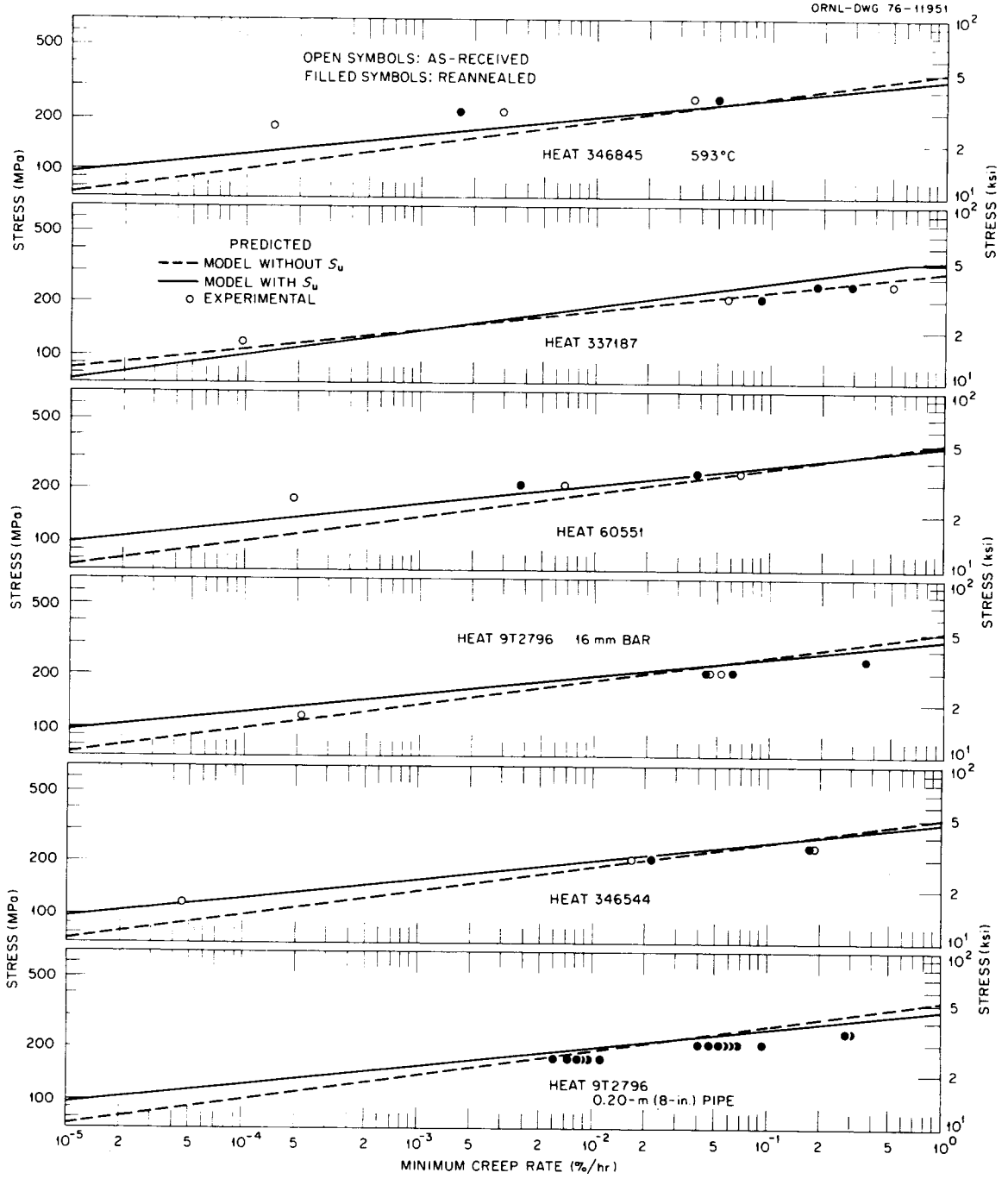

Fig. 26. Comparison of Experimental Minimum Creep Rate with Values Computed from Models With and Without Elevated-Temperature Ultimate Tensile Strength (S_u) for Several Heats of Type 304 Stainless Steel.

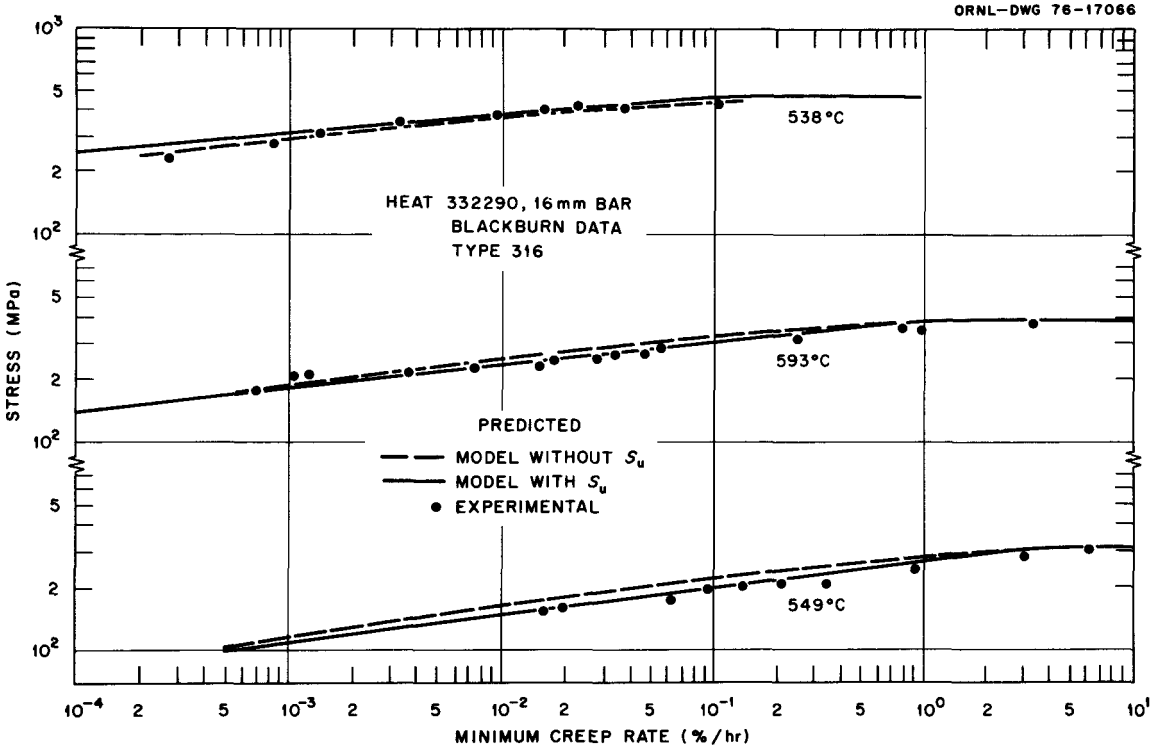

Fig. 27. Comparison of Experimental Minimum Creep-Rate Data with Values Computed from Models With and Without Elevated-Temperature Ultimate Tensile Strength (S_u) for Blackburn Data on Heat 332290 of Type 316 Stainless Steel.

experimental values by factors of 100 or greater. However, when the ultimate tensile strength of that particular heat at the creep-test temperatures was used in the model with S_u, the experimental and predicted values agreed within factors of 10 or less. Thus, with only the knowledge of an elevated-temperature ultimate tensile strength, the creep behavior of a new heat can be predicted with fair accuracy.

The experimental data on type 316 stainless steel can be compared with predicted values from models with and without S_u (Fig. 28*b*). The model without S_u by Stillman et al.[24] was derived from heats other than those used in the present study. As mentioned earlier, the present investigative model used only those data points for which elevated-temperature ultimate tensile strength values were available. However, that was not the consideration in the selection of data for the Stillman[24] model. The model with S_u improves significantly the agreement between the experimental and predicted values (Fig. 28). Although agreement between the experimental data and values predicted by the Stillman[24] model is also fair, it may just be coincidental. However, the model with S_u always yields closer agreement.

In summary the models of t_r and $\dot{e}_m$ containing S_u predicted fairly well, even for long-term data. Furthermore, such close agreement between the experimental and predicted values for heats melted in Japan supports the validity of the models proposed in the present investigation.

Using Eq. (9) we have predicted the values of 10^3, 10^4, and 10^5 hr creep-rupture strength and plotted them as a function of S_u at the creep-test temperature (Fig. 29). In Fig. 29 are also shown lines based on Eq. (5) and constants from Table 1. The values predicted from Eq. (9) fall on the same line regardless of the test temperature; this is consistent with Eq. (5). Furthermore, values predicted from Eq. (5) are in close agreement with values predicted from the generalized model in Eq. (9). A slight disagreement between the two models for 10^4 hr rupture strength probably results from the possible error in constants α and β of Eq. (5) due to a large data bias at 593°C (1100°F). Thus the only difference between Eqs. (5) and (9) is that the former relates log $S_R{}^t$ directly to S_u, whereas the latter expresses log t_r in terms of S, T, and S_u.

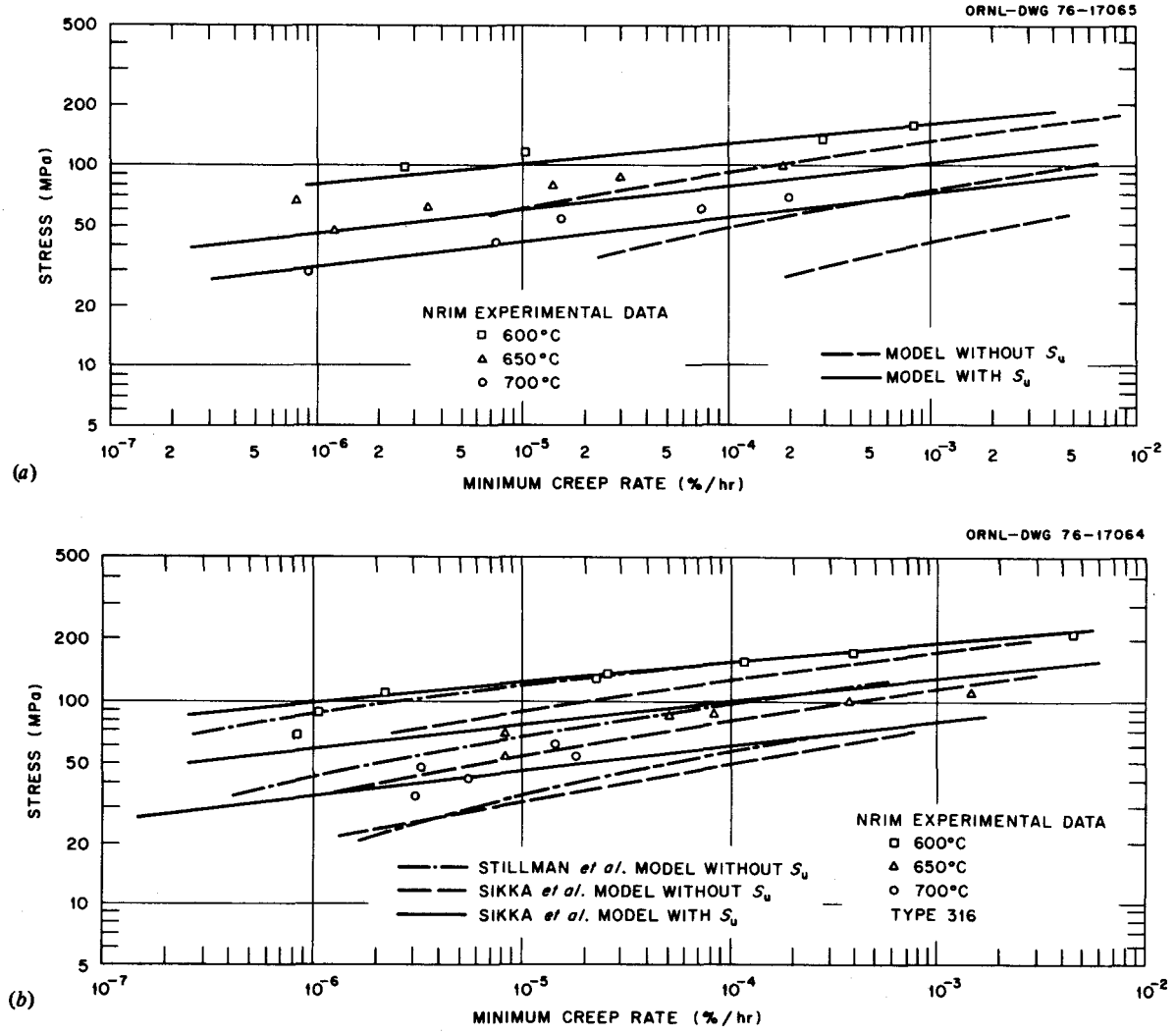

Fig. 28. Comparison of Experimental Minimum Creep-Rate Data with Values Computed from Models With and Without Elevated-Temperature Ultimate Tensile Strength (S_u) for Long-Term Data Obtained from NRIM on (*a*) Type 304 and (*b*) Type 316 Stainless Steel.

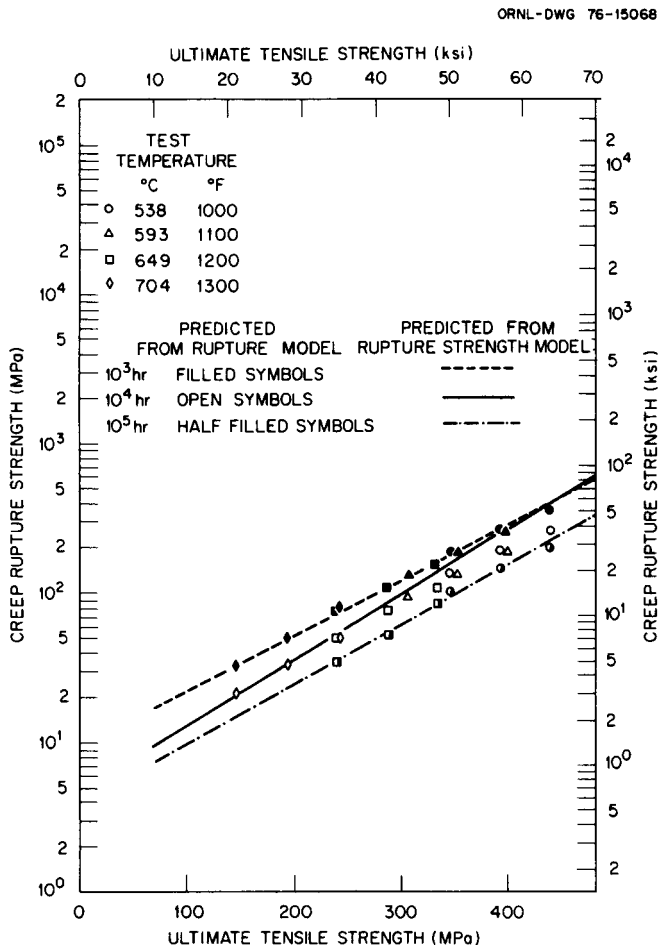

Fig. 29. Comparison of Creep-Rupture Strengths Predicted from Rupture Model and Rupture-Strength Model for Type 304 Stainless Steel.

4.3 EXTENSION OF t_r AND $\dot{e}_m$ MODELS IN TIME TO ONSET OF TERTIARY CREEP, t_{ss} (OR t_3), AND STRAIN TO ONSET OF TERTIARY, e_{ss} (OR e_3), BY MEANS OF EMPIRICAL RELATIONS

Booker and Sikka[25,26,27] have developed empirical relationships for predicting t_{ss} and e_{ss} from t_r and $\dot{e}_m$. These relationships for type 304 stainless steel are given for 482–816°C (900–1500°F) by three equations:

$$t_{ss} = 0.752\, t_r^{0.977} \text{ (from 277 data)}, \tag{20}$$

$$e_{ss} = \frac{e_{ss}}{t_{ss}} = 1.11\, \dot{e}_m^{0.974} \text{ (from 138 data)}, \tag{21}$$

and

$$e_{ss} = 0.835\, \dot{e}_m^{0.974}\, t_r^{0.977} \text{ [from Eqs. (20) and (21)]}. \tag{22}$$

The values of e_{ss} and t_{ss} are 0.2% offset points from the linear portion of the creep curve. The equations for predicting t_{ss} and e_{ss} for type 316 stainless steel in the range 593–816°C (1100–1500°F) are:

$$t_3 = 0.526\, t_r^{1.004} \text{ (for 183 data)}, \tag{23}$$

$$\dot{e}_3 = 1.602\, \dot{e}_m^{0.995} \text{ (for 120 data)}, \tag{24}$$

and

$$\dot{e}_3 = 0.84\, \dot{e}_m^{0.995}\, t_r^{1.004} \text{ [from Eqs. (23) and (24)]}. \tag{25}$$

The values of e_3 and t_3 in Eqs. (23) through (25) are points of divergence from the linear portion of the creep curve.

The constants in Eqs. (20) through (25) are relatively independent of heat-to-heat and temperature variations. However, these equations in combination with Eqs. (9), (10), and (16) can be used to predict the $t_{ss}(t_3)$ and $e_{ss}(e_3)$ values of a given heat if its elevated-temperature S_u value is known.

It has been shown (Sect. 4.2) that S_u models [Eqs. (9) and (10)] predict more accurately time to rupture (t_r) and minimum creep rate ($\dot{e}_m$) for a given heat than models without S_u. Equations (21), (22), (23), and (24) then suggest that accurate knowledge of t_r and $\dot{e}_m$ will also help predict $t_{ss}(t_3)$ and $e_{ss}(e_3)$ more accurately (Figs. 30–33).

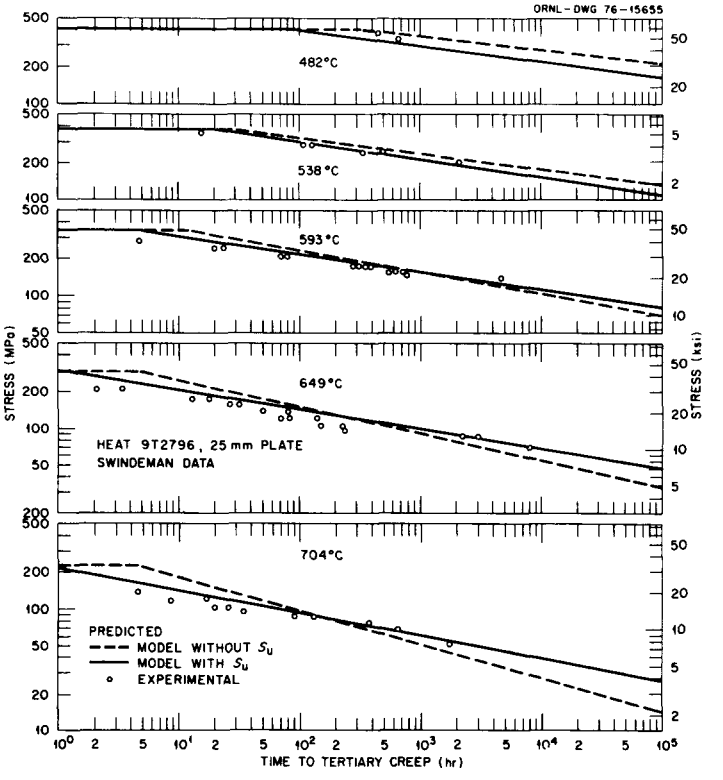

Fig. 30. Comparison of Experimental Time to Tertiary Creep with Values Computed from Models With and Without Elevated-Temperature Ultimate Tensile Strength (S_u) for 25-mm (1-in.) Plate of a Weak (9T2796) Heat of Type 304 Stainless Steel.

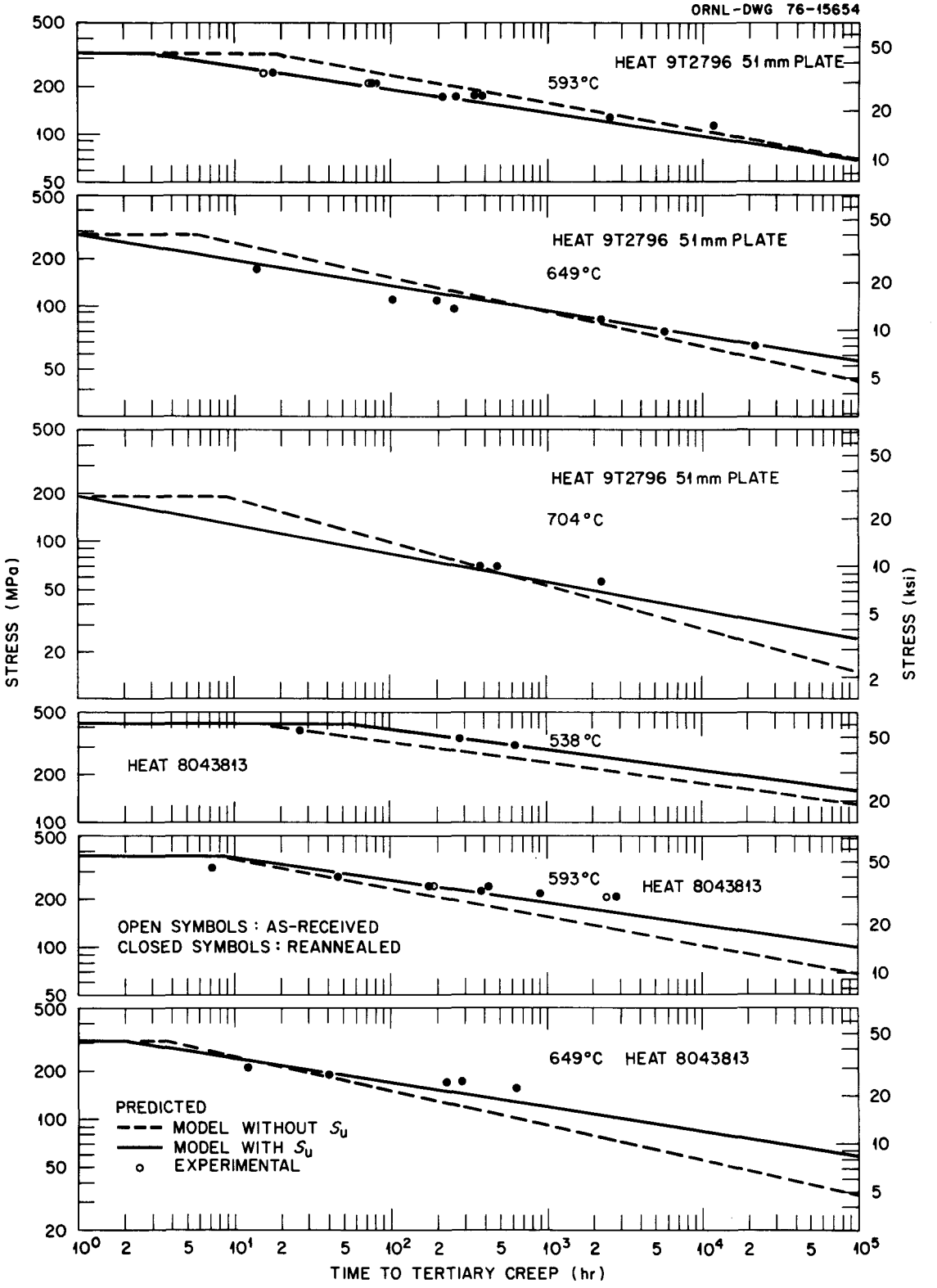

Fig. 31. Comparison of Experimental Time to Tertiary Creep with Values Computed from Models With and Without Elevated-Temperature Ultimate Tensile Strength (S_u) for a Weak (9T2796) and a Strong Heat (8043813) of Type 304 Stainless Steel.

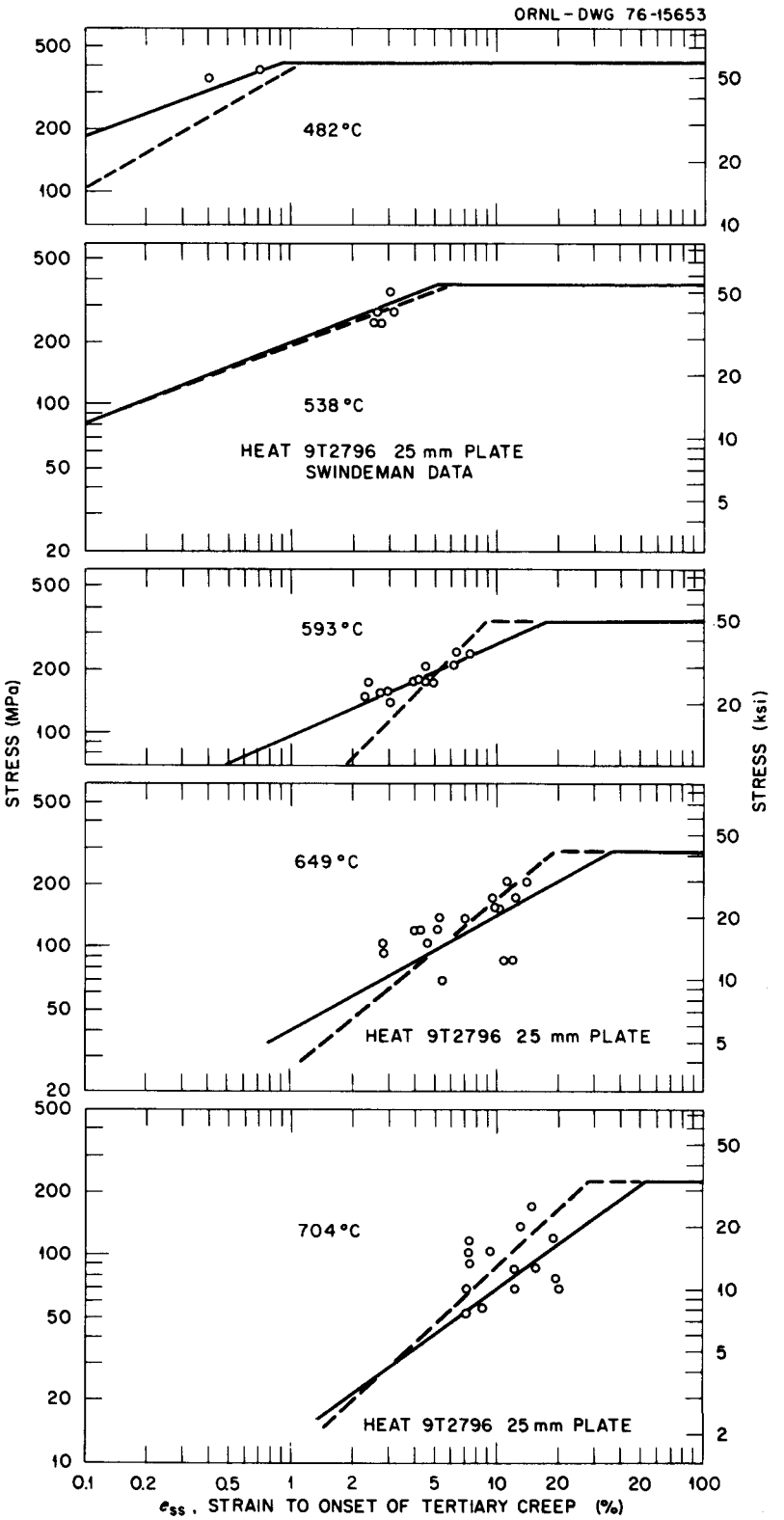

Fig. 32. Comparison of Experimental Strain to Onset of Tertiary Creep with Values Computed from Models With and Without Elevated-Temperature Ultimate Tensile Strength (S_u) for 25-mm (1-in.) Plate of a Weak Heat (9T2796) of Type 304 Stainless Steel. Dotted line – model without S_u; solid line – model with S_u.

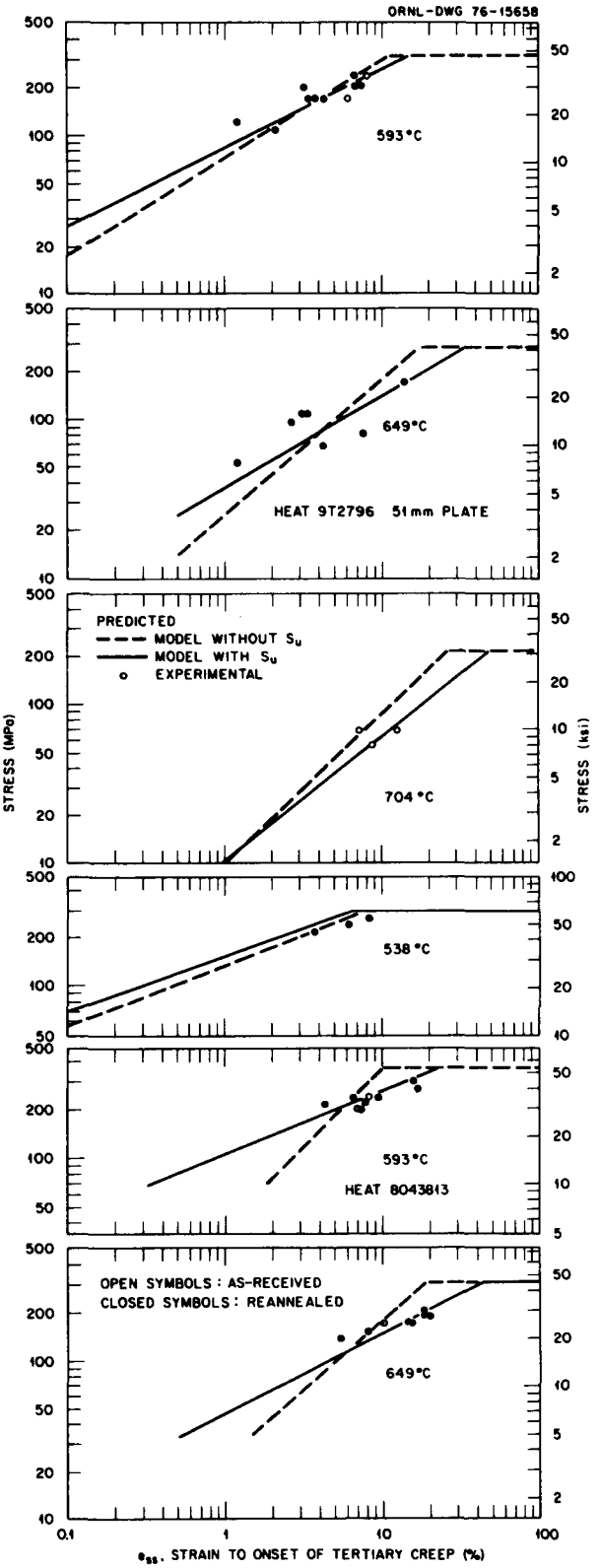

Fig. 33. Comparison of Experimental Strain to Onset of Tertiary Creep with Values Computed from Models With and Without Elevated-Temperature Ultimate Tensile Strength (S_u) for a Weak (9T2796) and a Strong Heat (8043813) of Type 304 Stainless Steel.

4.4 CREEP EQUATION AND ISOCHRONOUS STRESS-STRAIN CURVES

Booker and Sikka[28] have shown that strain-time behavior of type 304 stainless steel can be described by the rational polynomial creep equation:

$$e_c = \frac{Cpt}{1+pt} + \dot{e}_m t \ , \tag{26}$$

where

e_c = creep strain,
t = time, and
C = limiting value of the transient primary term.

The properties of this equation (Fig. 34) were described in detail by Hobson and Booker.[29] Equation (26) has been shown to be valid for 482–704°C.

The parameter p is related to the sharpness of the curvature of the primary creep region. Booker and Sikka[28] described C and p by the following equations:

$$c = e_3 - \dot{e}_m t_3 \ , \tag{27}$$

and

$$p = \frac{\dot{e}_o - \dot{e}_m}{c} \ , \tag{28}$$

where $\dot{e}_o$ = the initial creep rate, and $\dot{e}_o$ was expressed in terms of $\dot{e}_m$ by:

$$\dot{e}_o = 3.43\, \dot{e}_m^{0.80} \ . \tag{29}$$

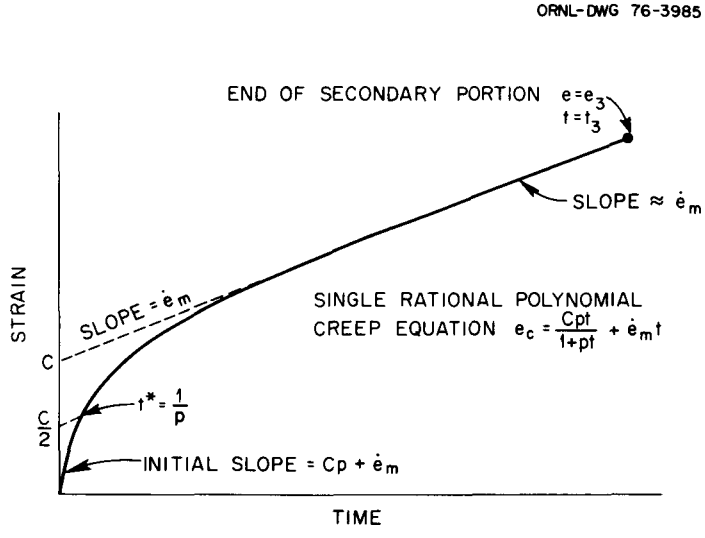

Fig. 34. Properties of the Rational Polynomial Creep Equation.

Thus, with Eqs. (20) through (29), it is possible to determine the strain-time behavior from values of $\dot{e}_m$ and t_r. Since Equations (9) and (10) can be used to estimate t_r and $\dot{e}_m$ of a given heat if its elevated-temperature S_u is known, then Eqs. (20) through (28) in combination with Eqs. (9) and (10) can be used to estimate the strain-time behavior of an individual heat subjected to simple uniaxial creep loads. Experimentally determined creep curves of several heats are compared with those predicted based on maximum, average, and minimum values of elevated-temperature ultimate tensile strength (S_u) (Fig. 3). The predicted curves describe the observed behavior closely. Comparisons of experimental and predicted creep curves for long-term tests on several individual heats (Figs. 35–37) show that long-term strain-time behavior of an individual heat can also be estimated with varying degrees of success if its elevated-temperature S_u is known. The Blacklun equation[30] predicts an average behavior of heats for which the data were used in developing the equation, but it does not contain any index for predicting heat-to-heat variations (Figs. 35–37).

The creep equation with heat-to-heat variations incorporated through elevated-temperature ultimate tensile strengths[28] in conjunction with a tensile stress-strain model[31] containing heat-to-heat variation through 0.2% yield strength has been used to predict isochronous stress-strain behavior for average, maximum and minimum S_u values. These curves are shown in Fig. 38 for three different test temperatures. Included in these figures are the values predicted from currently used tensile and creep models.[32]

Results presented above show that the use of an ultimate tensile strength term in creep law formulations for type 304 stainless steel gives better definition of the creep characteristics of individual heats. Further, the above methods permit the estimation of minimum isochronous stress-strain curves with some assurance which heretofore has not been possible. Long-term creep and creep-rupture tests in progress at ORNL will provide additional long-term data and answer questions concerning the role of residual element chemistry thereby providing the means for refining the models further if required.

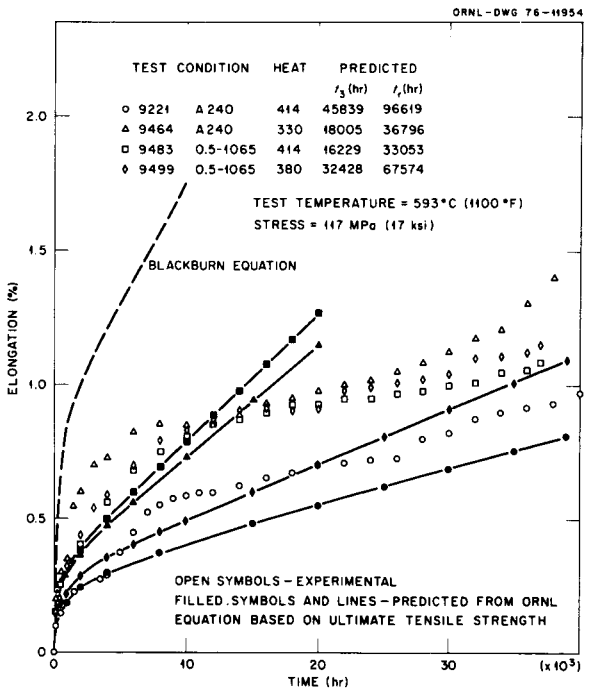

Fig. 35. Comparison Between Experimental and Predicted Creep Curves for Three Heats of Type 304 Stainless Steel. Condition 0.5-1065 means laboratory reannealing for 0.5 hr at 1065°C. The Blackburn equation is the presently approved equation in *Nuclear Systems Materials Handbook.*

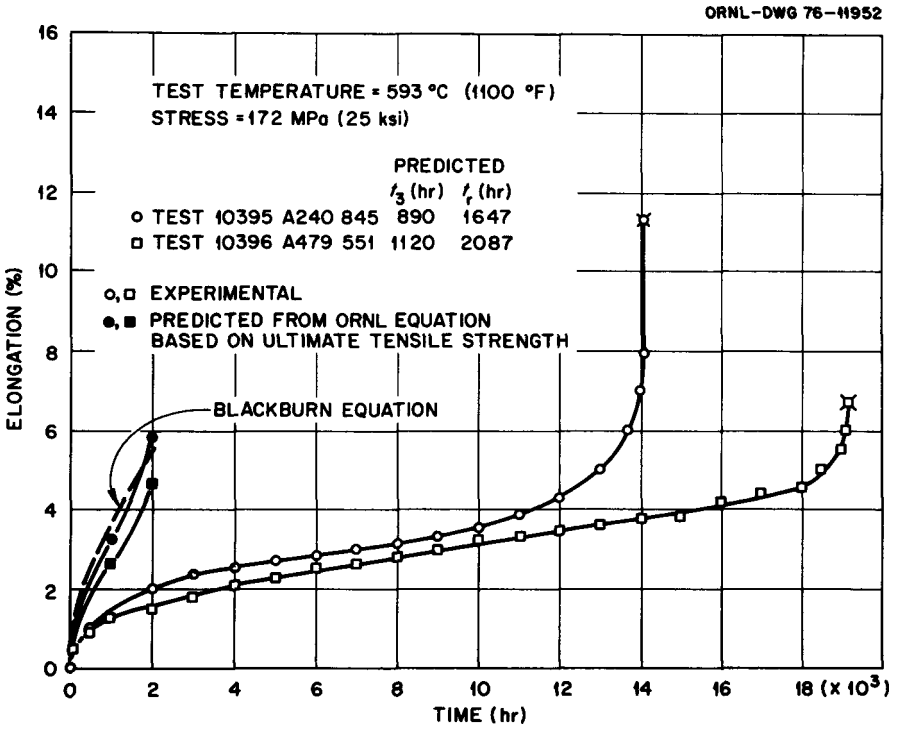

Fig. 36. Comparison Between Experimental and Estimated Creep Curves for Two Heats of Type 304 Stainless Steel. The Blackburn equation is the presently approved equation in *Nuclear Systems Materials Handbook.*

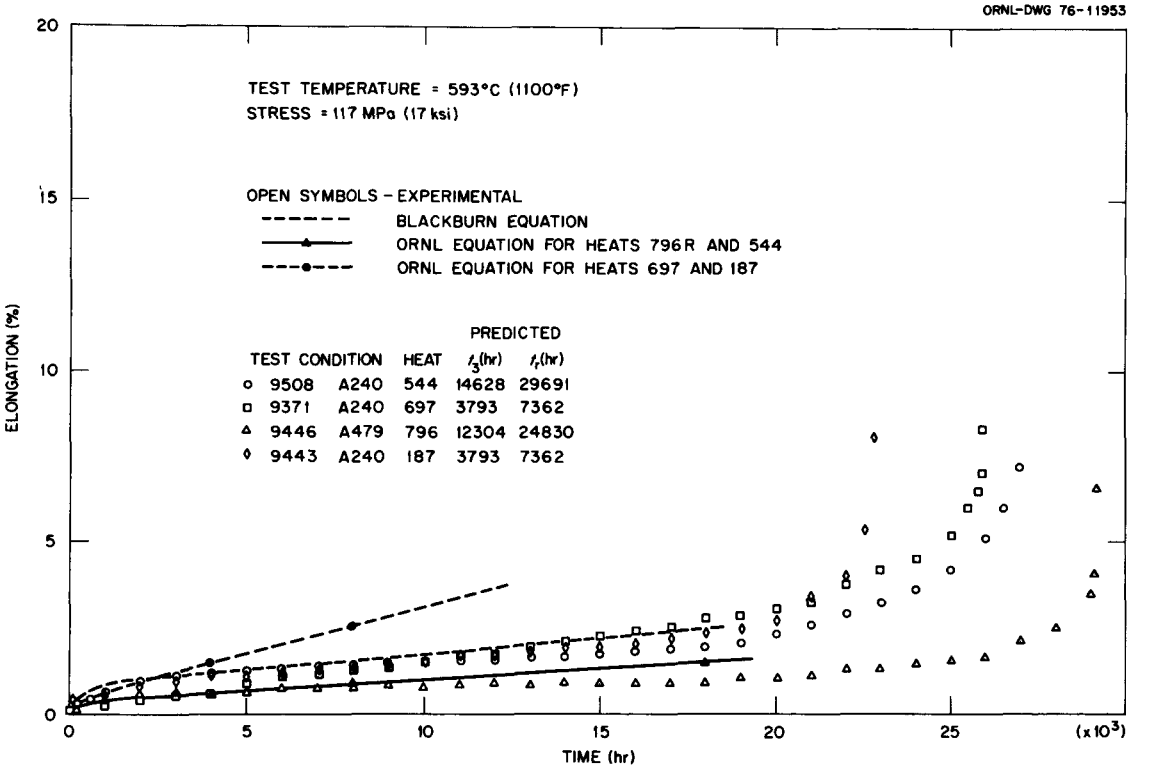

Fig. 37. Comparison Between Experimental and Estimated Creep Curves for Four Heats of Type 304 Stainless Steel. The Blackburn equation is the presently approved equation in *Nuclear Systems Materials Handbook.*

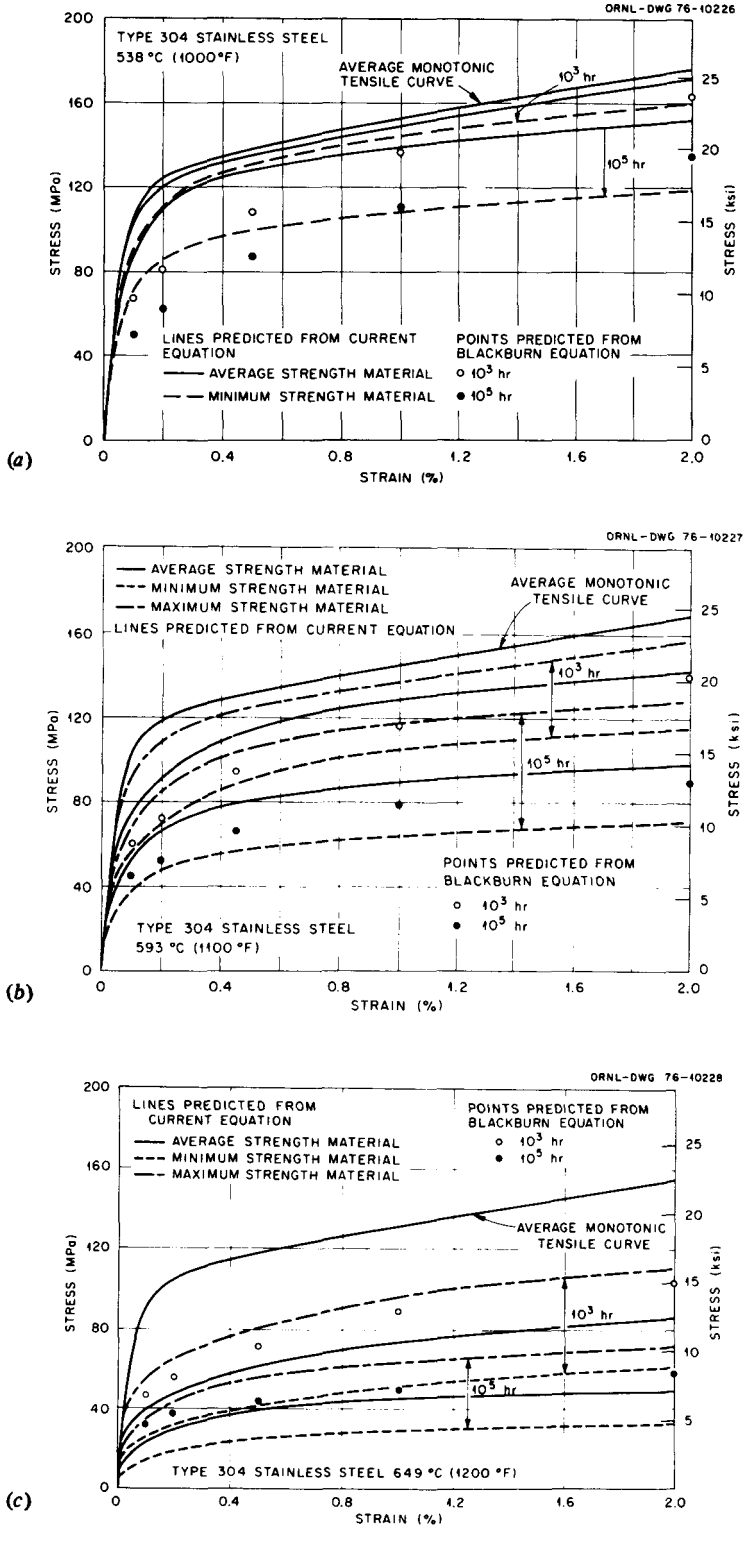

Fig. 38. Isochronous Stress-Strain Curves at 10^3 and 10^5 hr Predicted from the Creep Equation and the Rational Polynomial Equation for Average Stress-Strain Behavior. Shown are predictions for average, minimum, and maximum creep strength. Also shown are values from curves constructed from the Blackburn equation. (*a*) 538°C (1000°F), (*b*) 593°C (1100°F), and (*c*) 649°C (1200°F).

5. METALLURGICAL CONSIDERATIONS

Relationships presented in previous sections between short-term elevated-temperature ultimate tensile strength and long-term properties are empirical, but still some consideration must be given to the following:

1. metallurgical instability,
2. substructural difference between the tensile and creep modes of deformation, and
3. fracture mode differences between short-term tensile and long-term creep specimens.

5.1 METALLURGICAL INSTABILITY

Austenitic stainless steels undergo metallurgical changes during long-term creep testing.[33–36] For type 304 stainless steel, these changes include the precipitation of carbides at grain boundaries and in the matrix; whereas type 316 forms additional phases (η, χ, and σ). Time-temperature-precipitation diagrams for type 316 show that, for reannealed material, intermetallic phases form after long times ($\geq$10,000 hr) at 649°C (1200°F) and lower temperatures. However, at higher temperatures these changes can occur at much shorter times. Furthermore, precipitation processes can be enhanced to some extent under stress.[37]

Effects of long-term thermal aging on creep properties of types 304 and 316 stainless steels have been previously investigated[18,38–41] and are being studied at ORNL. A previous study[38] conducted on type 304 stainless steel for material preexposed for 100,000 hr (11.4 yr) at 565°C (1050°F) showed only minimal changes on the creep properties (Fig. 39). Still other data [18] obtained from type 316 stainless steel preexposed (aged) for 10,000 hr at three different temperatures show minimal effects of aging on creep properties (Fig. 40) as Steichen's data[41] does also (Fig. 41).

The ORNL data come from several heats of types 304 and 316 stainless steel. These heats are being exposed for various periods at temperatures of 482, 593 and 649°C (900, 1100 and 1200°F). Most of the post-aged creep tests are being done at a common test temperature of 593°C (1100°F). Additional tests at aging temperatures lower or higher than 593°C (1100°F) are also in progress.

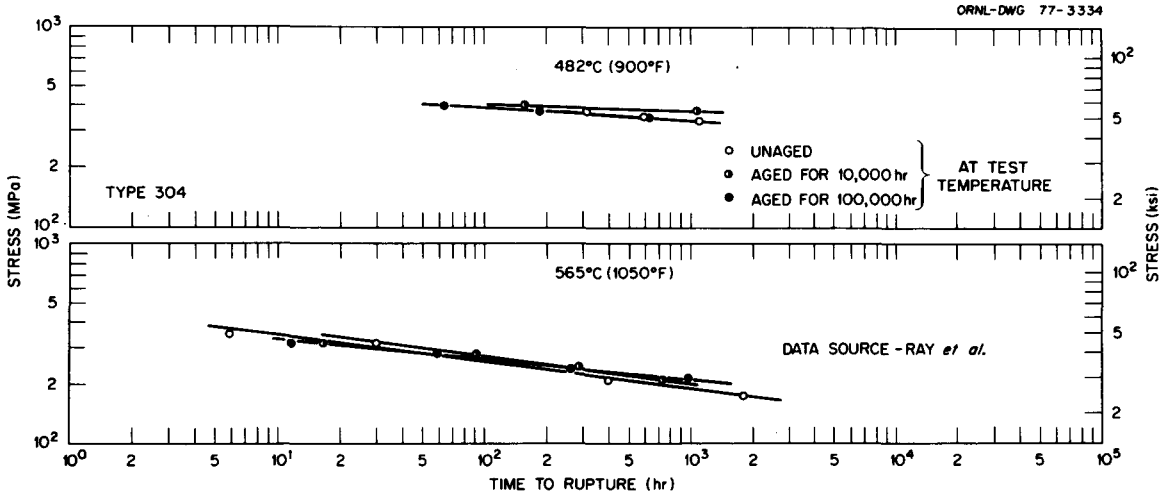

Fig. 39. Stress-Rupture Plots of Unaged and Aged Type 304 Stainless Steel. These data are taken from Ray et al. [38].

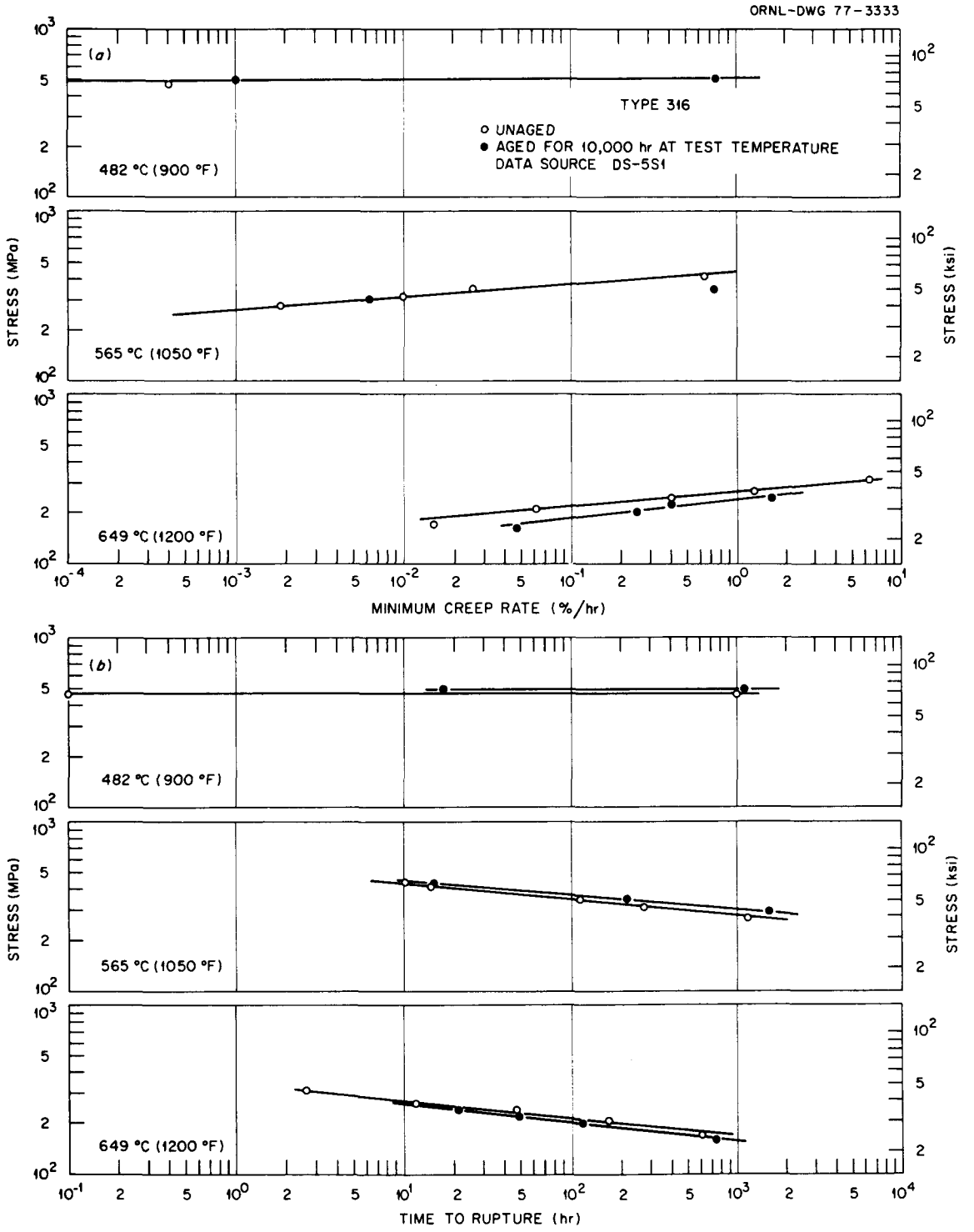

Fig. 40. Creep Properties of Unaged and Aged Type 316 Stainless Steel. (*a*) Stress versus minimum creep rate. (*b*) Stress versus time to rupture. These data are from DS-5S1 [*18*].

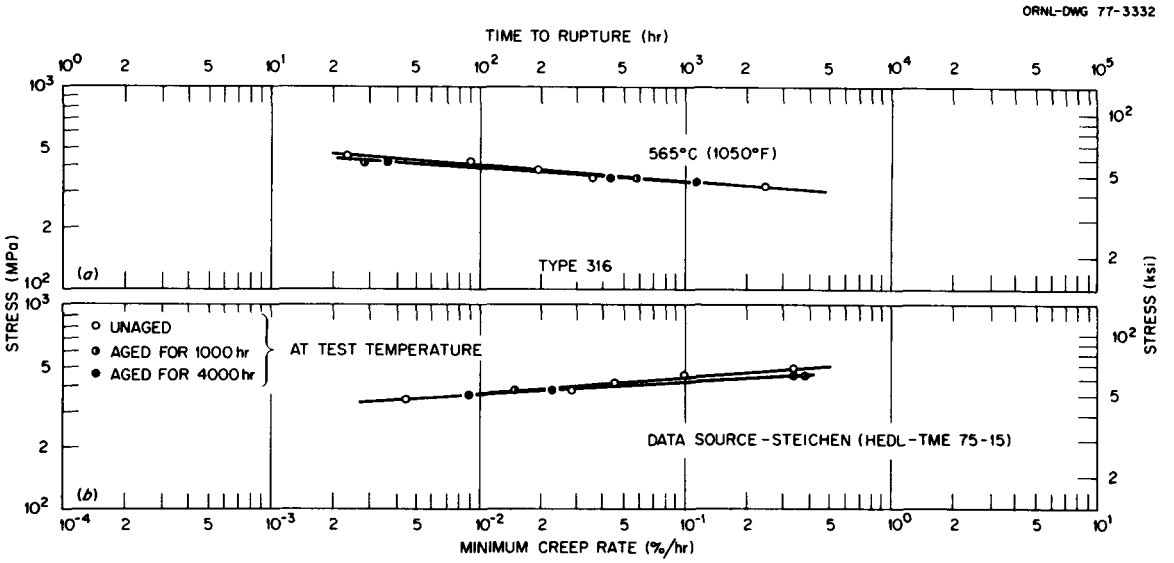

Fig. 41. Creep Properties of Unaged and Aged Type 316 Stainless Steel. (*a*) Stress versus time to rupture. (*b*) Stress versus minimum creep rate. These data are taken from the work of Steichen [41].

Figs. 42 and 43 show the effect of thermal aging conditions on creep properties of the reference heat (9T2796K) and another heat (346845). All creep tests were done at a test temperature of 593°C (1100°F) and a stress of 207 MPa (30 ksi). Figures 42 and 43 also show results obtained on material aged in both as-received and reannealed conditions. Thermal aging increases minimum creep rate for both heats with an increase in time to rupture for the reference heat and a decrease in time in rupture for heat 346845 (Figs. 42 and 43). The reference heat had a coarse grain size and was a weak heat; whereas heat 346845 had a fine grain size and accordingly was a strong heat of type 304 stainless steel. The changes produced in the reference heat as a consequence of a pretest aging treatment were much less than those for heat 346845 (Figs. 42 and 43). Aging at 649°C (1200°F) produced maximum changes in creep properties at a test temperature of 593°C (1100°F). Furthermore, for a given aging temperature, increasing exposure time increased the changes in time to rupture and minimum creep rate. For the same aging and test temperature [593°C (1100°F)], the short-term creep tests showed changes in time to rupture by a factor less than 2 and in minimum creep rate by a factor less than 10. The weak or strong character of a given heat is retained even after thermal aging (Fig. 44).

Long-term thermal aging had only a minimal effect on long-term creep tests of the reference heat and heat 346845. For creep stresses above the yield strength (Fig. 45) time to rupture for heat 346845 decreases from 14,077 to 10,630 hr and minimum creep rate increases from 1.6×10^{-4} to 4.4×10^{-4} % per hr. For the reference heat (Fig. 46) although minimum creep rate increased from 6.8×10^{-5} to 1.2×10^{-4} % per hr, time to rupture for the aged specimens appears to be increasing beyond that of the unaged specimen. Creep tests at stresses below the yield strength (Figs. 47 and 48) show only minor effects of thermal aging for test periods of 13,000 to 15,000 hr. The elevated-temperature ultimate tensile strength of the reference heat and heat 346845 changed from 357 to 350 MPa (5.18 to 50.7 ksi) and 322 to 323 MPa (46.7 to 46.9 ksi), respectively, for thermal aging of 10,000 hr at 593°C (1100°F).

In conclusion, we found that aging and subsequent testing at the same temperature [593°C (1100°F)] produces minimal changes in short-term ultimate tensile strength and short- and long-term creep properties

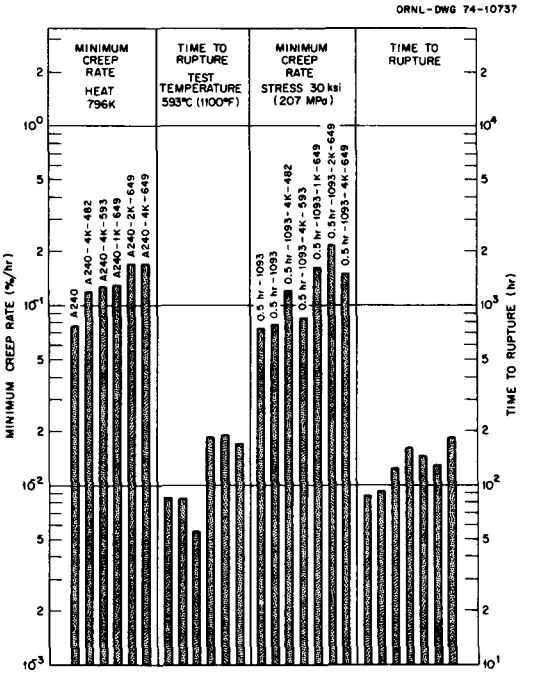

Fig. 42. Effect of Aging on Minimum Creep Rate and Time to Rupture at a Test Temperature of 593°C (1100°F) and a Stress of 30 ksi (207 MPa) for Heat 9T2796K Aged in Both As-Received and Reannealed Conditions. A240 stands for as-received condition and 0.5 hr-1093 for reannealed condition. Abbreviations 1K, 2K and 4K stand for aging times of 1000, 2000, and 4000 hr. Numbers 482, 593, and 649 are temperatures in °C and correspond to 900, 1100, and 1200°F. Number 796K is a short form of the heat number.

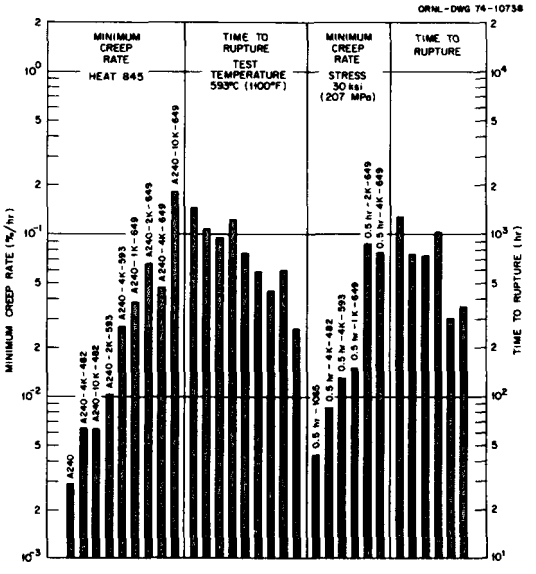

Fig. 43. Effect of Aging on Minimum Creep Rate and Time to Rupture at a Test Temperature of 593°C (1100°F) and a Stress of 30 ksi (207 MPa) for Heat 346845 Aged in Both As-Received and Reannealed Conditions. A240 stands for as-received condition and 0.5 hr-1065 for reannealed condition. Abbreviations 1K, 2K, and 4K stand for aging times of 1000, 2000, and 4000 hr. Numbers 482, 593, and 649 are temperatures in °C and correspond to 900, 1100, and 1200°F. Number 845 is a short form of the heat number.

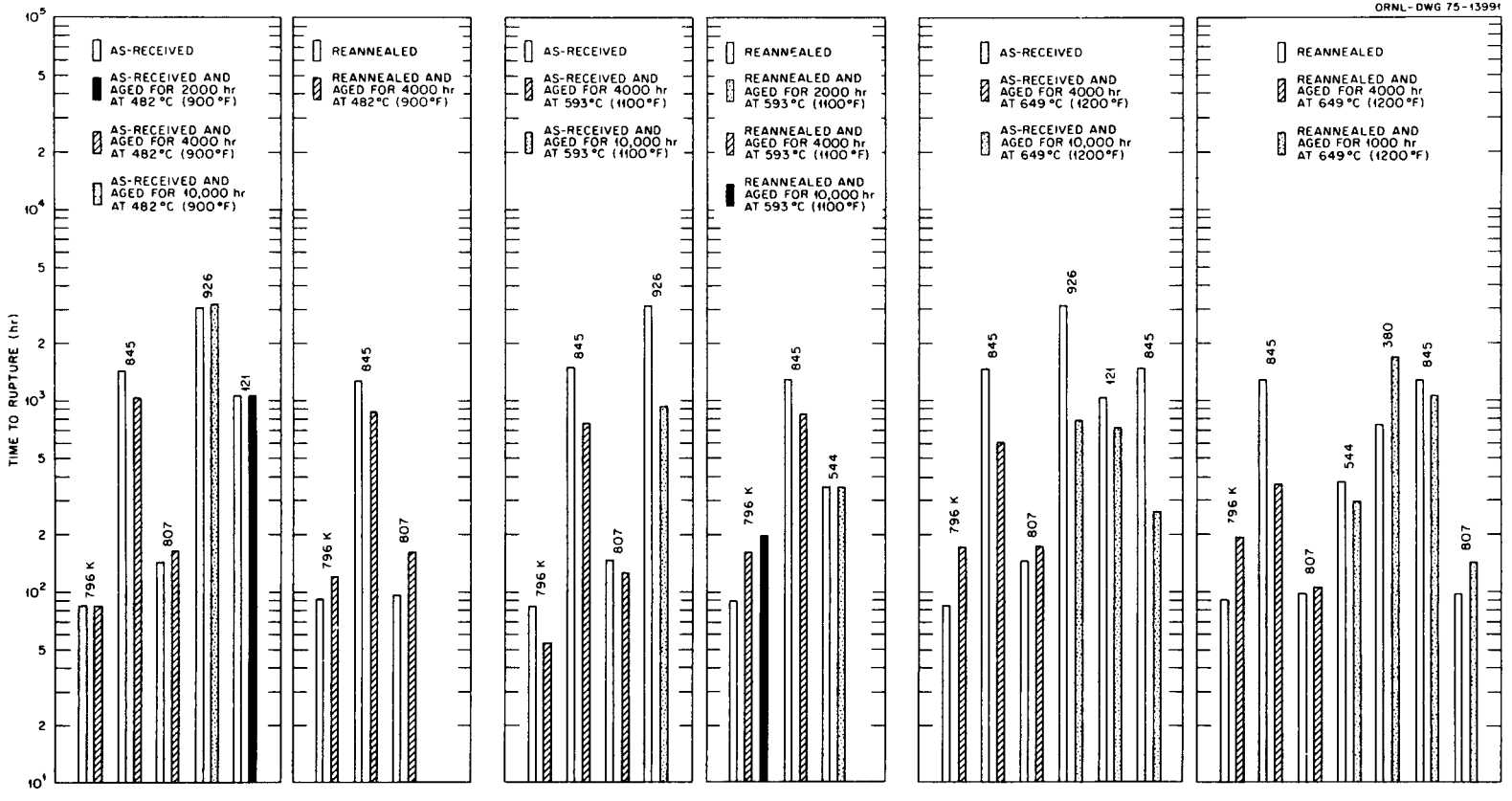

Fig. 44. Bar Charts Showing Heat-to-Heat Variation Observed in Unaged and Aged Conditions of Several Heats of Type 304 Stainless Steel. All tests were performed at 30 ksi (207 MPa) and 593°C (1100°F). Numbers above the bars are abbreviations for heat numbers, 9T2796K, 346845, X22807, R22926, 3121, and 346554 respectively.

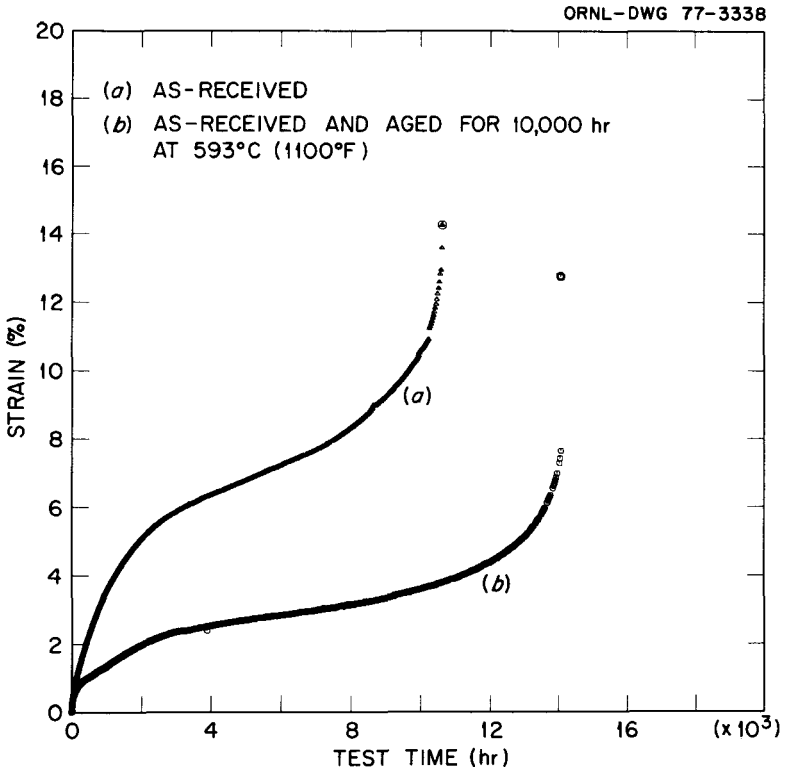

Fig. 45. Creep Curves at 593°C (1100°F) and 25 ksi (172 MPa) for Heat 346845 in Both Unaged and Aged Conditions. Aging was performed on as-received materials for 10,000 hr at 593°C (1100°F).

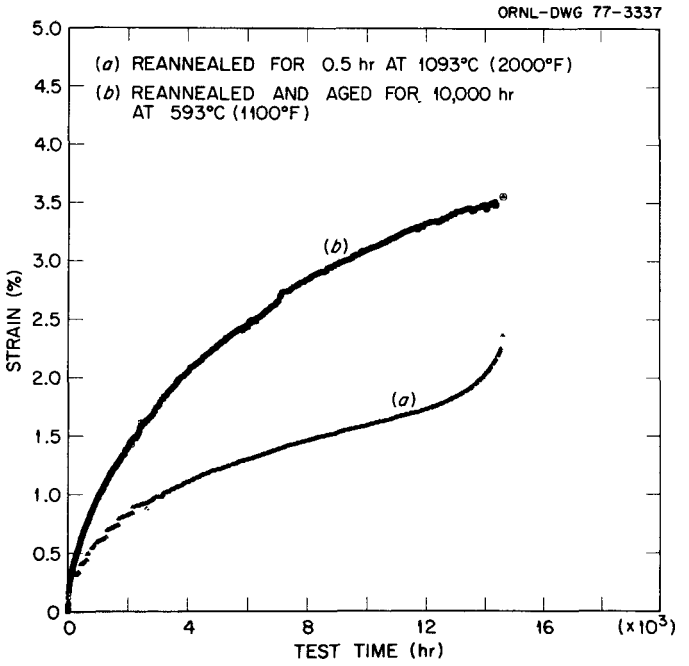

Fig. 46. Creep Curves at 593°C (1100°F) and 16 ksi (110 MPa) for Heat 9T2796K in Both Unaged and Aged Conditions. Aging was performed on reannealed material for 10,000 hr at 593°C (1100°F).

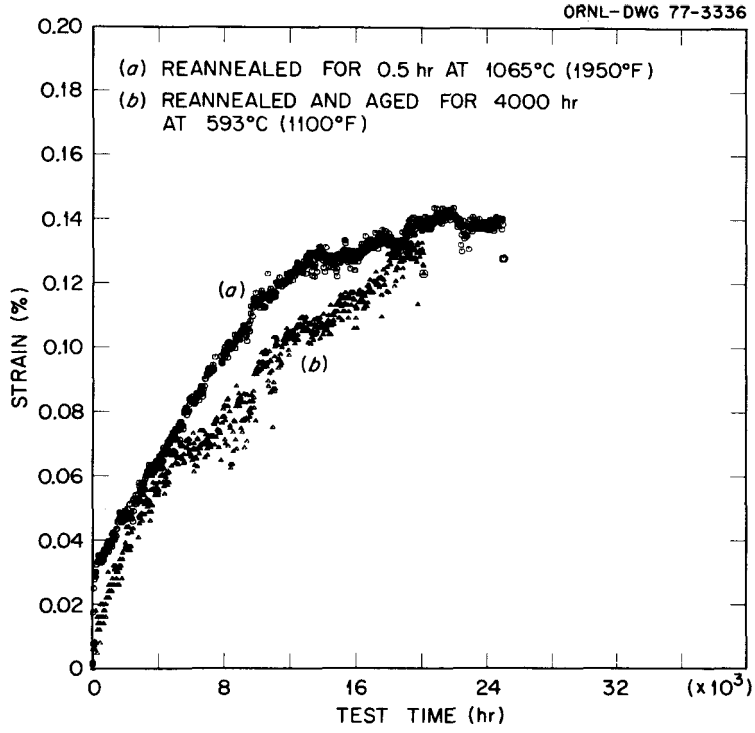

Fig. 47. Creep Curves at 593°C (1100°F) and 10 ksi (69 MPa) for Heat 346845 in Both Unaged and Aged Conditions. Aging was performed on reannealed material for 4,000 hr at 593°C (1100°F).

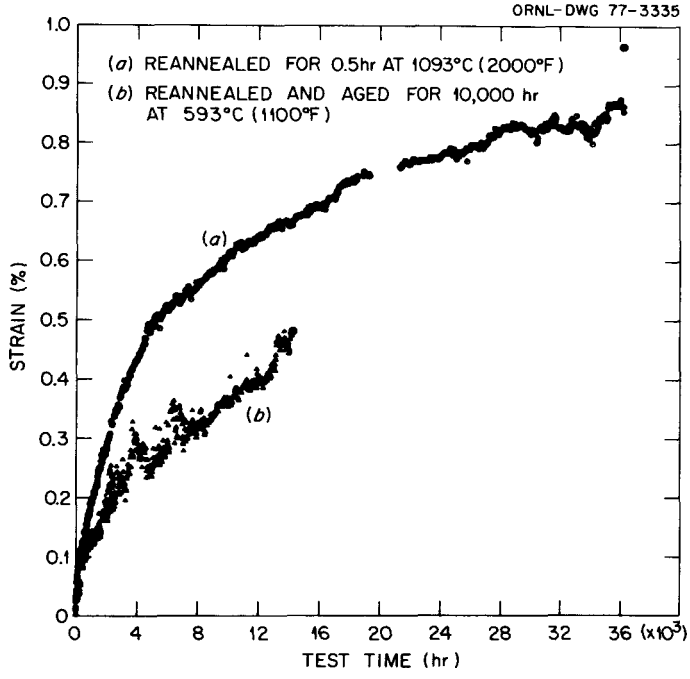

Fig. 48. Creep Curves at 593°C (1100°F) and 10 ksi (69 MPa) for Heat 9T2796K in Both Unaged and Aged Conditions. Aging was performed on reannealed material for 10,000 hr at 593°C (1100°F).

of type 304 stainless steel. Limited ORNL information on two heats of type 304 stainless steel for aging and testing at 649°C (1200°F) again showed only small changes in both short-term ultimate tensile strength and creep properties. The ORNL results presented above are consistent with those available in the literature[18,38–41] in that the effects of long-term prethermal exposure or aging on subsequent creep properties of types 304 and 316 stainless steel are minimal, depending upon individual heat chemistry and processing history. Work in progress is expected to provide additional information clarifying the roles of these last two variables.

5.2 SUBSTRUCTURAL DIFFERENCES BETWEEN TENSILE AND CREEP MODES OF DEFORMATION

Sherby and Dorn[11] suggested that a correlation between tensile and creep properties was possible because the same microstructures were observed for equal values of the Zener-Holloman parameter. Several substructural studies[42–45] on tensile and creep-tested specimens of types 304 and 316 stainless steel have shown that the dislocation substructure sizes have the following relationships:

$$\lambda(\text{cell}) \propto (Gb/S)^2 , \tag{30}$$

and

$$\lambda(\text{subgrain}) \propto Gb/S , \tag{31}$$

where

S = stress,

d = average dislocation cell or subgrain size,

G = shear modulus, and

b = Burger's vector.

Dislocation cell formation occurs at low temperatures where the deformation mode is glide controlled, whereas subgrains form at temperatures where the deformation mode is climb controlled and recovery can occur. However, these substructures form independently of the deformation mode (tensile or creep). Thus, relations given by Eqs. (30) and (31) suggest that if substructure controls the deformation, then elevated-temperature ultimate tensile strength and creep and creep-rupture properties are related. More work is needed to further clarify the role of substructure in various deformation modes resulting from high and low strain-rate deformation at temperatures approaching and within the creep range.

5.3 FRACTURE MODE DIFFERENCE BETWEEN SHORT-TERM TENSILE AND LONG-TERM CREEP

For austenitic stainless steels, the fracture mode observed from short-term tensile tests conducted at moderate to high strain rates is generally transgranular, whereas creep deformation generally produces an intergranular fracture. The transgranular fracture is accompanied by intragranular deformation whereas intergranular fracture is accompanied by grain-boundary deformation. The observed relationship between short-term elevated-temperature ultimate tensile strength and creep properties then suggests that

intragranular strength should relate to the intergranular or grain boundary strength. This observed relationship may also mean that the chemical composition and other factors which control the intragranular strength are also responsible for controlling the grain boundary strength. Manjoine,[46] while describing flow and fracture, has suggested that the relative strengths of grains and the boundaries are functions of the same factors.

The tensile reduction of area is a function of test temperature for heats of varying strength of types 304 and 316 stainless steel in terms of S_u (Fig. 49). The weak heats show a drop in ductility at temperatures in the creep range (temperature $\geq$538°C). This drop in tensile ductility is commonly referred to as the ductility minimum; Rhines and Wray[47] have offered the following explanation for it. At low temperatures, fracture occurs by the usual transgranular crack propagation mechanism, and ductility is high. At temperatures near the minimum, deformation occurs by grain-boundary shear and the intergranular voids formed at triple points grow unhindered, causing drastic loss in ductility. At high temperatures, recrystallization occurs simultaneously with intergranular void formation continuously breaking up the intergranular fracture path so that the ductility increases again.

The ductility minimum associated with intergranular crack initiation and propagation occurs in the weak heats and is postponed to a higher temperature in the strong heats (Fig. 48). Such an observation suggests that the strong heats also have higher grain-boundary strength during creep. It has already been shown that the strong heats in creep have higher ultimate tensile strengths. These two observations show that the inter- and intragranular strengths are related and are probably controlled by the same factors.[46] Such reasoning also supports the observed relationships between the short-term tensile and creep properties.

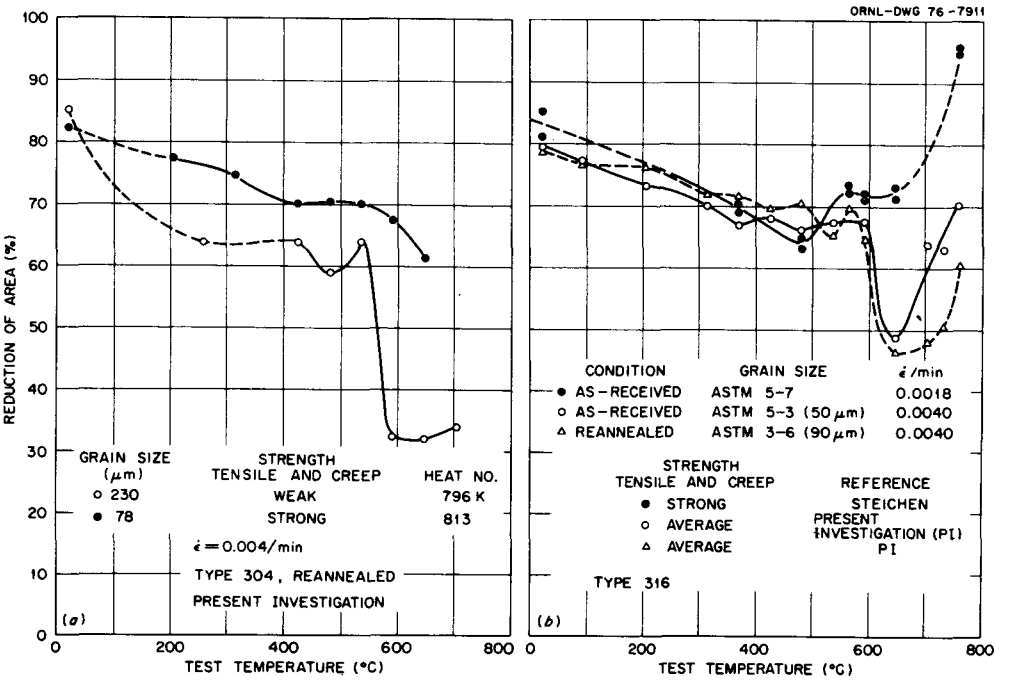

Fig. 49. Plot of Tensile Reduction of Area as a Function of Test Temperature for Type 304 and 316 Stainless Steel. (*a*) Effect of weak and strong heat on ductility minima for type 304. (*b*) Effect of heat strength on ductility minima for type 316.

6. DISCUSSION

6.1 IMPLICATION OF RESULTS

The empirical relationships described in Sect. 5 are useful in predicting creep and creep-rupture properties of an individual heat based on the knowledge of its elevated-temperature ultimate tensile strength. The generalized models of log t_r and log $\dot{e}_m$ in terms of S, T, and S_u were derived from data over a temperature range of 538 to 704°C (1000–1300°F) and for S_u values at the creep-test temperature obtained at a strain rate of 6.7×10^{-4} per sec. For S_u values given at any other strain rate, a correction must be applied (Appendix B).

The S_u models help to estimate creep properties more accurately than the models without S_u but cannot predict exactly the behavior of every individual heat. The exact description of an individual heat is not possible partially because of inherent experimental errors and scatter inherent in tensile and creep properties (Appendix C). Although the use of S_u provides a convenient, useful means for describing heat-to-heat variations for design purposes, it does not totally define all of the factors that influence creep strength.

Models derived in the present investigation were based mainly on short-term tests and a few tests approaching 40,000 hr and one 65,000 hr test. Although modelling of the data has suggested linear plots of log S versus log t_r and log S versus log $\dot{e}_m$, long-term testing (periods exceeding 50,000 hr) is needed to check these models. Such long-term tests are in progress at ORNL.

Results presented in this report also suggest that it *may* be possible to use elevated-temperature ultimate tensile strength as a characterization test.

6.2. IMPLICATIONS FOR ELEVATED-TEMPERATURE DESIGN AND MATERIALS ENGINEERING

This study had two objectives: (1) to determine if the elevated-temperature tensile strength of a given heat of type 304 or 316 stainless steel obtained from a short-term tensile test could be an index for predicting long-term time dependent behavior of that heat at temperatures within the creep regime and (2) to examine how such an index could be used in elevated-temperature design. The analysis presented in previous sections of this report supports the concept that strong heats (particularly of type 304 stainless steel), as determined by their elevated-temperature tensile strengths, also remain comparatively strong in creep and creep-rupture behavior. Further, it was shown that for type 304 stainless steel, ultimate strength factors could be incorporated into empirical relationships for creep rupture, minimum creep rate, creep strain, and time-to-tertiary creep. Therefore, estimates of the behavior of individual heats can be made once the elevated-temperature tensile strength is known.

Elevated-temperature design to prevent failure by one or more of the several possible failure mechanisms guarded against by the ASME code uses stress- or strain-limit values which are arrived at by multiplying minimum property values by factors of safety. However, constitutive equations for depicting flow behavior presently use average material properties. Furthermore, the cost of using time-dependent analysis is high, probably an order of magnitude greater than time-independent analysis for LMFBR design conditions.[48]

As was indicated in the introduction, variability in creep deformation properties for type 304 stainless steel is high (e.g., minimum creep rates can vary by factors as high as 140–200). Consequently, there may

be instances when greater assurance is required for a given heat than is given by simply using average and indirectly minimum properties. Also, it may be desirable to more closely match the properties of several heats used in a multi-heat component such as a pressure vessel. Thus better defined relationships which can give guidance concerning individual heat behavior on a comparative basis have high value.

In a sensitivity study done at ORNL in conjunction with the analysis of a pipe ratchetting experiment[49] (TTT-1) (Fig. 50), the pipe specimen from the ORNL reference heat (heat 9T2796) was

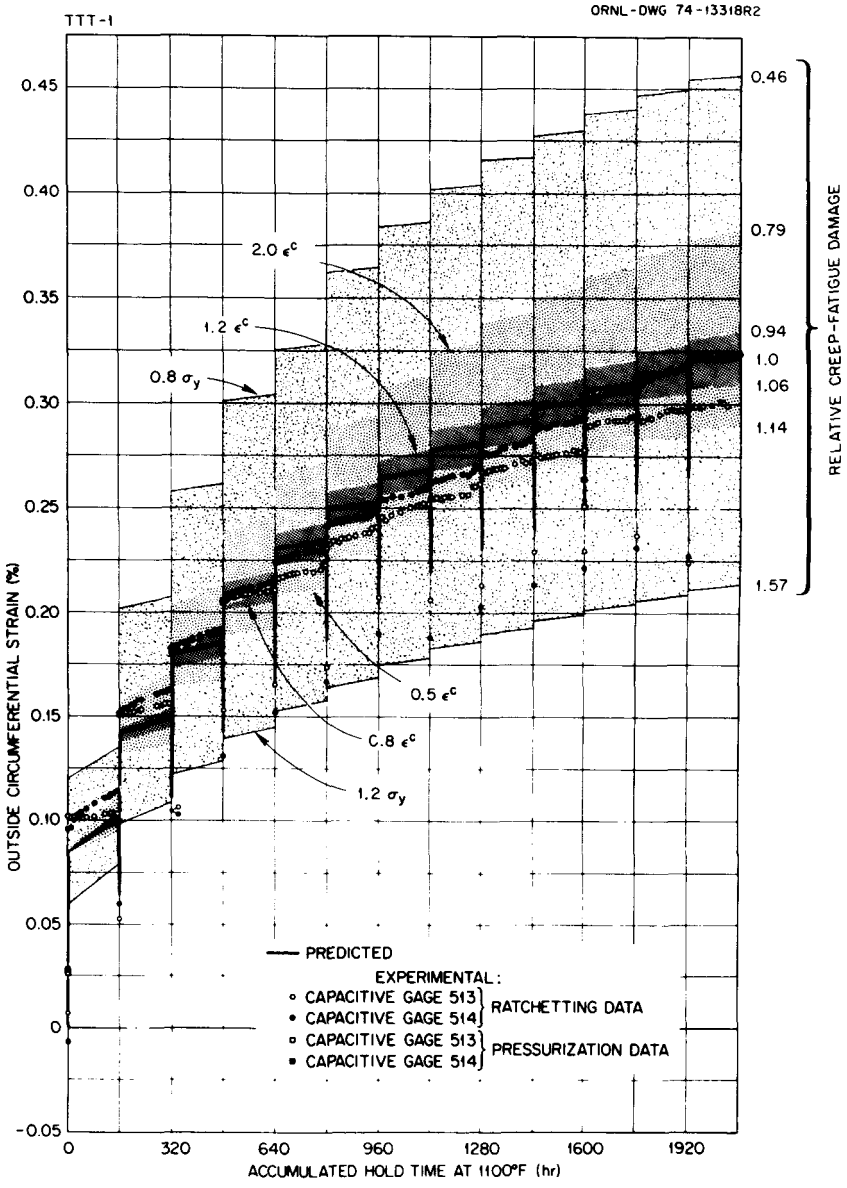

Fig. 50. Comparison of Measured and Predicted Circumferential Ratchetting Strains for Pipe Thermal Ratchetting Test TTT-1. The solid prediction curve is based on the best available elastic-plastic and creep data for the specimen material. The extremes of the shaded bands represent predictions based on increasing or decreasing the yield stresses and the creep strain response as indicated. The relative creep-fatigue damage factors shown to the right were calculated according to the inelastic analysis rules of Code Case 1592. This figure illustrates the range of behavior that can result from normal heat-to-heat material variations.

tested; the cyclic stress-strain and creep data used in calculating the predicted pipe outside circumferential ratchetting strain were also from this heat of type 304 stainless steel. The differences between predicted and observed circumferential ratchetting strain are small when the known properties of this heat of material were used. However, the designer usually has no way of knowing the specific properties of the heat of material he is dealing with. Therefore, in this study the predictive calculations were repeated with variations of the yield strength, σ_y (up to ± 20%), and creep strain, ϵ_c (up to ± a factor of 2), response from mean values. Large deviations from experimental results in both calculated ratchetting strains and creep-fatigue damage factors are possible when typical uncertainties in the data are introduced into the calculations. Therefore, mechanical property correlations which can more closely predicate individual heat behavior are advantageous in design calculations.

Turning next to the materials engineering and alloy development benefits, consider again the mechanical properties of two heats of type 304 stainless steel:

A comparison of heat 8043813 with heat 9T2796 using the appropriate tensile strengths, shows the former to be stronger (Table 5). Comparisons between the creep-rupture and minimum creep-rate properties of these two heats by actual data and by the indicated mathematical formulations (Figs. 51 and 52) show heat 8043813 to be the stronger in stress-rupture properties throughout the data range and beyond. Heat 8043813 is consistently the most creep resistant (lower creep rate at a given stress and temperature) of the two.

Table 5. Mechanical Properties of two heats of type 304 stainless steel

	Heat 8043813	Heat 9T2796
Yield strength (room temperature)[a] A240/annealed[b] (MPa)	214/204	187/185
Tensile strength (room temperature)[a] A240/annealed[b] (MPa)	637/605	515/540
Yield strength (593°C)[a] A240/annealed[b] (MPa)	105/82	101/70
Tensile strength (593°C)[a] A240/annealed[b] (MPa)	345/354	328/322
Yield strength (649°C)[a] A240/annealed[b] (MPa)	112/79	93/72
Tensile strength (649°C)[a] A240/annealed[b] (MPa)	285/300	281/277
Niobium content, wt %	0.02%	0.008%
Grain size (ASTM)	4	<1

[a]Strain rate 0.04 per min unless specified otherwise.
[b]Annealed is for 0.5 hr at 1065°C. As received indicated by the ASTM specification by which fabricated (A240 for plate).

Several years ago,[50] elevated-temperature fatigue and creep-fatigue tests were run on heat 8043813 and heat 9T2796 along with several other heats (Fig. 53). As the duration of the hold period increases for each cycle, the time to failure increases and generally the number of cycles to failure decreases for a given strain range (Fig. 53). However, for heat 8043813 (dashed lines, Fig. 53) the reduction in fatigue life with increasing duration of the tensile hold period is minimal compared with that of the other heats. Simply stated, heat 8043813 has good creep-rupture and remarkably good creep-fatigue resistance in comparison to other heats of type 304 stainless steel. Probably this is due to differences in residual element content, especially niobium.

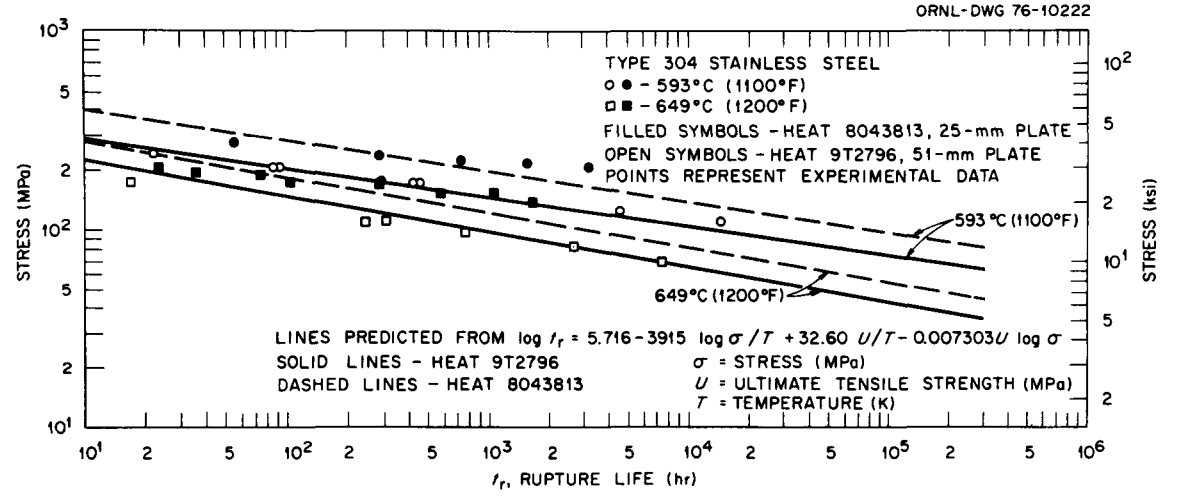

Fig. 51. Comparisons of the Stress-Rupture Properties of Two Heats of Type 304 Stainless Steel at 593°C (1100°F) and 649°C (1200°F).

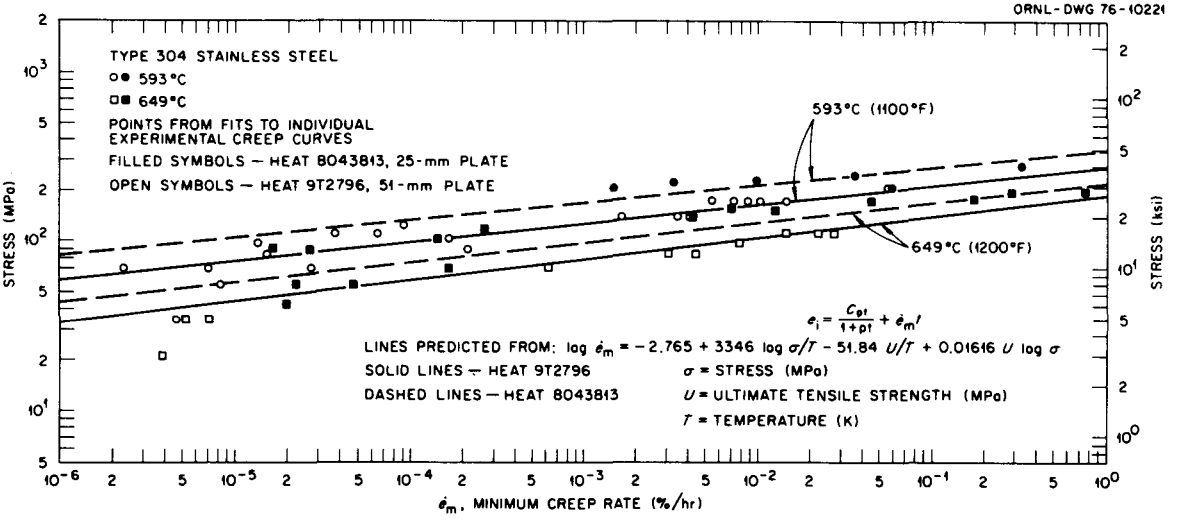

Fig. 52. Comparisons of the Minimum Creep-Rate Properties of Two Heats of Type 304 Stainless Steel at 593°C (1100°F) and 649°C (1200°F).

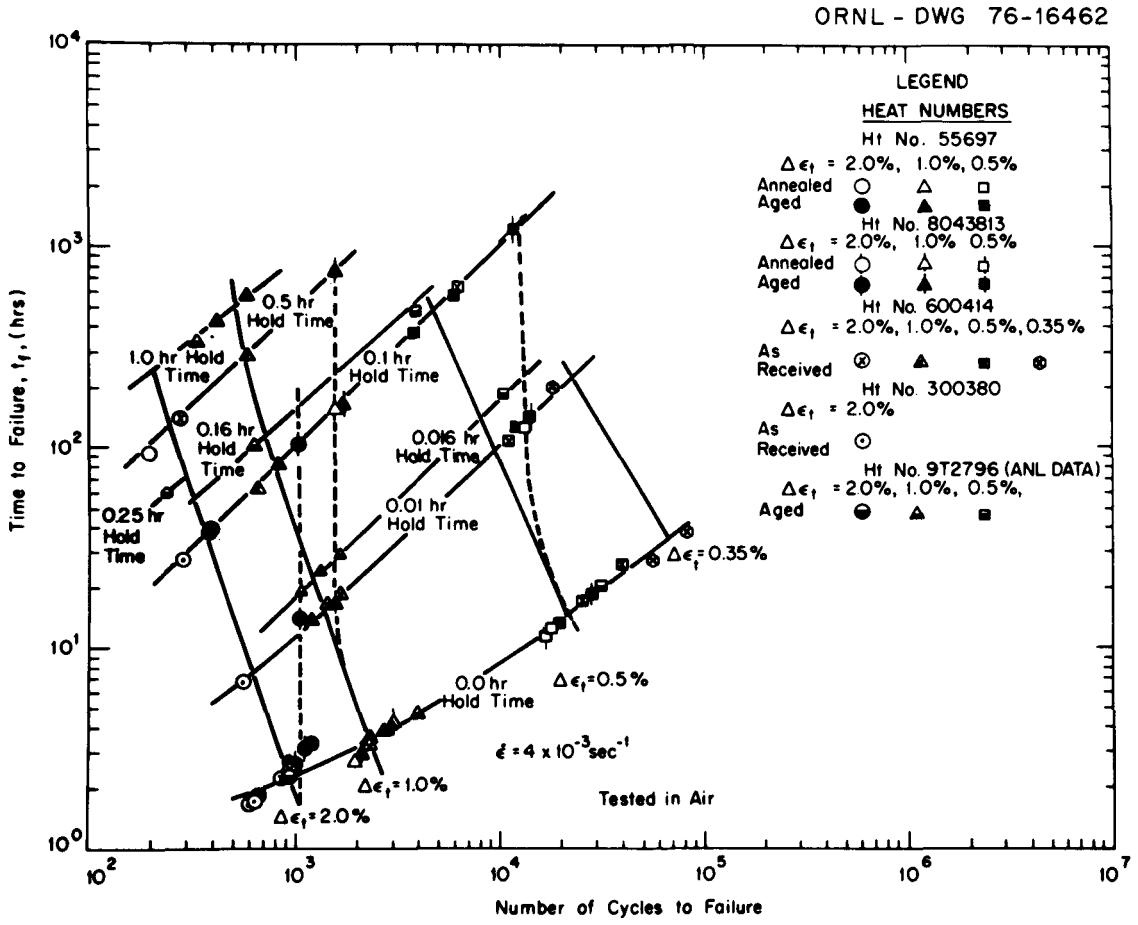

Fig. 53. Time to Failure Versus Number of Cycles to Failure for Five Different Heats of 304 Stainless Steel Tested at 593°C (1100°F) with Various Tensile Hold Times. This data from tests with either continuous cycling (zero hold time) or tension-only hold periods for those periods indicated in fully reversed strain-controlled cycling.

That niobium content affects creep behavior of type 304 stainless steel is clearly shown by plotting the time to rupture values of several different heats of material tested at 593°C (1100°F) and 206.8 MPa (30 ksi) against the niobium content (Fig. 54); increasing the niobium content improves the stress-rupture properties. Niobium is a ferrite, sigma, and chi phase former (>0.5%)[51,52] and when found in steels is usually found as a carbide or a nitride. The superior creep-fatigue resistance of heat 8043813 is due probably to the presence of a fine precipitate of niobium carbide (Nb_4C_3 or NbC) or nitride at the grain boundaries. These precipitates strengthen the grain boundaries by possibly restricting sliding and reducing cavitation,[53,54] thereby providing additional resistance to intergranular crack propagation. This suggests that controlled small additions of this element might improve the overall time-dependent mechanical properties of type 304 stainless steel. However, the additions would have to be small if the resulting product forms were to be weldable, since it has been clearly shown that heat-affected zone cracking in weld joints of type 347 stainless steel[54] was due to the presence of as little as 0.10% niobium. Further, fusion line porosity has occasionally been noted in welding types 321 and 347 stainless (Nb > 0.4%) due to thermally induced disassociation of the niobium carbonitrides. Work is in progress to vary the niobium concentration in several experimental alloys to determine if an optimum niobium concentration can be found.

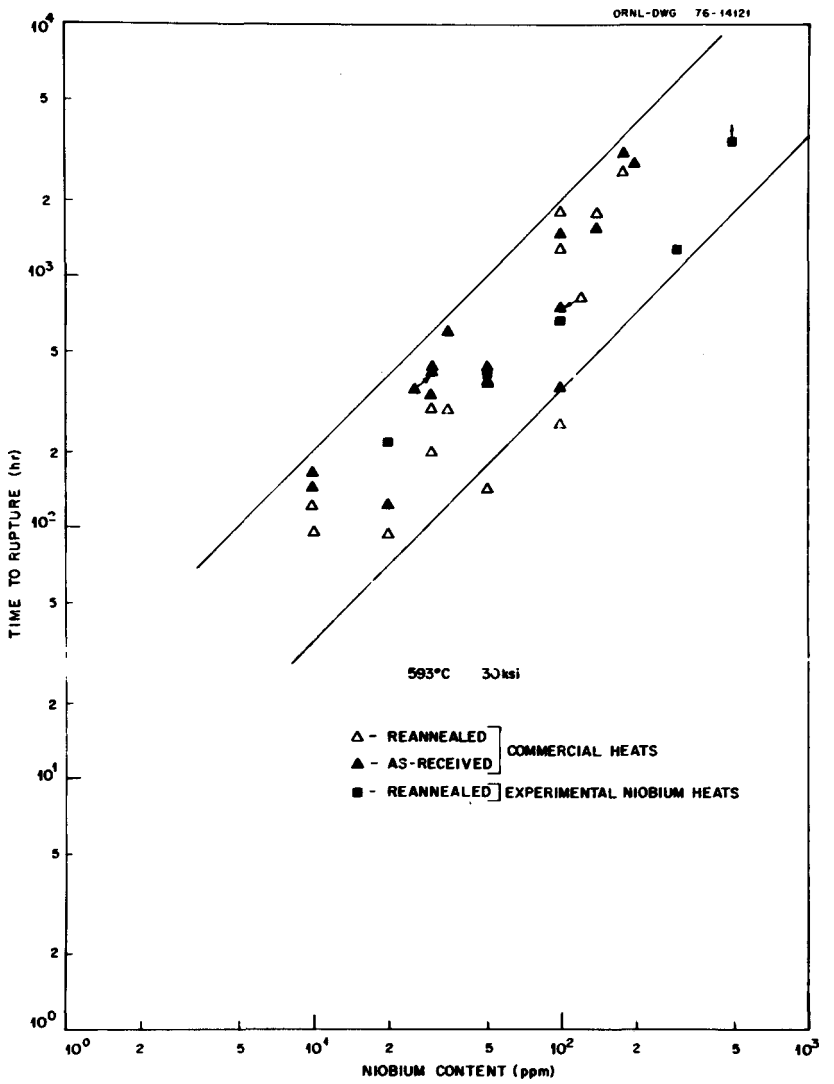

Fig. 54. Time-to-Rupture as a Function of Niobium Content for Several Commercial and Experimental Heats of Type 304 Stainless Steel Tested at 593°C (1100°F) at 207 MPa (30 ksi).

Variations in other residual elements besides niobium can also influence the strength, and therefore account for heat-to-heat variations in the mechanical properties of the austenitic stainless steels. Titanium in concenrations of about 0.14 to 0.15% (wt) in 304 stainless steel increases creep-rupture strength and lowers minimum creep rates.[55] Also, carbon and nitrogen content as well as grain size affect properties of types 304 and 316 stainless steel (Figs. 55 and 56).

Still another indication that relative strengths of these types of materials tend to remain constant as the elevated-temperature test time increases can be seen in Figs. 57 and 58. The scatter band of the ultimate strengths of many heats of type 316 stainless can be plotted as a function of temperature (Fig. 57). The average as well as maximum and minimum expected values are defined in comparison with the current Nuclear Systems Materials Handbook minimum expected values for type 316 stainless steel (Fig. 57). Also superimposed on the plot (Fig. 57) are the ultimate strength values of specimens taken from fabricated 16-8-2 stainless steel submerged-arc weld metal. Comparison of the data shows that the weld metal is

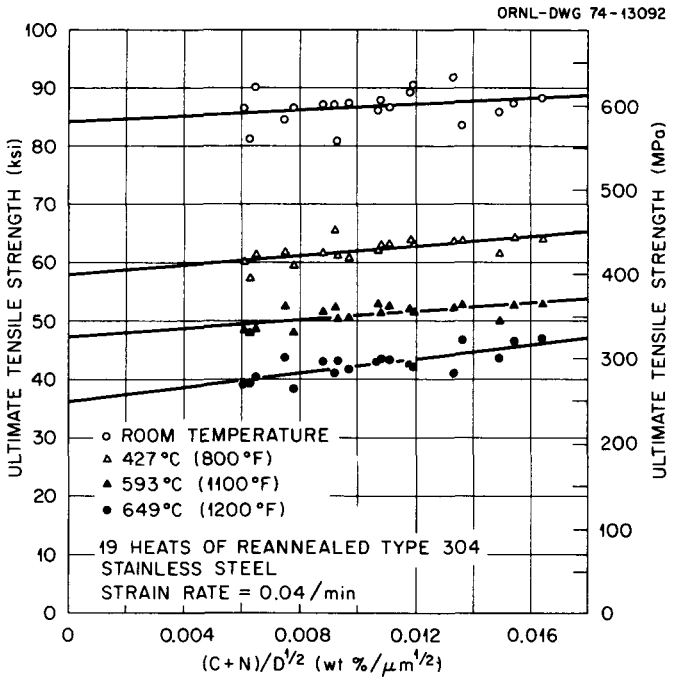

Fig. 55. Plot of Ultimate Tensile Strength as a Function of $(C + N)d^{-1/2}$ for 19 Heats of Type 304 Stainless Steel.

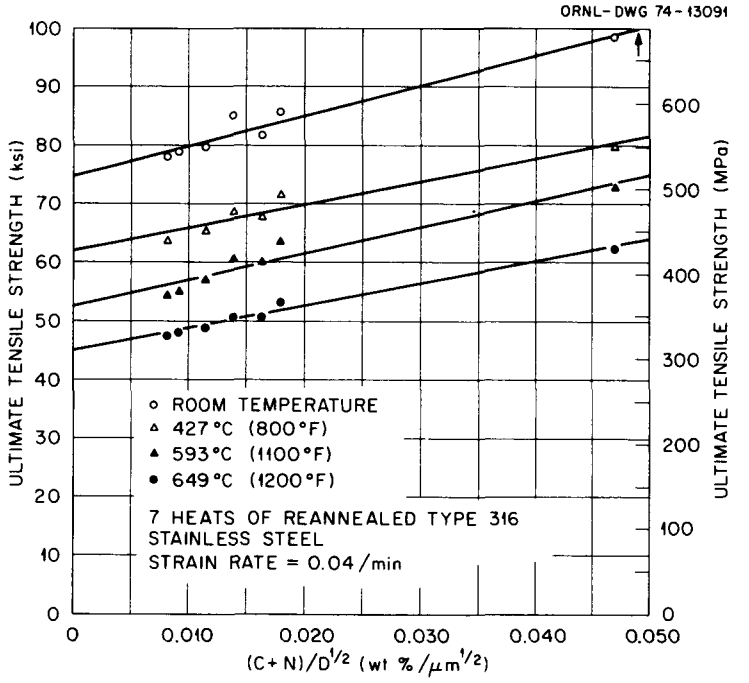

Fig. 56. Plot of Ultimate Tensile Strength as a Function of $(C + N)d^{-1/2}$ for Seven Heats of Type 316 Stainless Steel.

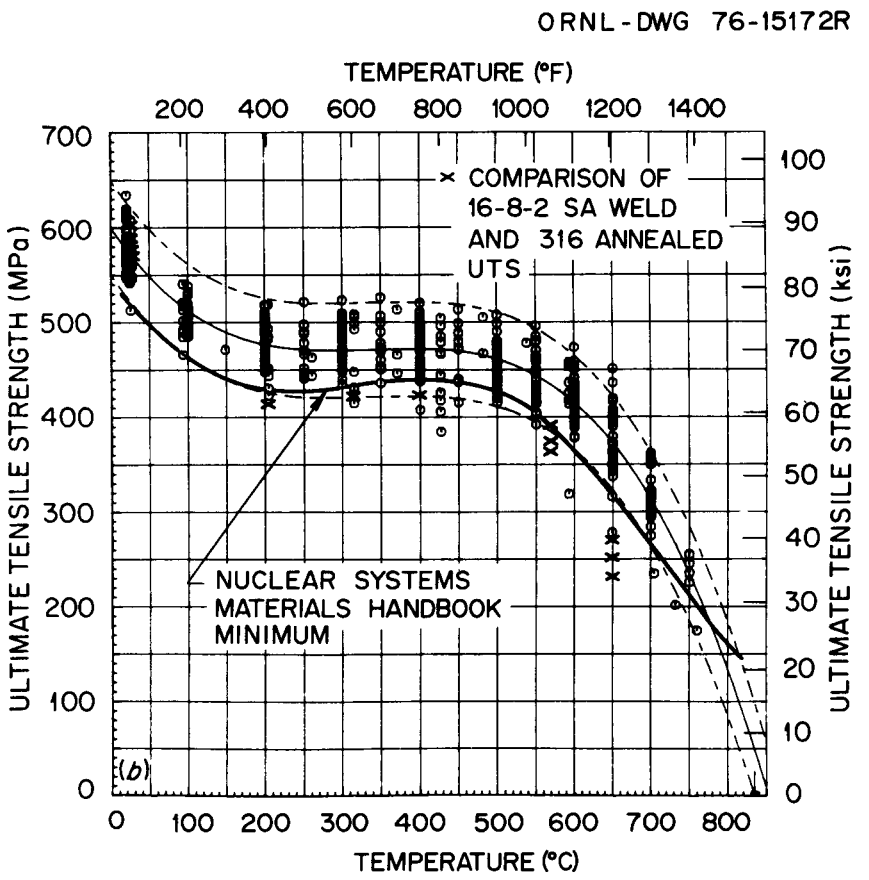

Fig. 57. Comparison of the Ultimate Tensile Strengths of Type 316 Stainless Steel and 16-8-2 Weld Metal as a Function of Temperature. The symbol o indicates type 316 stainess; x indicates 16-8-2 weld metal.

generally weaker in short term tensile tests than the base material, that is, type 316 stainless (Fig. 58). Again experimental results available so far show the stress-rupture values for 16-8-2 stainless steel to be generally below or within the lower half of the scatter band for type 316 stainless steel base material.

Summarizing, heat-to-heat variability in the elevated-temperature mechanical properties of the austenitic stainless steels is due to many factors; however, these factors are being identified and relationships have been formulated which will allow the designer as well as the materials engineer greater certainty in estimating long-term individual heat behavior. Again, however, it should be emphasized that the methods presented herein should *not* be taken as a substitute for long-term experimental data. The designer and manufacturer who are anxious to proceed safely with design and construction of elevated-temperature energy conversion systems generally consider data in the range of 10^4 to 10^5 hrs to be long-term information. However, owners and operators require information about material behavior in terms of 30 to 40 years of useful service life, and they, in turn, may become much concerned about the low stress temperature induced changes that may be only partially reflected in short-term test results. This situation may be particularly true when a new generation of engineers faces the economic decision of whether or not to continue operation or replace an expensive unit that was designed and built by the preceding generation. Accordingly, in the interim until more long-term data and documented service experience become available, methods for estimating material behavior in the elevated-temperature regime have great value, but must be used with care.

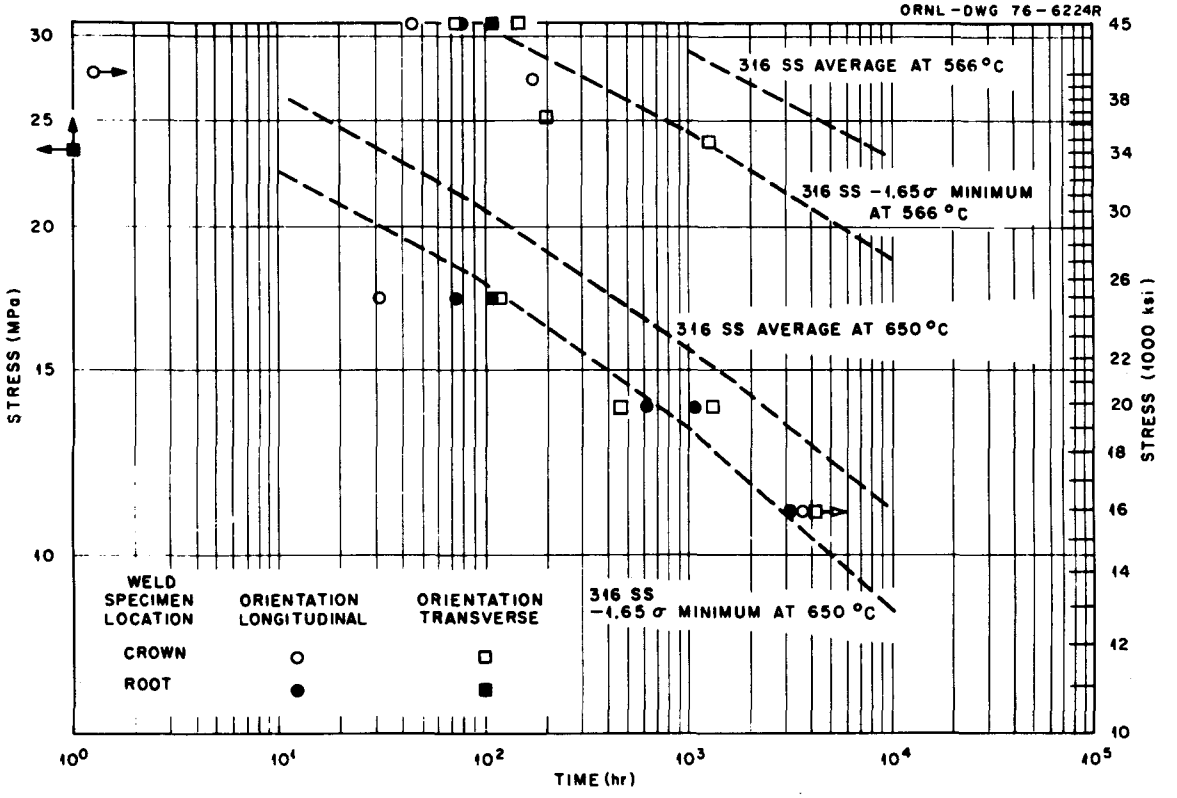

Fig. 58. Comparison of Creep-Rupture Properties of Type 16-8-2 Stainless Steel Submerged-Arc Weld Specimens with Type 316 Stainless Steel Base Metal (After Blackburn).

7. SUMMARY AND CONCLUSIONS

Elevated-temperature tensile and creep properties for several heats of types 304 and 316 stainless steel were used to show that ultimate tensile strengths obtained at the creep-test temperature and at a fixed strain rate can be used as an index for correlating and estimating creep and creep-rupture properties. The following are general observations and conclusions:

1. A literature search showed that several past investigations in both the United States and the USSR attempted to correlate short-term tensile properties with long-term creep properties. The USSR study was done on 116 different materials and used a linear relationship between tensile and creep properties as opposed to an exponential relation observed in this study and by other investigators in the United States.

2. Ultimate tensile strength (S_u) and creep and creep-rupture strength ($S_{1\%}{}^t$ and $S_r{}^t$) were related by:

$$S_{1\%}{}^t = \alpha_1 \exp(\beta_1 S_u) ,$$

and

$$S_r{}^t = \alpha \exp(\beta S_u) .$$

Both of the above relations were independent of test temperature and were observed to be appropriate in the range of 538–816°C (1000–1500°F).

3. Stress-rupture isotherms constructed with and without ultimate tensile-strength terms for 20 heats of type 304 stainless steel indicated that ultimate tensile-strength corrections could rearrange heats according to their strength, and thereby minimize the uncertainty in predicting the creep properties of an individual heat.

4. Generalized models for time to rupture (t_r) and minimum creep rate ($\dot{e}_m$) in terms of stress (S), temperature (T), and ultimate tensile strength (S_u), derived from Oak Ridge National Laboratory (ORNL) data[1] on 20 heats of type 304 stainless steel were:

$$\log t_r = 5.716 - \frac{3915}{T} \log S + 32.60 \frac{S_u}{T} - 0.007303\, S_u \log S \ , \tag{9}$$

and

$$\log \dot{e}_m = -2.765 + \frac{3346}{T} \log S - 51.84 \frac{S_u}{T} + 0.01616\, S_u \log S \ , \tag{10}$$

with S and S_u in MPa and T in K. The S_u values for ORNL data were measured at a strain rate of 6.67×10^{-4} per sec.

5. Time-to-rupture data for type 316 stainless steel showed less variation than data for type 304, and the effectiveness of an ultimate tensile-strength term (S_u) in creep-rupture models was reduced in comparison to type 304 stainless steel. However, for minimum creep rate, heat-to-heat variations were almost twice those found for t_r and the following model containing S_u was obtained:

$$\text{Log}\, \dot{e}_m = -3.534 + 2.0734 \log S - 45.064 \frac{S_u}{T} + 0.01836\, S_u \log S \ , \tag{16}$$

with S and S_u in MPa and T in K.

6. Visual inspection of the maximum-minimum value bands derived from $S_u \pm$ twice the standard error of estimate in S_u, showed them to be in close agreement with total heat-to-heat variations observed in t_r and $\dot{e}_m$ for type 304 stainless steel. Close agreement was also observed for predicting or accounting for heat-to-heat variations in Japanese data.[22]

7. Comparisons between the experimental data on t_r and $\dot{e}_m$ and the values estimated from generalized models with and without S_u showed that data from models containing an S_u term always agreed more closely with the experimental data than did the values from models without an S_u term.

8. Elevated-temperature ultimate tensile-strength values were used in estimating creep strain-time behavior of individual heats. Agreements was generally close between the experimental creep curves for short-term creep tests on 20 heats of type 304 stainless steels and those curves estimated with maximum, minimum, and average values of S_u. Agreement was also close for long-term creep tests, approaching 40,000 hr. Further, the creep equation containing S_u terms is a way to compute average and minimum isochronous stress-strain curves.

9. Inclusion of an S_u term in t_r and $\dot{e}_m$ models or a creep equation can reduce the uncertainty in predicted values but cannot define behavior exactly. Inherent experimental errors in both the tensile and creep properties as well as other complicating metallurgical factors introduce some measure of uncertainty. These factors such as residual element chemistry are being investigated and will be addressed in subsequent reports.

10. The present investigation has shown that a linear model (log-log coordinates) describes the log S vs log t_r and log S vs log $\dot{e}_m$ plots. However, more long-term creep data for periods extended to >50,000 hr are required to check the validity of linear models.

ACKNOWLEDGMENTS

The authors gratefully acknowledge R. H. Baldwin and E. B. Patton for doing the creep tests, L. T. Ratcliff for doing the tensile tests, D. O. Hobson and J. R. Ellis for reviewing, P. Patriarca and G. M. Slaughter for approving the report, George Griffith for editing, and M. S. Guy for typing the manuscript.

APPENDIX A

Data Summaries

Table A.1. Creep-rupture-strength data for type 304 stainless steel

Data	Temperature		Creep rupture strength (MPa)			Ultimate tensile strength MPa	Data source
	°C	°F	10^3 hr	10^4 hr	10^5 hr		
				Type 304			
1	538	1000	222	167	119[a]	376	ORNL
2	538	1000	308			421	ORNL
3	538	1000	239			379	ORNL
4	593	1100	150	110	84[a]	322	ORNL
5	593	1100	226	193		354	ORNL
6	593	1100	166	124		333	ORNL
7	593	1100	157	112	74[a]	340	ORNL
8	593	1100		134		337	ORNL
9	593	1100	212			360	ORNL
10	593	1100	214	176		357	ORNL
11	593	1100	169	131		336	ORNL
12	593	1100	197			350	ORNL
13	593	1100	191	139		360	ORNL
14	593	1100	190	135	91[b]	356[c]	AR-2
15	593	1100	152			352	DS-5S1
16	593	1100	190			401	DS-5S1
17	593	1100	207			354	DS-5S1
18	593	1100	207			387	DS-5S1
19	593	1100		182		345	DS-5S1
20	649	1200	93	71	52[a]	277	ORNL
21	649	1200	103	68	43[a]	282	ORNL
22	649	1200	112			269	ORNL
23	649	1200	157			300	ORNL
24	649	1200	121	83	55[b]	311[c]	AR-2
25	649	1200	97			296	DS-5S1
26	649	1200	141			333	DS-5S1
27	649	1200	151			354	DS-5S1
28	649	1200			90[d]	332[c]	Spaeder and Defilppi
29	649	1200			85[d]	328[c]	Spaeder and Defilppi
30	649	1200			76[d]	334[c]	Spaeder and Defilppi
31	649	1200			76[d]	320[c]	Spaeder and Defilppi
32	649	1200			74[d]	330[c]	Spaeder and Defilppi
33	649	1200			72[d]	334[c]	Spaeder and Defilppi
34	649	1200			67[d]	334[c]	Spaeder and Defilppi
35	649	1200			74[d]	324[c]	Spaeder and Defilppi
36	649	1200			72[d]	334[c]	Spaeder and Defilppi
37	649	1200			79[d]	340[c]	Spaeder and Defilppi
38	649	1200			92[d]	356[c]	Spaeder and Defilppi
39	649	1200			99[d]	340[c]	Spaeder and Defilppi
40	649	1200			98[d]	334[c]	Spaeder and Defilppi
41	649	1200			96[d]	340[c]	Spaeder and Defilppi
42	704	1300	64	42		228	ORNL
43	704	1300	64	45		215	ORNL
44	704	1300	63			248	DS-5S1
45	704	1300	60			243	DS-5S1
46	732	1350	82			246	DS-5S1

Table A.1 (continued)

Data	Temperature		Creep rupture strength (MPa)			Ultimate tensile strength MPa	Data source
	°C	°F	10^3 hr	10^4 hr	10^5 hr		
47	760	1400	41			192	DS-5S1
48	816	1500	29			152	DS-5S1
49	816	1500	27			145	DS-5S1
				Type 304H			
50	593	1100	207			387	DS-5S1
51	593	1100	207			354	DS-5S1
52	649	1200	141			333	DS-5S1
				Type 304L			
53	550	1020	157	100	69[e]	354[f]	SWISS
54	593	1100	108	70	45[e]	328[f]	SWISS
55	649	1200	77	48	30[e]	289[f]	SWISS
56	704	1300	54	35	19[e]	246[f]	SWISS
57	750	1380	41	22	<7[e]	206[f]	SWISS
58	565	1050	172			348	DS-5S1
59	649	1200	117			295	DS-5S1
				Type 304LN			
60	565	1050	190			383	DS-5S1
61	649	1200	133			340	DS-5S1

[a]Data extrapolated from tests of duration 10,000 hr and less. MCM method used for extrapolation.

[b]Linearly extrapolated on log-log plot from data up to 65,000 hr.

[c]Ultimate tensile strength known only at room temperature. The elevated-temperature values were obtained by using tensile-strength ratio data from DS-5S2.

[d]Extrapolation method not known.

[e]Data not extrapolated. Obtained from 11-year-long creep testing.

[f]No tensile data available. Elevated-temperature tensile-strength values were obtained by using the average room temperature. Value and the ultimate tensile-strength ratio data from DS-5S2.

Table A.2. Summary of creep-rupture-strength data for type 316 stainless steel

Data	Temperature		Creep rupture strength (MPa)			Ultimate tensile strength	Data source	
	°C	°F	10^3 hr	10^4 hr	10^5 hr	MPa		
				Type 316				
1	538	1000	310			456		HEDL
2	550	1020	359			486		Bloom-ORNL
3	593	1100	325			501		ORNL
4	593	1100	245			418		ORNL
5	593	1100	240			393		ORNL
6	593	1100	228			366		ORNL
7	593	1100	193	138		425		Spaeder and Brickner
8	593	1100	200	159		419		Spaeder and Brickner
9	593	1100	228			434		DS-5S1
10	593	1100	234			434		DS-5S1
11	593	1100	241			421		DS-5S1
12	593	1100	234			398		DS-5S1
13	649	1200	159			308		HEDL
14	649	1200	162			328		Bloom-ORNL
15	649	1200	172			417		DS-5S1
16	649	1200	155	114		341		DS-5S1
17	649	1200	191	123		335	DS-5S1	DS-5S1
18	649	1200	155			332		DS-5S1
19	649	1200	145			341		DS-5S1
20	649	1200	160	128		360		Cullen and Davis
21	649	1200	149	121		345		Cullen and Davis
22	649	1200	175	128		376		Cullen and Davis
23	649	1200	201	146		405		Cullen and Davis
24	704	1300	90	59		319		Spaeder and Brickner
25	704	1300	124	83		310		Spaeder and Brickner
26	704	1300	117			317		DS-5S1
27	704	1300	122			346		DS-5S1
28	732	1350	83	51		231		DS-5S1
29	732	1350	76			236		DS-5S1
30	732	1350	86			226		DS-5S1
31	732	1350	76			341		DS-5S1
32	732	1350	76			269		DS-5S1
33	750	1382	63			197		Bloom-ORNL
34	760	1400	76			269		DS-5S1
35	816	1500	42	26		252		Spaeder and Brickner
36	816	1500	56	34		207		Spaeder and Brickner
37	816	1500	49			193		DS-5S1
38	816	1500	48			193		DS-5S1
39	816	1500	41	19		139		DS-5S1
40	816	1500	41			150		DS-5S1
41	816	1500	46			150		DS-5S1
				Type 316L				
42	565	1050	252			378		DS-5S1
43	565	1050	248			387		DS-5S1
44	649	1200	145			327		DS-5S1
				Type 316N				
45	649	1200	212			403		Cullen and Davis

Table A.3. Summary of creep-strength data for type 304 stainless steel

Data	Temperature		Creep rupture strength (MPa)				Ultimate tensile strength	Data source
	°C	°F	0.001/hr	0.0001/hr	0.00001/hr	0.000001/hr	MPa	
				Type 304				
1	538	1000		124	74		371	DS-5S1
2	565	1050			124	78	394	DS-5S1
3	565	1050			98		404	DS-5S1
4	593	1100	156	128			359	ORNL
5	593	1100	194				358	ORNL
6	593	1100	190	165			360	ORNL
7	593	1100	141	114			322	ORNL
8	593	1100	146	121			336	ORNL
9	593	1100	197	154	117		363	ORNL
10	593	1100	156	131	111		356	ORNL
11	593	1100	145	114	90		337	ORNL
12	593	1100	209				370	ORNL
13	593	1100	200				359	ORNL
14	593	1100		90			352	DS-5S1
15	593	1100		90			336	DS-5S1
16	649	1200	74	59			277	ORNL
17	649	1200			57	34	338	DS-5S1
18	649	1200			45		319	DS-5S1
19	649	1200		54	30		296	DS-5S1
20	704	1300	46				215	ORNL
21	704	1300		36			248	DS-5S1
22	704	1300			31	12	192	DS-5S1
23	732	1350			28		213	DS-5S1
24	816	1500		14			152	DS-5S1
25	816	1500		17	11		145	DS-5S1
				Type 304H				
26	593	1100			110		354	DS-5S1
27	649	1200			72		333	DS-5S1

Table A.4. Summary of creep-strength data for type 316 stainless steel

Data	Temperature		Creep rupture strength (MPa)				Ultimate tensile strength MPa	Data source
	°C	°F	0.001/hr	0.0001/hr	0.00001/hr	0.000001/hr		
				Type 316				
1	538	1100		207	102		507	DS-5S1
2	593	1100		179			434	DS-5S1
3	593	1100		162	83		476	DS-5S1
4	593	1100	217	169	131		434	DS-5S1
5	593	1100			107		398	DS-5S1
6	593	1100	145	103			419	Spaeder and Brickner
7	593	1100	152	110			425	Spaeder and Brickner
8	649	1200						
9	649	1200						
10	649	1200		99	47		417	DS-5S1
11	649	1200			45		332	DS-5S1
12	649	1200			45		341	DS-5S1
13	704	1300		67			317	DS-5S1
14	704	1300		62	29		346	DS-5S1
15	704	1300	90	64	41		317	DS-5S1
16	704	1300	61	43			310	Spaeder and Brickner
17	704	1300	59	41			319	Spaeder and Brickner
18	732	1350		36	18		217	DS-5S1
19	732	1350			21		215	DS-5S1
20	732	1350			29		236	DS-5S1
21	816	1500		22			193	DS-5S1
22	816	1500		15	8		141	DS-5S1
23	816	1500		29	13		217	DS-5S1
24	816	1500	34	18	10		193	DS-5S1
25	816	1500	26	17			207	Spaeder and Brickner
26	816	1500	26	17			252	Spaeder and Brickner
				Type 316L				
27	649	1200		86	68		328	DS-5S1
28	649	1200		62	40		351	DS-5S1

Table A.5. Summary of time to rupture, minimum creep rate and elevated-temperature ultimate tensile-strength data for type 304 stainless steel. This summary includes both ORNL and the data collected from literature. All ORNL tensile-strength values were at a strain rate of 0.04/min.

Heat number	Temp (C)	Stress (MPa)	Ultimate tensile strength (MPa)	Rupture life (hr)	Minimum creep rate (%/hr)
ORNL796P	482.	310.	410.	0.0	0.0001300
ORNL796P	482.	345.	410.	884.8	0.0002800
ORNL796P	482.	379.	410.	668.0	0.0015000
ORNL796P	538.	172.	378.	0.0	0.0001000
ORNL796P	538.	207.	378.	2219.0	0.0006500
ORNL796P	538.	207.	378.	0.0	0.0006300
ORNL796P	538.	241.	378.	350.4	0.0065000
ORNL796P	538.	241.	378.	594.8	0.0040000
ORNL796P	538.	276.	378.	139.7	0.0240000
ORNL796P	538.	276.	378.	162.8	0.0210000
ORNL796P	538.	310.	378.	60.1	0.0300000
ORNL796P	538.	345.	378.	21.0	0.2399999
ORNL 813	538.	310.	421.	837.0	0.0052000
ORNL 813	538.	345.	421.	348.0	0.0210000
ORNL 813	538.	379.	421.	33.8	0.3200000
ORNL 070	593.	241.	364.	864.6	0.0065000
ORNL 070	593.	241.	363.	1174.5	0.0047000
ORNL 086	593.	207.	354.	428.1	0.0250000
ORNL 086	593.	207.	354.	331.9	0.0140000
ORNL 086	593.	241.	354.	52.6	0.2000000
ORNL 086	593.	241.	354.	78.0	0.1300000
ORNL 111	593.	241.	362.	287.0	0.0130000
ORNL 111	593.	241.	371.	295.7	0.0130000
ORNL 187	593.	117.	336.	22622.2	0.0000960
ORNL 187	593.	207.	336.	120.5	0.0560000
ORNL 187	593.	207.	331.	98.7	0.0880000
ORNL 187	593.	241.	336.	18.3	0.5000000
ORNL 187	593.	241.	331.	25.9	0.2900000
ORNL 187	593.	241.	331.	59.2	0.1830000
ORNL 283	593.	207.	348.	331.6	0.0350000
ORNL 283	593.	207.	355.	290.4	0.0380000
ORNL 283	593.	241.	355.	60.8	0.2200000
ORNL 283	593.	241.	348.	70.0	0.2300000
ORNL 330	593.	207.	360.	254.1	0.0240000
ORNL 330	593.	207.	364.	355.3	0.0140000
ORNL 330	593.	241.	360.	116.1	0.0880000
ORNL 330	593.	241.	360.	133.1	0.0829999
ORNL 330	593.	241.	364.	56.0	0.1300000
ORNL 330	593.	241.	360.	70.1	0.0860000
ORNL 330	593.	241.	360.	91.2	0.1300000
ORNL 330	593.	317.	364.	4.1	4.0999994
ORNL 380	593.	207.	376.	738.4	0.0023000
ORNL 380	593.	207.	364.	741.5	0.0034000
ORNL 380	593.	241.	364.	102.8	0.0460000
ORNL 380	593.	241.	364.	323.3	0.0170000

Table A.5 (continued)

Heat number	Temp (C)	Stress (MPa)	Ultimate tensile strength (MPa)	Rupture life (hr)	Minimum creep rate (%/hr)
ORNL 380	593.	241.	376.	168.1	0.0220000
ORNL 414	593.	200.	383.	1958.6	0.0012000
ORNL 414	593.	207.	362.	1795.7	0.0024000
ORNL 414	593.	241.	362.	415.6	0.0120000
ORNL 414	593.	241.	362.	119.5	0.0250000
ORNL 414	593.	241.	383.	325.9	0.0120000
ORNL 414	593.	241.	362.	658.9	0.0076000
ORNL 414	593.	241.	362.	582.6	0.0108000
ORNLK544	593.	117.	360.	26875.2	0.0000450
ORNLK544	593.	207.	360.	431.0	0.0166000
ORNL 544	593.	207.	359.	356.1	0.0216000
ORNL 544	593.	241.	359.	62.1	0.1730000
ORNLK544	593.	241.	360.	66.3	0.1830000
ORNL 551	593.	172.	345.	19180.0	0.0001900
ORNL 551	593.	207.	345.	1507.5	0.0067000
ORNL 551	593.	207.	362.	1788.5	0.0037000
ORNL 551	593.	241.	362.	299.5	0.0380000
ORNL 697	593.	207.	337.	406.4	0.0270000
ORNL 697	593.	207.	337.	412.6	0.0430000
ORNL 697	593.	207.	333.	195.0	0.0490000
ORNL 697	593.	241.	333.	24.0	0.3400000
ORNL 697	593.	241.	337.	46.0	0.1500000
ORNL796A	593.	172.	343.	604.5	0.0060000
ORNL796A	593.	172.	351.	724.7	0.0084000
ORNL796A	593.	172.	355.	630.4	0.0110000
ORNL796A	593.	172.	356.	763.4	0.0095000
ORNL796A	593.	172.	354.	765.2	0.0086000
ORNL796A	593.	172.	343.	766.8	0.0082000
ORNL796A	593.	172.	355.	776.8	0.0071000
ORNL796A	593.	207.	343.	109.4	0.0919999
ORNL796A	593.	207.	356.	214.7	0.0460000
ORNL796A	593.	207.	354.	140.2	0.0570000
ORNL796A	593.	207.	355.	143.7	0.0670000
ORNL796A	593.	207.	355.	148.4	0.0610000
ORNL796A	593.	207.	343.	150.5	0.0610000
ORNL796A	593.	207.	355.	187.8	0.0400000
ORNL796A	593.	207.	351.	194.4	0.0530000
ORNL796A	593.	241.	355.	27.0	0.3000000
ORNL796A	593.	241.	355.	37.4	0.2800000
ORNL796P	593.	138.	340.	0.0	0.0006500
ORNL796P	593.	147.	340.	1230.0	0.0021400
ORNL796P	593.	155.	340.	1247.0	0.0030000
ORNL796P	593.	155.	340.	1063.0	0.0028000
ORNL796P	593.	155.	340.	878.1	0.0035000
ORNL796P	593.	172.	340.	619.2	0.0090000

Table A.5 (continued)

Heat number	Temp (C)	Stress (MPa)	Ultimate tensile strength (MPa)	Rupture life (hr)	Minimum creep rate (%/hr)
ORNL796P	593.	172.	340.	440.1	0.0110000
ORNL796P	593.	172.	340.	552.9	0.0106000
ORNL796P	593.	172.	340.	0.0	0.0100000
ORNL796P	593.	207.	340.	110.8	0.0460000
ORNL796P	593.	207.	340.	98.5	0.0760000
ORNL796P	593.	241.	340.	25.1	0.3400000
ORNL796P	593.	241.	340.	29.2	0.2300000
ORNL796P	593.	276.	340.	4.9	2.0999994
ORNL796P	593.	276.	340.	5.8	1.6999998
ORNLK796	593.	110.	322.	14647.1	0.0000680
ORNLR796	593.	117.	356.	29253.4	0.0000210
ORNLK796	593.	124.	322.	4544.0	0.0002500
ORNLK796	593.	172.	322.	423.3	0.0080000
ORNLK796	593.	172.	322.	244.1	0.0068000
ORNLK796	593.	172.	322.	453.4	0.0072000
ORNLK796	593.	172.	322.	291.7	0.0102000
ORNLR796	593.	207.	344.	168.8	0.0610000
ORNLR796	593.	207.	356.	274.2	0.0520000
ORNLR796	593.	207.	356.	281.4	0.0450000
ORNLK796	593.	207.	325.	84.4	0.0770000
ORNLR796	593.	207.	356.	286.7	0.0440000
ORNLK796	593.	207.	322.	86.8	0.0739999
ORNLK796	593.	207.	322.	92.8	0.0800000
ORNLK796	593.	241.	325.	17.6	0.5000000
ORNLK796	593.	241.	322.	22.2	0.3600000
ORNLR796	593.	241.	344.	43.7	0.3500000
ORNL 797	593.	207.	347.	138.9	0.0390000
ORNL 797	593.	207.	345.	352.6	0.0170000
ORNL 797	593.	241.	345.	39.8	0.2399999
ORNL 797	593.	241.	347.	27.9	0.2200000
ORNL 779	593.	207.	350.	599.3	0.0100000
ORNL 779	593.	207.	364.	280.4	0.0210000
ORNL 779	593.	241.	350.	80.1	0.1000000
ORNL 779	593.	241.	364.	82.8	0.0960000
ORNL 807	593.	207.	312.	143.2	0.1500000
ORNL 807	593.	207.	330.	96.4	0.1600000
ORNL 807	593.	241.	312.	16.8	1.0999994
ORNL 807	593.	241.	330.	18.1	0.9700000
ORNL 813	593.	207.	345.	2765.6	0.0023000
ORNL 813	593.	207.	370.	3184.0	0.0015000
ORNL 813	593.	221.	370.	1570.0	0.0033000
ORNL 813	593.	228.	370.	723.0	0.0100000
ORNL 813	593.	241.	370.	721.0	0.0110000
ORNL 813	593.	241.	345.	284.2	0.0330000
ORNL 813	593.	241.	370.	287.0	0.0360000

Table A.5 (continued)

Heat number	Temp (C)	Stress (MPa)	Ultimate tensile strength (MPa)	Rupture life (hr)	Minimum creep rate (%/hr)
ORNL 813	593.	276.	370.	55.3	0.3300000
ORNL 813	593.	310.	370.	9.9	2.1999998
ORNLK845	593.	172.	357.	14077.0	0.0001425
ORNLK845	593.	207.	357.	1459.6	0.0028750
ORNLK845	593.	207.	360.	1275.4	0.0016250
ORNLK845	593.	241.	360.	247.7	0.0480000
ORNLK845	593.	241.	357.	287.0	0.0347500
ORNL 866	593.	207.	334.	121.0	0.1700000
ORNL 866	593.	207.	325.	162.3	0.1300000
ORNL 866	593.	241.	334.	25.2	0.7500000
ORNL 866	593.	241.	334.	30.4	0.7675000
ORNL 866	593.	241.	325.	33.8	0.7000000
ORNL 926	593.	207.	359.	3074.4	0.0018000
ORNL 926	593.	207.	348.	2580.2	0.0020000
ORNL 926	593.	241.	348.	713.4	0.0120000
ORNL 926	593.	241.	348.	625.1	0.0160000
ORNL 926	593.	241.	359.	332.5	0.0350000
ORNL 926	593.	241.	348.	673.7	0.0150000
ORNL 086	649.	172.	293.	77.0	0.2399999
ORNL 187	649.	172.	277.	36.8	0.5599999
ORNL 330	649.	172.	297.	74.9	0.2800000
ORNL 380	649.	172.	328.	303.9	0.0260000
ORNL 414	649.	172.	299.	308.1	0.0360000
ORNL 414	649.	172.	299.	253.1	0.0480000
ORNL 414	649.	172.	299.	266.3	0.0390000
ORNL 544	649.	172.	296.	44.5	0.4550000
ORNL 544	649.	172.	294.	47.0	0.5950000
ORNL796P	649.	52.	286.	0.0	0.0000350
ORNL796P	649.	69.	286.	0.0	0.0005000
ORNL796P	649.	86.	286.	3960.0	0.0032000
ORNL796P	649.	86.	286.	0.0	0.0043500
ORNL796P	649.	95.	286.	1053.0	0.0097000
ORNL796P	649.	95.	286.	0.0	0.0080000
ORNL796P	649.	103.	286.	1524.0	0.0170000
ORNL796P	649.	103.	286.	730.0	0.0150000
ORNL796P	649.	121.	286.	250.0	0.0500000
ORNL796P	649.	121.	286.	484.7	0.0290000
ORNL796P	649.	121.	286.	288.2	0.0400000
ORNL796P	649.	134.	286.	177.9	0.0770000
ORNL796P	649.	138.	286.	111.2	0.0870000
ORNL796P	649.	155.	286.	40.0	0.3300000
ORNL796P	649.	155.	286.	53.8	0.2700000
ORNL796P	649.	172.	286.	18.8	0.8699999
ORNL796P	649.	172.	286.	27.7	0.4600000
ORNL796P	649.	207.	286.	2.8	4.6999998

Table A.5 (continued)

Heat number	Temp (C)	Stress (MPa)	Ultimate tensile strength (MPa)	Rupture life (hr)	Minimum creep rate (%/hr)
ORNL796P	649.	207.	286.	4.6	3.6999998
ORNLK796	649.	55.	277.	20059.2	0.0000544
ORNLK796	649.	69.	277.	7273.5	0.0006300
ORNLK796	649.	83.	277.	2674.0	0.0032400
ORNLK796	649.	97.	277.	760.7	0.0081500
ORNLK796	649.	110.	277.	303.6	0.0170000
ORNLK796	649.	110.	277.	244.9	0.0280000
ORNLK796	649.	172.	277.	17.0	0.9097000
ORNLR796	649.	172.	292.	62.7	0.3600000
ORNLR796	649.	172.	292.	67.2	0.3300000
ORNL 807	649.	172.	264.	43.5	0.7000000
ORNL 807	649.	241.	271.	26.8	1.5999994
ORNL 813	649.	155.	310.	1072.0	0.0070000
ORNL 813	649.	172.	310.	385.9	0.0250000
ORNL 813	649.	172.	310.	293.7	0.0450000
ORNL 813	649.	190.	310.	74.5	0.2900000
ORNL 813	649.	207.	310.	23.1	1.0999994
ORNL 813	649.	241.	310.	4.7	7.6999998
ORNLK845	649.	172.	283.	152.3	0.1410000
ORNLK845	649.	172.	296.	186.1	0.0755000
ORNL 866	649.	172.	263.	17.8	1.5999994
ORNL 926	649.	172.	276.	50.1	0.4500000
ORNL796P	704.	52.	228.	2296.0	0.0042000
ORNL796P	704.	69.	228.	1027.0	0.0280000
ORNL796P	704.	78.	228.	562.7	0.0500000
ORNL796P	704.	86.	228.	244.4	0.1199999
ORNL796P	704.	86.	228.	170.5	0.1300000
ORNL796P	704.	95.	228.	83.1	0.2100000
ORNL796P	704.	103.	228.	46.9	0.3300000
ORNL796P	704.	103.	228.	70.1	0.3200000
ORNL796P	704.	117.	228.	22.1	0.8000000
ORNL796P	704.	121.	228.	23.3	1.0499992
ORNL796P	704.	138.	228.	8.7	2.7999992
ORNL796P	704.	172.	228.	1.6	15.6999998
ORNLK796	704.	55.	215.	2760.1	0.0041000
ORNLK796	704.	69.	215.	653.0	0.0250000
ORNLK796	704.	69.	215.	567.9	0.0200000
ORNL796P	760.	52.	174.	697.7	0.0440000
ORNL796P	760.	59.	174.	195.9	0.1400000
ORNL796P	760.	69.	174.	45.7	0.4299999
ORNL796P	760.	69.	174.	61.4	0.3550000
ORNL796P	760.	86.	174.	16.1	1.5000000
ORNL796P	760.	86.	174.	19.9	1.4299994
ORNL796P	760.	103.	174.	5.3	5.1999998
ORNL796P	760.	121.	174.	2.1	14.5000000
ORNL796P	760.	138.	174.	0.8	42.0000000

Table A.5 (continued)

Heat number	Temp (C)	Stress (MPa)	Ultimate tensile strength (MPa)	Rupture life (hr)	Minimum creep rate (%/hr)
MPCAR-2	538.	276.	396.	435.0	0.0
HEDL 697	538.	310.	379.	81.3	0.0512000
HEDL 697	538.	276.	379.	261.7	0.0109000
HEDL 697	538.	310.	379.	112.1	0.0
HEDL 697	538.	310.	379.	142.2	0.0395000
HEDL 697	538.	276.	379.	182.3	0.0126000
HEDL 697	538.	207.	379.	4022.0	0.0005410
HEDL 697	538.	172.	379.	7034.0	0.0002470
HEDL 697	538.	310.	379.	75.6	0.0950000
HEDL 697	538.	310.	379.	135.6	0.0358000
HEDL 697	538.	345.	379.	26.6	0.0
HEDL 697	538.	241.	379.	1506.1	0.0019200
HEDL 697	538.	310.	379.	57.2	0.1050000
HEDL 697	538.	310.	379.	88.2	0.0640000
HEDL 697	538.	276.	379.	208.8	0.0175000
HEDL 697	538.	365.	379.	19.0	1.8999996
HEDL 697	538.	345.	379.	19.6	0.2300000
HEDL 697	538.	345.	379.	29.1	0.1330000
B-W 216	566.	138.	394.	0.0	0.0000170
B-W 216	566.	90.	394.	0.0	0.0000019
B-W 216	566.	186.	394.	32505.5	0.0
B-W 216	566.	310.	394.	186.7	0.0
B-W 216	566.	255.	394.	977.5	0.0
B-W 216	566.	207.	394.	13629.7	0.0
B-W 219	566.	138.	404.	0.0	0.0000417
B-W 219	566.	90.	404.	0.0	0.0000062
B-W 219	566.	186.	404.	4201.3	0.0
B-W 219	566.	165.	404.	7863.4	0.0
B-W 219	566.	283.	404.	326.1	0.0
B-W 219	566.	207.	404.	3127.2	0.0
MPCAR-2	593.	117.	356.	31770.0	0.0000600
MPCAR-2	593.	152.	356.	4530.0	0.0
MPCAR-2	593.	167.	356.	2090.0	0.0
MPCAR-2	593.	186.	356.	1180.0	0.0
MPCAR-2	593.	221.	356.	210.0	0.0
MPCAR-2	593.	248.	356.	60.0	0.0
MPCAR-2	593.	276.	356.	10.6	0.0
MPCAR-2	593.	110.	356.	33712.0	0.0000500
MPCAR-2	593.	131.	356.	11122.0	0.0
MPCAR-2	593.	207.	356.	432.0	0.0
MPCAR-2	593.	103.	356.	48923.0	0.0000360
MPCAR-2	593.	262.	356.	25.0	0.0
MPCAR-2	593.	283.	356.	15.0	0.0
MPCAR-2	593.	103.	356.	46406.0	0.0000250
MPCAR-2	593.	97.	356.	65028.0	0.0

Table A.5 (continued)

Heat number	Temp (C)	Stress (MPa)	Ultimate tensile strength (MPa)	Rupture life (hr)	Minimum creep rate (%/hr)
1PCAR-2	593.	241.	356.	68.0	0.0
TIMKN 746	593.	276.	372.	20.0	0.0
TIMKN 746	593.	241.	372.	655.0	0.0
TIMKN 746	593.	207.	372.	736.0	0.0
TIMKN 718	593.	276.	391.	27.0	0.0
TIMKN 718	593.	207.	391.	927.0	0.0
TIMKN 718	593.	241.	391.	178.0	0.0
TIMKN 057	593.	276.	397.	383.0	0.0
TIMKN 057	593.	241.	397.	966.0	0.0
TIMKN 367	593.	117.	354.	0.0	0.0000120
TIMKN 367	593.	90.	354.	0.0	0.0000050
TIMKN 367	593.	241.	354.	225.0	0.0
TIMKN 367	593.	200.	354.	1378.0	0.0
TIMKN 973	593.	276.	374.	101.0	0.0
TIMKN 973	593.	241.	374.	555.0	0.0
HEDL 697	593.	152.	333.	0.0	0.0029000
HEDL 697	593.	138.	333.	0.0	0.0018100
HEDL 697	593.	345.	333.	0.8	12.5000000
HEDL 697	593.	183.	333.	440.1	0.0180000
HEDL 697	593.	193.	333.	241.4	0.0338000
HEDL 697	593.	276.	333.	22.1	0.7420000
HEDL 697	593.	172.	333.	372.0	0.0112000
HEDL 697	593.	310.	333.	5.2	2.3199997
HEDL 697	593.	276.	333.	15.5	0.7580000
HEDL 697	593.	207.	333.	195.6	0.0455000
HEDL 697	593.	193.	333.	375.2	0.0100000
HEDL 697	593.	172.	333.	627.0	0.0100000
HEDL 697	593.	207.	333.	198.8	0.0424000
HEDL 697	593.	172.	333.	628.7	0.0116000
HEDL 697	593.	241.	333.	49.0	0.1970000
B-W 220	649.	186.	354.	211.9	0.0
B-W 220	649.	152.	354.	742.8	0.0
B-W 220	649.	114.	354.	10646.4	0.0
B-W 220	649.	138.	354.	1517.3	0.0
B-W 220	649.	124.	354.	5597.7	0.0
B-W 220	649.	103.	354.	18208.1	0.0
MPCAR-2	649.	76.	311.	0.0	0.0002900
MPCAR-2	649.	59.	311.	0.0	0.0000200
MPCAR-2	649.	117.	311.	1470.0	0.0
MPCAR-2	649.	179.	311.	40.0	0.0
MPCAR-2	649.	159.	311.	140.0	0.0
MPCAR-2	649.	131.	311.	500.0	0.0
MPCAR-2	649.	103.	311.	2850.0	0.0
MPCAR-2	649.	276.	311.	1.0	0.0
MPCAR-2	649.	66.	311.	49052.0	0.0000430

Table A.5 (continued)

Heat number	Temp (C)	Stress (MPa)	Ultimate tensile strength (MPa)	Rupture life (hr)	Minimum creep rate (%/hr)
MPCAR-2	649.	138.	311.	322.0	0.0
MPCAR-2	649.	214.	311.	13.0	0.0
MPCAR-2	649.	124.	311.	533.0	0.0
MPCAR-2	649.	69.	311.	20074.0	0.0000840
MPCAR-2	649.	62.	311.	36614.0	0.0000150
MPCAR-2	649.	69.	311.	21985.0	0.0000820
MPCAR-2	649.	207.	311.	16.1	0.0
MPCAR-2	649.	172.	311.	67.0	0.0
MPCAR-2	649.	72.	311.	26603.0	0.0000760
MPCAR-2	649.	83.	311.	10039.0	0.0004000
B-W 216	649.	54.	338.	0.0	0.0000082
B-W 216	649.	41.	338.	0.0	0.0000024
B-W 216	649.	207.	338.	31.6	0.0
B-W 216	649.	114.	338.	3651.5	0.0
B-W 216	649.	107.	338.	7473.6	0.0
B-W 216	649.	138.	338.	1596.6	0.0
B-W 216	649.	165.	338.	249.2	0.0
B-W 219	649.	54.	319.	0.0	0.0000420
B-W 219	649.	45.	319.	0.0	0.0000100
B-W 219	649.	38.	319.	0.0	0.0000040
B-W 219	649.	152.	319.	260.7	0.0
B-W 219	649.	114.	319.	3872.8	0.0
B-W 219	649.	107.	319.	9752.1	0.0
B-W 219	649.	138.	319.	1095.3	0.0
B-W 219	649.	186.	319.	96.6	0.0
B-W 213	649.	152.	321.	340.7	0.0650000
B-W 213	649.	114.	321.	7823.2	0.0003000
B-W 213	649.	138.	321.	1646.7	0.0060000
B-W 213	649.	124.	321.	4337.7	0.0013600
UMICH 323	649.	255.	296.	1.0	0.0
UMICH 323	649.	193.	296.	11.3	0.0
UMICH 323	649.	97.	296.	1002.0	0.0
UMICH 323	649.	214.	296.	3.7	0.0
UMICH 323	649.	83.	296.	3074.0	0.0011300
UMICH 323	649.	117.	296.	308.0	0.0
TIMKN 367	649.	83.	333.	0.0	0.0000160
TIMKN 367	649.	62.	333.	0.0	0.0000060
TIMKN 367	649.	165.	333.	240.0	0.0
TIMKN 367	649.	114.	333.	4903.0	0.0
TIMKN 367	649.	138.	333.	1398.0	0.0
HEDL 697	649.	97.	281.	0.0	0.0079400
HEDL 697	649.	193.	281.	22.0	0.0
HEDL 697	649.	152.	281.	82.8	0.3010000
HEDL 697	649.	172.	281.	44.9	0.5310000
HEDL 697	649.	110.	281.	625.3	0.0159000

Table A.5 (continued)

Heat number	Temp (C)	Stress (MPa)	Ultimate tensile strength (MPa)	Rupture life (hr)	Minimum creep rate (%/hr)
HEDL 697	649.	165.	281.	67.3	0.2890000
HEDL 697	649.	152.	281.	147.5	0.1450000
HEDL 697	649.	138.	281.	217.1	0.0447000
HEDL 697	649.	138.	281.	257.7	0.0766000
HEDL 697	649.	207.	281.	3.3	1.9099998
HEDL 697	649.	159.	281.	89.0	0.2070000
HEDL 697	649.	145.	281.	239.3	0.0871000
HEDL 697	649.	124.	281.	589.7	0.0341000
HEDL 697	649.	262.	281.	1.0	19.1999969
HEDL 697	649.	241.	281.	1.3	16.0499921
HEDL 697	649.	241.	281.	2.2	11.3999996
HEDL 697	649.	276.	281.	0.6	31.2999878
MPCAR-2	704.	138.	260.	24.8	0.0
UMICH 323	704.	207.	243.	0.4	0.0
UMICH 323	704.	152.	243.	3.3	0.0
UMICH 323	704.	124.	243.	13.3	0.0
UMICH 323	704.	69.	243.	614.0	0.0
UMICH 323	704.	83.	243.	185.0	0.0
B-W 220	732.	63.	246.	6551.0	0.0
B-W 220	732.	103.	246.	202.5	0.0
B-W 220	732.	83.	246.	882.5	0.0
B-W 220	732.	69.	246.	3202.5	0.0
B-W 220	732.	62.	246.	7342.4	0.0
B-W 220	732.	55.	246.	15529.1	0.0
B-W 216	732.	26.	192.	0.0	0.0000071
B-W 216	732.	20.	192.	0.0	0.0000033
B-W 216	732.	14.	192.	0.0	0.0000014
B-W 216	732.	103.	192.	84.7	0.0
B-W 216	732.	59.	192.	3225.9	0.0
B-W 216	732.	83.	192.	486.6	0.0
B-W 216	732.	52.	192.	6438.6	0.0
B-W 216	732.	40.	192.	30368.4	0.0
B-W 219	732.	31.	213.	0.0	0.0000270
B-W 219	732.	26.	213.	0.0	0.0000067
B-W 219	732.	103.	213.	46.9	0.0
B-W 219	732.	83.	213.	416.1	0.0
B-W 219	732.	59.	213.	3776.3	0.0
B-W 219	732.	48.	213.	8537.7	0.0
MPCAR-2	760.	138.	198.	4.0	0.0
UMICH 323	760.	152.	192.	0.5	0.0
UMICH 323	760.	48.	192.	740.0	0.0
UMICH 323	760.	34.	192.	3430.0	0.0
UMICH 323	760.	117.	192.	2.3	0.0
UMICH 323	760.	41.	192.	1112.0	0.0
UMICH 323	760.	97.	192.	6.4	0.0

Table A.5 (continued)

Heat number	Temp (C)	Stress (MPa)	Ultimate tensile strength (MPa)	Rupture life (hr)	Minimum creep rate (%/hr)
MPCAR-2	816.	34.	141.	2710.0	0.0
UMICH 323	816.	103.	145.	0.3	0.0
UMICH 323	816.	28.	145.	1092.0	0.0064000
UMICH 323	816.	41.	145.	133.0	0.0
UMICH 323	816.	76.	145.	4.4	0.0
UMICH 323	816.	66.	145.	5.8	0.0
UMICH 323	816.	57.	145.	26.7	0.0
UMICH 323	816.	34.	145.	277.0	0.0

Table A.6. Time to rupture and minimum creep rate and elevated-temperature ultimate tensile-strength data for type 316 stainless steel. This summary includes all but ORNL data.

Heat number	Temp (C)	Stress (MPa)	Ultimate tensile strength (MPa)	Rupture life (hr)	Minimum creep rate (%/hr)
HEDL2990	538.	434.	468.	60.5	0.1020000
HEDL2990	538.	414.	468.	106.0	0.0225000
HEDL2990	538.	414.	468.	129.6	0.0335000
HEDL2990	538.	400.	468.	203.9	0.0156000
HEDL2990	538.	379.	468.	263.1	0.0092500
HEDL2990	538.	345.	468.	432.9	0.0032500
HEDL2990	538.	310.	468.	1032.0	0.0020500
HEDL2990	538.	276.	468.	2795.0	0.0008400
HEDL2990	538.	239.	468.	0.0	0.0002670
55318	566.	414.	477.	67.3	0.1149999
55319	566.	414.	475.	60.5	0.1860000
55319	566.	331.	475.	0.0	0.0105000
55320	566.	448.	476.	23.4	0.3189999
55320	566.	414.	476.	91.5	0.0950000
55320	566.	379.	476.	194.0	0.4390000
55320	566.	345.	476.	360.5	0.0270000
55320	566.	310.	476.	2483.5	0.0043000
HEDL2990	593.	345.	384.	11.2	0.9750000
HEDL2990	593.	310.	384.	22.8	0.2500000
HEDL2990	593.	276.	384.	196.9	0.0544000
HEDL2990	593.	262.	384.	481.1	0.0342000
HEDL2990	593.	262.	384.	0.0	0.0464000
HEDL2990	593.	248.	384.	359.2	0.0172000
HEDL2990	593.	248.	384.	236.2	0.0276000
HEDL2990	593.	234.	384.	338.1	0.0150000
HEDL2990	593.	372.	384.	5.6	0.4199991
HEDL2990	593.	359.	384.	8.4	0.8030000
HEDL2990	593.	221.	384.	1113.2	0.0073700
HEDL2990	593.	214.	384.	2395.0	0.0037000
HEDL2990	593.	207.	384.	0.0	0.0010800
HEDL2990	593.	207.	384.	0.0	0.0012300
HEDL2990	593.	179.	384.	0.0	0.0007040
HEDL2990	593.	179.	384.	0.0	0.0003900
USS 373	593.	414.	434.	4.8	0.7440000
USS 373	593.	400.	434.	8.5	0.3279999
USS 373	593.	386.	434.	11.6	0.2880000
USS 373	593.	372.	434.	14.7	0.2160000
USS 373	593.	331.	434.	38.0	0.0
USS 373	593.	276.	434.	163.0	0.1160000
USS 373	593.	248.	434.	593.0	0.0025600
USS 373	593.	172.	434.	0.0	0.0001020
B-W 230	649.	228.	341.	56.3	0.0
B-W 230	649.	172.	341.	3006.9	0.0
B-W 230	649.	152.	341.	4407.5	0.0
B-W 230	649.	62.	341.	0.0	0.0000150

Table A.6 (continued)

Heat number	Temp (C)	Stress (MPa)	Ultimate tensile strength (MPa)	Rupture life (hr)	Minimum creep rate (%/hr)
B-W 230	649.	228.	370.	67.9	0.0
B-W 230	649.	172.	370.	3499.5	0.0
B-W 230	649.	103.	370.	23146.4	0.0
B-W 230	649.	197.	341.	833.2	0.0
B-W 230	649.	134.	341.	6379.4	0.0
B-W 230	649.	114.	341.	12931.4	0.0
B-W 230	649.	107.	341.	16730.4	0.0
B-W 230	649.	197.	370.	690.4	0.0
B-W 230	649.	155.	370.	4881.5	0.0
B-W 230	649.	121.	370.	8597.9	0.0
HEDL2990	649.	296.	312.	3.5	6.0799999
HEDL2990	649.	276.	312.	5.2	3.0000000
HEDL2990	649.	241.	312.	24.9	0.9110000
HEDL2990	649.	207.	312.	141.2	0.2120000
HEDL2990	649.	207.	312.	95.0	0.3419999
HEDL2990	649.	200.	312.	115.0	0.1440000
HEDL2990	649.	193.	312.	165.4	0.0944000
HEDL2990	649.	172.	312.	374.5	0.0638000
HEDL2990	649.	159.	312.	989.0	0.0198000
HEDL2990	649.	152.	312.	1294.2	0.0159000
HEDL2990	649.	124.	312.	0.0	0.0015800
55319	649.	241.	393.	88.8	0.2640000
55319	649.	207.	393.	367.6	0.0450000
55320	649.	276.	393.	30.3	0.7660000
55320	649.	234.	393.	120.6	0.1790000
55320	649.	207.	393.	448.8	0.0393000
55320	649.	179.	393.	970.0	0.0210000
55320	649.	165.	393.	2132.6	0.0093900
55318	649.	241.	393.	76.9	0.3099999
55318	649.	207.	393.	290.5	0.0568000
302-16P	649.	145.	341.	6000.0	0.0004200
B-W 232	649.	228.	335.	105.8	0.0
B-W 232	649.	172.	335.	3882.3	0.0
B-W 232	649.	145.	335.	5246.7	0.0
B-W 232	649.	110.	335.	14584.7	0.0
B-W 232	649.	197.	335.	391.8	0.0
TIMKN 372	649.	372.	417.	0.4	0.0
TIMKN 372	649.	303.	417.	2.4	0.0
TIMKN 372	649.	262.	417.	10.4	0.0
TIMKN 372	649.	172.	417.	984.0	0.0
TIMKN 372	649.	117.	417.	13056.0	0.0
TIMKN 372	704.	303.	346.	0.2	0.0
TIMKN 372	704.	241.	346.	2.5	0.0
TIMKN 372	704.	221.	346.	7.0	0.0
TIMKN 372	704.	152.	346.	290.0	0.0

Table A.6 (continued)

Heat number	Temp (C)	Stress (MPa)	Ultimate tensile strength (MPa)	Rupture life (hr)	Minimum creep rate (%/hr)
TIMKN 372	704.	131.	346.	671.0	0.0
TIMKN 372	704.	117.	346.	1472.0	0.0
USS 373	704.	76.	317.	0.0	0.0002180
USS 373	704.	55.	317.	0.0	0.0000426
USS 373	704.	255.	317.	3.8	4.5999994
USS 373	704.	221.	317.	12.2	1.1299992
USS 373	704.	165.	317.	93.0	0.1540000
USS 373	704.	138.	317.	327.0	0.0446000
B-W 230	732.	138.	217.	37.0	0.0
B-W 230	732.	103.	217.	283.8	0.0
B-W 230	732.	48.	217.	9133.0	0.0
B-W 230	732.	41.	217.	0.0	0.0002310
B-W 230	732.	21.	217.	0.0	0.0000138
B-W 230	732.	138.	215.	38.7	0.0
B-W 230	732.	103.	215.	218.1	0.0
B-W 230	732.	48.	215.	13848.2	0.0
B-W 230	732.	21.	215.	0.0	0.0000100
B-W 230	732.	114.	217.	93.4	0.0
B-W 230	732.	79.	217.	1560.5	0.0
B-W 230	732.	66.	217.	3137.0	0.0
B-W 230	732.	31.	217.	0.0	0.0000400
B-W 230	732.	114.	215.	115.1	0.0
B-W 230	732.	79.	215.	1080.4	0.0
B-W 230	732.	66.	215.	2865.2	0.0
B-W 230	732.	52.	215.	6779.4	0.0
B-W 230	732.	45.	215.	0.0	0.0000625
302-3	732.	41.	217.	11420.0	0.0002400
B-W 232	732.	138.	231.	89.6	0.0
B-W 232	732.	117.	231.	150.2	0.0
B-W 232	732.	103.	231.	319.6	0.0
B-W 232	732.	48.	231.	13913.4	0.0
B-W 232	732.	58.	231.	6402.2	0.0
B-W 232	732.	114.	231.	159.7	0.0
HEDL2990	760.	131.	171.	18.0	1.8399992
HEDL2990	760.	117.	171.	27.5	0.8780000
HEDL2990	760.	103.	171.	72.2	0.4600000
HEDL2990	760.	103.	171.	69.4	0.4119999
HEDL2990	760.	83.	171.	274.6	0.0904000
HEDL2990	760.	69.	171.	1050.5	0.0285000
HEDL2990	760.	62.	171.	1810.1	0.0161000
55318	760.	97.	248.	196.2	0.1560000
55319	760.	97.	248.	222.3	0.1420000
55320	760.	138.	262.	65.2	0.8540000
55320	760.	103.	262.	79.3	0.2000000
55320	760.	83.	262.	65.9	0.0480000

Table A.6 (continued)

Heat number	Temp (C)	Stress (MPa)	Ultimate tensile strength (MPa)	Rupture life (hr)	Minimum creep rate (%/hr)
TIMKN 372	760.	159.	269.	6.8	0.0
TIMKN 372	760.	97.	269.	254.0	0.0
TIMKN 372	760.	76.	269.	985.0	0.0
TIMKN 372	760.	214.	269.	0.8	0.0
TIMKN 372	760.	190.	269.	2.1	0.0
TIMKN 372	760.	52.	269.	6336.0	0.0
B-W 230	816.	21.	141.	14233.0	0.0
B-W 230	816.	21.	141.	0.0	0.0003820
B-W 230	816.	14.	141.	0.0	0.0000625
B-W 230	816.	21.	148.	13145.8	0.0
B-W 230	816.	31.	141.	3166.5	0.0
B-W 230	816.	31.	148.	2845.5	0.0
B-W 230	816.	24.	148.	7871.2	0.0
B-W 230	816.	59.	141.	200.4	0.0
B-W 230	816.	39.	141.	1216.7	0.0
B-W 230	816.	59.	148.	190.2	0.0
B-W 230	816.	39.	148.	1353.1	0.0
B-W 230	816.	6.	141.	0.0	0.0000069
302-7	816.	21.	141.	10200.0	0.0002525
B-W 232	816.	28.	139.	3443.9	0.0
B-W 232	816.	47.	139.	690.9	0.0
B-W 232	816.	40.	139.	1077.2	0.0
TIMKN 372	816.	172.	217.	0.4	0.0
TIMKN 372	816.	138.	217.	1.9	0.0
TIMKN 372	816.	110.	217.	7.9	0.0
TIMKN 372	816.	34.	217.	2841.0	0.0000157
TIMKN 372	816.	51.	217.	817.0	0.0
TIMKN 372	816.	66.	217.	312.0	0.0
USS 373	816.	83.	193.	43.0	0.5810000
USS 373	816.	62.	193.	251.0	0.0892000
USS 373	816.	28.	193.	0.0	0.0002360
USS 373	816.	52.	193.	742.0	0.0213000
USS 373	816.	10.	193.	0.0	0.0000096
TIMKN 372	871.	124.	170.	0.4	0.0
TIMKN 372	871.	97.	170.	2.5	0.0
TIMKN 372	871.	83.	170.	6.3	0.0
TIMKN 372	871.	34.	170.	684.0	0.0
TIMKN 372	871.	23.	170.	1247.0	0.0
TIMKN 372	871.	45.	170.	206.0	0.0
HEDL2990	649.	317.	312.	1.3	19.2999878
USS 373	816.	138.	193.	1.8	14.3999996
HEDL2990	649.	331.	312.	0.9	23.8599854
USS 373	704.	276.	317.	0.6	39.6999969
302-6	816.	21.	141.	4750.0	500.0012207
USS 373	816.	165.	193.	0.4	89.0000000

APPENDIX B

Strain-Rate Dependence of Ultimate Tensile Strengths

Ultimate tensile strength was a function of strain rate for ORNL data[21] on a reannealed reference heat of type 304 stainless steel (Figs. B.1 and B.2). For the strain-rate range (1×10^{-5} to 10.0 per min) (Figs. B.1 and B.2) ultimate tensile strength (S_u) is given by:

$$S_u = S_u^{\,o} + B \log \dot{e} \ , \tag{B1}$$

where

$\dot{e}$ = strain rate per min,

$S_u^{\,o} = S_u$ at a strain rate of unity, and

B = constant dependent on temperature.

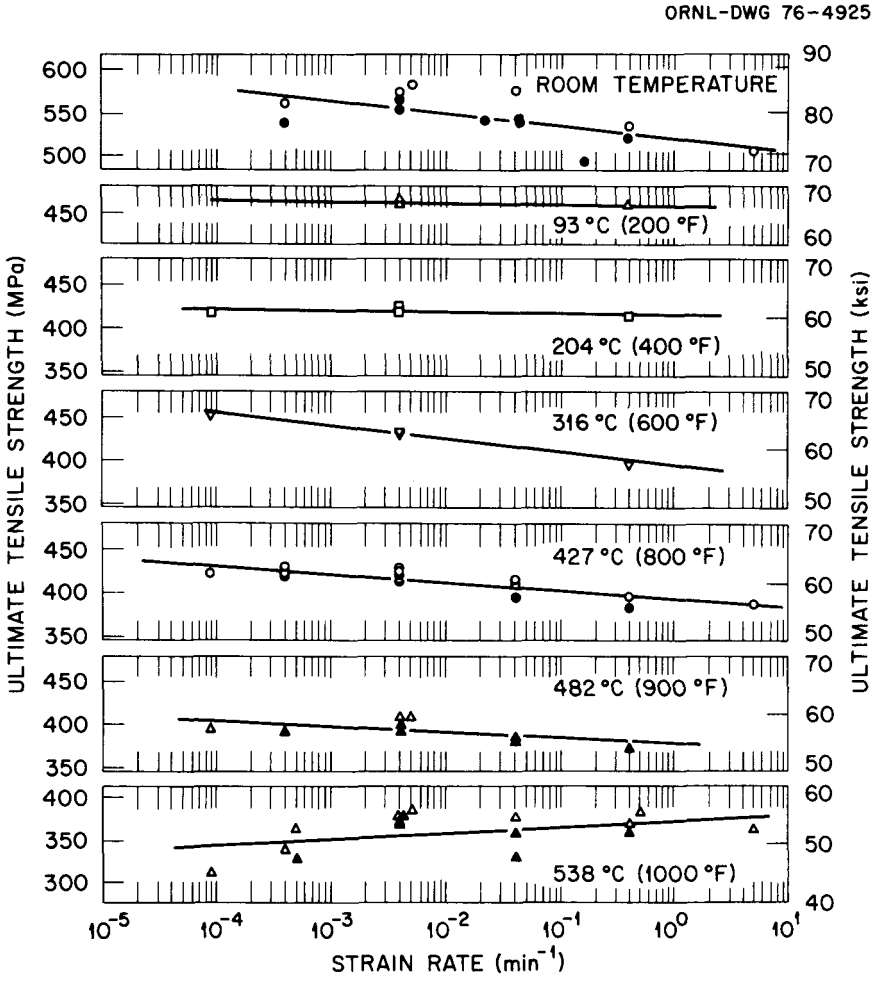

Fig. B.1. Ultimate Tensile Strength as a Function of Strain Rate for Reannealed Reference Heat of Type 304 Stainless Steel. Test temperature range room temperature to 538°C (1000°F).

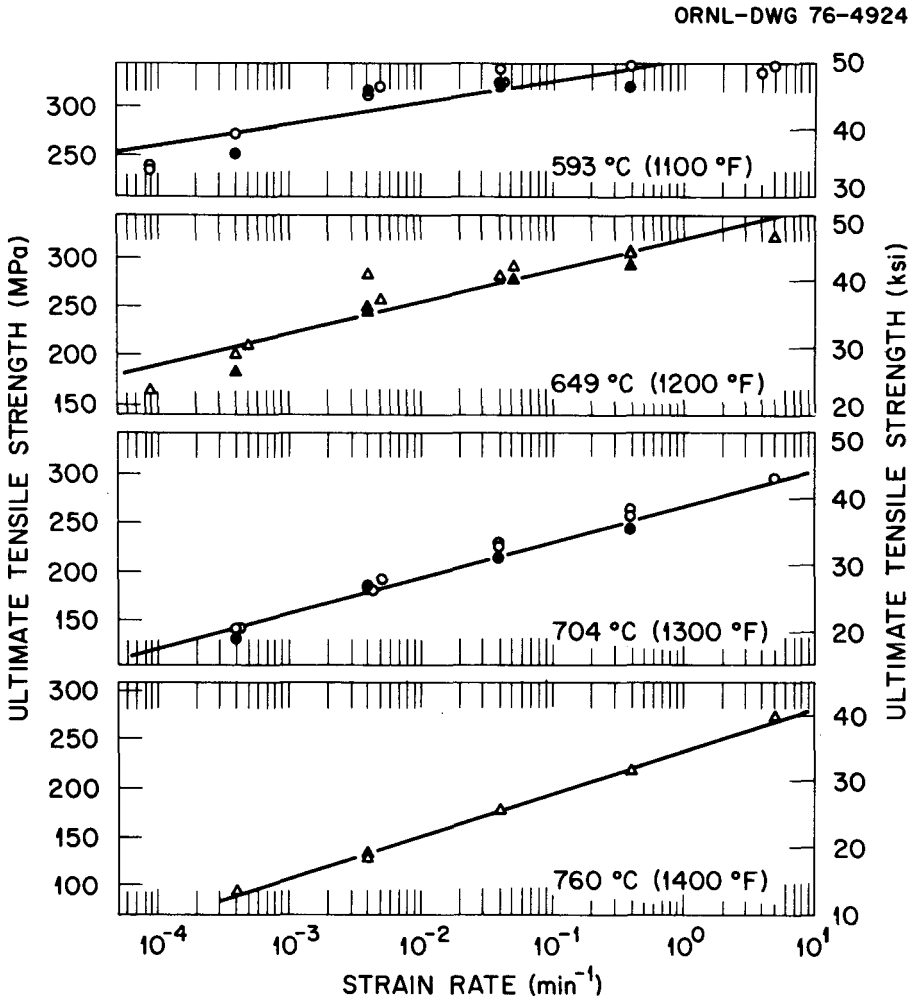

Fig. B.2. Ultimate Tensile Strength as a Function of Strain Rate for Reannealed Reference Heat of Type 304 Stainless Steel. Test temperature range 593–760°C (1100–1400°F).

Equation (B1) can be modified to obtain the S_u values at a strain rate of 0.04 per min (6.67×10^{-4} per sec).

$$S_u^* = S_u + B \log (0.04/\dot{e}), \tag{B2}$$

where

S_u^* = ultimate tensile strength at a strain rate of 0.04/min, and

S_u = ultimate tensile strength at any other strain rate, $\dot{e}$.

Least squares analysis was done on data shown in Figs. B.1 and B.2 and values of S_u^o and B so obtained are summarized in Table B.1. Values of S_u^o will change from heat to heat, but values of B are expected to be independent.

It is recommended that Equation (B2) and constants listed in Table B.1 be used in computing S_u^*, the value of ultimate tensile strength at the desired strain rate of predicting creep properties from models presented in this report.

Table B-1. Summary of constants in equation UTS = UTS_o + B log $\dot{e}$, for reannealed[a] reference heat of type 304 stainless steel[b]

Test temperature		No. of data points	Summary of constants,[c] ksi				RSE,[e] ksi	R^{2f} (%)
°C	°F		UTS_o	SE[d] in UTS_o	B	SE[d] in B		
25	77	14	75.57	1.42	−2.11	0.72	3.02	32
93	200	3	66.48	0.85	−0.30	0.43	0.71	42
204	400	4	60.31	0.64	−0.18	0.24	0.63	21
316	600	4	57.25	0.42	−2.21	0.16	0.41	90
427	800	14	57.10	0.61	−1.40	0.25	1.25	72
482	900	9	54.96	1.25	−0.94	0.51	1.57	33
538	1000	16	53.98	1.30	1.01	0.56	2.91	19
593	1100	16	50.36	1.10	3.13	0.47	2.70	76
649	1200	15	46.30	1.16	4.74	0.51	2.59	91
704	1300	14	39.80	0.46	5.66	0.22	1.00	83
760	1400	6	34.55	0.39	6.42	0.19	0.65	100

[a] 0.5 hr at 1093°C (200°F).

[b] Data for 1 and 2 in. (25 and 51 mm) plates have been treated together.

[c] Constants are for data in strain-rate range of 9×10^{-5} to 0.4 per min.

[d] SE = standard error in value of constants.

[e] RSE = residual standard error = $\sqrt{y^2/n-\nu}$, where n is the number of data points and ν = number of coefficients in the model (here $\nu = 2$) and $\Sigma_y{}^2 = \Sigma(UTS_{predicted} - UTS_{experimental})^2$.

[f] R^2 = Coefficient of determination (square of the multiple correlation).

APPENDIX C

Error Estimate in Determining Elevated-Temperature Ultimate Tensile Strength

A statistical sample of 12 specimens of reannealed type 316 stainless steel was selected for three tensile tests each in four different Instron machines. All tensile tests were done on 16-mm plate of reference heat (8092297) of type 316 stainless steel at 593°C (110°F) and a strain rate of 6.7×10^{-4} per sec (Table C.1). Statistical analysis showed that machine-to-machine variability in determining elevated-temperature ultimate tensile strength was not significant.

Table C.1. Summary of ultimate tensile strength at 593°C (1100°F) and 6.7×10^{-4} per sec on a single heat of type 316 stainless steel in the reannealed condition[a]

Test	Machine	Ultimate tensile strength		Standard error of estimate (SEE)[b]
		MPa	ksi	
1	1	417.7	60.58	
2	1	421.1	61.07	
3	1	419.9	60.90	
4	2	421.1	61.07	
5	2	424.5	61.56	
6	2	418.7	60.73	±3.40 MPa
7	3	424.0	61.50	
8	3	425.8	61.75	±0.49 ksi
9	3	418.4	60.68	
10	4	415.1	60.20	
11	4	417.2	60.50	
12	4	424.3	61.53	
	Average:	420.7	61.01	

[a] 0.5 hr at 1065°C (1950°F).

[b] SEE = $\sqrt{\Sigma(\bar{X} - X)^2/n - \nu}$ where $\bar{X}$ = average value and X is the experimental value. The symbol n is the number of data points and ν is the number of coefficients (here $\nu = 1$).

NOTE: The machine-to-machine variability was not significant statistically.

The standard error of estimate for 12 repeated tests on type 316 stainless steel is 3.4 MPa, which is significantly smaller than observed values of 26.5 and 32 MPa, for several heats of types 304 and 316 stainless steels respectively.

Table C.2 shows a summary of elevated-temperature ultimate tensile data on 14 products of reference heat (9T2796) of type 304 stainless steel. The standard error of estimate for 14 products of a single heat, 7.45 MPa, exceeded a value of 3.4 MPa observed for 12 repeated tests on a single product form of a given heat.

In conclusion, we can say that error in determining elevated-temperature ultimate tensile strength of a given heat is significantly smaller than the observed heat-to-heat variations.

Table C.2. Ultimate tensile strength at 593°C (1100°F) and 6.7×10^{-4} per sec of 14 products of a single heat (9T2796) of type 304 stainless steel in the reannealed condition[a]

Test	Product	Size		Ultimate tensile strength		Standard error of estimate
		(mm)	(in.)	(MPa)	(ksi)	
1	Plate	9.5	0.37	336	48.73	
2	Plate	12.7	0.50	341	49.46	
3	Plate	19	0.75	341	49.46	
4	Plate	25	1.0	339	49.17	
5	Plate	50	2.0	321	46.56	
6	Pipe	102	4.0	341	49.46	
7	Pipe	203	8.0	339	49.17	
8	Pipe	64	2.5	349	50.62	
9	Bar	16	0.6	346	50.18	±7.45 MPa
10	Bar	16	0.6	344	49.89	(±1.08 ksi)
11	Bar	44	1.7	336	48.73	
12	Bar	48	1.9	336	48.73	
13	Bar	114	4.5	325	47.14	
14	Gundrilled Bar	64	2.5	337	48.48	
		Average:		337.9	49.01	

[a]0.5 hr at 1065°C (1950°F).

REFERENCES

1. V. K. Sikka, H. E. McCoy, M. K. Booker, and C. R. Brinkman, "Heat-to-Heat Variations in Creep Properties of Types 304 and 316 Stainless Steels," *J. Pressure Vessel Techol.* **97**: 243–51 (1975).

2. V. K. Sikka and M. K. Booker, "Assessment of Tensile and Creep Data for Types 304 and 316 Stainless Steel," ASME Paper No. 76-PVP-31, 1976, accepted for publication in *Journal of Pressure Vessel Technology*.

3. V. K. Sikka, "An Understanding of Heat-to-Heat Variations in Type 304 Stainless Steel," report in preparation, 1977.

4. V. K. Sikka and C. R. Brinkman, "Relation Between Short- and Long-Term Elevated-Temperature Properties of Several Austenitic Stainless Steels," *Scr. Metall.* **10**: 25–28 (1976).

5. E. P. Bens, "Hardness Testing of Metals and Alloys at Elevated Temperatures," *Trans. ASM*, **38**: 505–516 (1947).

6. F. Garofalo, P. R. Malenock, and G. V. Smith, "Hardness of Various Steels at Elevated Temperatures," *Trans. ASM*, **45**: 377–96 (1953).

7. "High Temperature Hardness Testing, Some Recent Russian Work," *Metallurgia*, 207–208 (September 1950).

8. E. E. Underwood, "Creep Properties from Short Time Test," *Material Methods*, **45**: 127–129 (1957).

9. F. S. Novik and A. A. Klypin, "Correlations Between the Properties of Certain Heat-Resisting Alloys," *Strength of Materials* (translated from *Problemy Prochnosti*), **4**: 1119–1124 (1972).

10. V. V. Krivenyik, "Relationship Between Short-Time Mechanical Characteristics and Long-Term Characteristics and Long-Term Strength," *Strength of Materials* (translated from *Problemy Prochnosti*) **6**: 295–299 (1974).

11. O. D. Sherby and J. E. Dorn, "Creep Correlations in Alpha Solid Solutions of Aluminum," *Trans. AIME, J. Metal*, **192**: 959–64 (1952).

12. G. V. Smith, *Supplemental Report on the Elevated-Temperature Properties of Chromium-Molybdenum Steels (An Evaluation of 2 1/4 Cr-1 Mo Steel), ASTM Data Ser. Publ.*, DS 6S2, American Society for Testing and Materials, Philadelphia, March 1971.

13. G. N. Emmanuel, W. E. Leyda, and H. J. Rozic, "Versatility of 2 1/4 Cr-1 Mo Steel as a Pressure Vessel Material," pp. 78–122 in *Symposium on 2 1/4-Cr-1 Mo Steel in Pressure Vessels and Piping*, ed. by A. E. Schaefer, American Society of Mechanical Engineers, New York, 1970.

14. R. Viswanathan, "Strength and Ductility of 2 1/4 Cr-1 Mo Steels in Creep at Elevated Temperatures," *Met. Technol.*, **1**: 284–94 (June 1974).

15. M. K. Booker, T. L. Hebble, D. O. Hobson, and C. R. Brinkman, *Mechanical Property Correlations for 2 1/4 Cr-1 Mo Steel in Support of Nuclear Reactor Systems Design*, ORNL/TM-5329 (June 1976).

16. R. W. Swindeman and C. E. Pugh, *Creep Studies on Type 304 Stainless Steel (Heat 8043813) Under Constant and Varying Loads*, ORNL/TM-4427 (June 1974).

17. R. W. Swindeman, "Creep-Rupture Correlations for Type 304 Stainless Steel (Heat 9T2796)," pp. 1–30 in *Structural Materials for Service at Elevated Temperatures in Nuclear Power Generation*, MPC-1, ed. by A. O. Schaefer, American Society of Mechanical Engineers, New York, 1975.

18. W. F. Simmons and J. A. Van Echo, *Report on the Elevated-Temperature Properties of Stainless Steels, ASTM Data Ser. Publ.*, DS 5S1, American Society for Testing and Materials, Philadelphia, 1965.

19. L. D. Blackburn, Hanford Engineering Development Laboratory, private communication, November 1973.

20. M. K. Booker, *Mathematical Description of the Elevated-Temperature Creep Behavior of Type 304 Austenitic Stainless Steel,* in preparation.

21. V. K. Sikka, T. L. Hebble, M. K. Booker, and C. R. Brinkman, *Influence of Laboratory Annealing on Tensile Properties and Time-Independent Design Stress Intensity Limits for Type 304 Stainless Steel,* ORNL-5175 (December 1976).

22. *NRIM Creep Data Sheets: Elevated-Temperature Materials Manufactured in Japan, 1973,* National Research Institute for Metals, Tokyo, 153, Japan.

23. Yoshio Monma, National Research Institute for Metals, Tokyo, 153, Japan, private communication, March 1976.

24. W. E. Stillman, M. K. Booker, and V. K. Sikka, "Mathematical Description of the Creep-Strain-Time Behavior of Type 316 Stainless Steel," pp. 424–28 in *Proc. 2nd Int. Conf. Mechanical Behavior of Materials,* American Society for Metals, Metals Park, Ohio, 1976.

25. M. K. Booker and V. K. Sikka, *Empirical Relationships Among Creep Properties of Four Elevated-Temperature Structural Materials,* ORNL/TM-5399 (June 1976).

26. M. K. Booker and V. K. Sikka, *Interrelationships Between Creep Life Criteria for Four Nuclear Structural Materials,* ORNL/TM-4997 (August 1975).

27. M. K. Booker and V. K. Sikka, *Predicting the Strain to Tertiary Creep for Elevated-Temperature Structural Materials,* ORNL/TM-5403 (July 1976).

28. M. K. Booker and V. K. Sikka, *Analysis of the Creep Strain-Time Behavior of Type 304 Stainless Steel,* ORNL-5190 (October 1976).

29. D. O. Hobson and M. K. Booker, *Materials Applications and Mathematical Properties of the Rational Polynomial Creep Equation,* ORNL-5202 (December 1976).

30. Hanford Engineering Development Laboratory, *Nuclear Systems Materials Handbook,* TID-26666 (continually updated).

31. V. K. Sikka, M. K. Booker, and J. P. Hammond, "Rational Polynomial Tensile Stress-Strain Equation for Low-Strain Behavior of Types 304 and 316 Stainless Steels," in preparation.

32. L. D. Blackburn, "Isochronous Stress-Strain Curves for Austenitic Stainless Steels," pp. 15–48 in *The Generation of Isochronous Stress-Strain Curves,* ed. by A. O. Schaefer, American Society of Mechanical Engineers, New York, 1972.

33. R. Strickler and A. Vinckier, "Morphology of Grain-Boundary Carbides and Its Influence on Intergranular Corrosion of 304 Stainless Steel," *Trans. ASM* **24**: 362–80 (1961).

34. B. Weiss and R. Strickler, "Phase Instabilities During High Temperature Exposure of 316 Austenitic Stainless Steel," *Met. Trans.* **3**: 851–66 (1973).

35. J. E. Spruiell et al. "Microstructural Stability of Thermal-Mechanically Pretreated Type 316 Stainless Steel," *Met. Trans.* **4**: 1533–1544 (1973).

36. C. F. Etienne, W. Dortland, and H. B. Zeedijk, "On the Capability of Austenitic Steel to Withstand Cyclic Deformation During Service at Elevated Temperature," paper presented at *International Conference on Creep and Fatigue in Elevated Temperatures Applications,* Philadelphia, September, 1973, and Sheffield, U.K., April, 1974.

37. R. K. Bhargara, J. Moteff, and R. W. Swindeman, "Metallographic Examination of Type 304 Stainless Steel Specimens Tested in Creep and Fatigue Modes," in preparation.

38. W. E. Ray et al., "Selection of Steam Generator Tubing Material for the Westinghouse LMFBR Demonstration Plant," *Nucl. Tech.* **11**: 222–31 (1971).

39. V. K. Sikka, C. R. Brinkman, and H. E. McCoy, "Effect of Thermal Aging on Tensile and Creep Properties of Types 304 and 316 Stainless Steels," pp. 316–50 in *Symposium on Structural Materials for Service at Elevated Temperatures in Nuclear Power Generation,* American Society of Mechanical Engineers, New York, 1975.

40. D. J. Wilson, "The Influence of Simulated Service Exposure on the Rupture Strengths of Grade 11, Grade 22, and Type 304 Steels," *J. Eng. Mat. Tech.* **96**: 10–21 (1974).

41. F. Garofalo, F. Von Gemmingen, and W. F. Dorris, "The Creep Behavior of an Austenitic Stainless Steel as Affected by Carbides Precipitated on Dislocations," *ASM Trans. Quart.* **54**: 430–44 (1961).

42. K. D. Challanger and J. Moteff, "Quantitative Characterization of the Substructure of AISI 316 Stainless Steel Resulting from Creep," *Met. Trans.* **4**: 749–55 (1973).

43. D. J. Michel, J. Moteff, and A. J. Lovell, "Substructure of Type 316 Stainless Steel from Deformation in Slow Tension at Temperature Between 21 and 816°C," *Acta Met.* **21**: 1269–1277 (1973).

44. V. K. Sikka, H. Nahm, and J. Moteff, "Some Aspects of Sub-boundary and Mobile Dislocations During High Temperature Creep of AISI 316 and 304 Stainless Steels," *Mat. Sci. Eng.* **20**: 55–62 (1975).

45. R. K. Bhargava, J. Moteff, and R. W. Swindeman, "Correlation of the Microstructure with the Creep and Tensile Properties of AISI 304 Stainless Steel," pp. 31–54 in *Symposium on Structural Materials for Service at Elevated Temperatures in Nuclear Power Generation,* American Society of Mechanical Engineers, New York, 1975.

46. M. J. Manjoine, "Basic Creep-Rupture Testing at 1100°F (593°C) of Uniaxially Loaded Specimens with Uniform Sections of Type 304 Stainless Steel," WARD-HT-3045-9, July 1975.

47. F. N. Rhines and R. J. Wary, "Investigation of the Intermediate Temperature Ductility Minimum," *Trans. ASM,* **54**: 117–28 (1961).

48. *Summary of U.S. LMFBR Programs on High Temperature Structural Design and Associated Materials Testing, October 1976,* ERDA-76/146, compiled by Oak Ridge National Laboratory, p. 25.

49. J. M. Corum, J. A. Clinard, W. K. Sartory, "An Assessment of the Validity of Inelastic Design Analysis Methods by Comparisons of Predictions With Test Results," in *Proceedings of Specialists' Meeting on High-Temperature Structural Design Technology,* Seven Springs Resort, Champion, Pennsylvania, April 27–30, 1976 (Oak Ridge National Laboratory).

50. C. R. Brinkman and G. E. Korth, "Heat-to-Heat Variations In The Fatigue and Creep-Fatigue Behavior of AISI Type 304 Stainless Steel at 593°C," *J. Nucl. Mat.* **48**: 293–306 (1973).

51. J. J. Heger, "Residual Elements in Stainless Steel – General Characteristics," pp. 120–136 in *Effects of Residual Elements on Properties of Austenitic Stainless Steels,* ASTM STP 418, American Society for Testing Materials, 1967.

52. G. E. Linnert, "Weldability of Austenitic Stainless Steels as Affected by Residual Elements," pp. 105–119 in *Effects of Residual Elements on Properties of Austenitic Stainless Steels,* ASTM STP 418, American Society for Testing Materials, 1967.

53. J. Wadsworth, S. R. Keown, and J. H. Woodhead, "The Effect of Niobium Carbide Precipitation on the Density Changes and Creep Properties of Type 347 Austenitic Stainless Steels," *Metal Science,* 105–112 (March 1976).

54. H. E. McCoy, *Studies of British Niobium-Stabilized Stainless Steels,* ORNL/TM-891, Oak Ridge National Laboratory (November 1964).

55. E. E. Bloom, *Effect of Titanium Additions on the Stress-Rupture Properties of Type 304 Stainless Steel,* ORNL/TM-1807, Oak Ridge National Laboratory (1967).